NASA
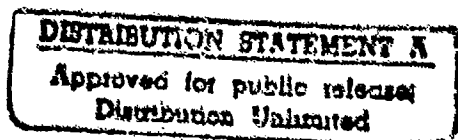Technical Memorandum 102340

AVSCOM
Technical Memorandum 89-C-005

AD-A217 844

An Investigation of Gear Mesh Failure Prediction Techniques

DTIC
ELECTE
FEB 0 8 1990
S D

James J. Zakrajsck
Lewis Research Center
Cleveland, Ohio

November 1989

NASA

US ARMY
AVIATION
SYSTEMS COMMAND
AVIATION R&T ACTIVITY

90 02 07 065

TABLE OF CONTENTS

1.0 OVERVIEW

This thesis is based upon experimental and theoretical work in the area of gear mesh failure diagnostics. More specifically, passive diagnostic instrumentation was installed on a single mesh gear fatigue tester, located at NASA Lewis Research Center, to periodically record the gear mesh induced vibration from initiation to failure. This information was analyzed using several existing gear diagnostic methodologies to determine if a correlation exists between the various prediction techniques and the observed modes of failure. This thesis presents the methods used and results obtained when applying the diagnostic techniques to the experimental data.

The experimental data collected during this thesis consisted of discrete vibration signatures taken from the eleven gear sets that were run to failure. Two accelerometers, both with a frequency range of 0 to 10,000 Hertz, and an optical sensor, used for a shaft synchronous signal, were installed on an existing spur gear fatigue tester. A timer was installed so that the vibration data could be periodically recorded on an FM tape recorder. Of the eleven gear sets monitored, five failed by heavy wear and scoring, two failed by single tooth pitting, two failed by tooth breakage, and two failed by distributed pitting.

The analytical work consisted of investigating and applying several gear mesh failure predication techniques. Two of the methods investigated were the FM0 and FM4 techniques developed by Stewart [1]. FM0 is a general method used to detect a variety of failures, whereas FM4 is more sensitive to a single tooth fault, such as single tooth fatigue cracks. Also used was the technique utilizing the Hilbert transform to demodulate the time signal. This technique, proposed by McFadden [2], is predominately used to detect fatigue cracks early in their development. The remaining three techniques investigated were the crest factor, sideband level ratio, and the non-harmonic to harmonic RMS level energy ratio. [3]

This thesis is divided into five chapters to help separate the main areas of this investigation. The remaining two sections of the introduction present the significance of condition monitoring in rotorcraft, and a brief overview of various transmission condition monitoring methods. Chapter II covers basic signal processing theory and techniques used in this analysis, and specific theory on each of the diagnostic methods investigated. Chapter III addresses the experimental work conducted during this study including a detailed description of the various gear failures found, and the results of frequency response measurements performed on the fatigue test rig. Results of applying the various gear diagnostic methods to the data collected are correlated to the actual gear failure modes in Chapter IV. Finally, Chapter V presents the conclusions of this research and recommendations applicable to further investigations into gear diagnostics.

1.1 SIGNIFICANCE OF GEAR CONDITION MONITORING IN ROTORCRAFT

In aerospace applications, where weight and size are premiums, gear systems are usually designed close to their projected limits. For rotorcraft transmissions, this design constraint translates into frequent transmission overhauls and frequent transmission related accidents resulting in death, injury, costly damage, and fleet grounding. Current on-board condition monitoring systems not only provide insufficient time between warning and failure,

but also result in many false alarms causing unnecessary and costly repairs. Thus the need for a reliable gear train condition monitoring system is paramount to the increased safety and cost efficient operation of current and future rotorcraft.

Some specific examples can be given illustrating the effects of transmission related problems on fleet readiness and safety. The entire Marine Corps fleet of 93 CH-53E Super Stallion Helicopters were grounded in February, 1987, due to a defective gear. [4] Also, The United Kingdom Department of Transport Air Accidents Investigation Branch (AAIB) released an official accident report on the November 1986 accident involving a Boeing 234 Commercial Chinook in the North Sea, which killed 45 people. [5] The main cause of the accident was determined to be a catastrophic failure of a modified gear in the forward transmission. This failure led to the desynchronization of the twin rotors such that the forward and aft rotors clashed.

The early detection of incipient failure in a rotorcraft transmission is not only important for safety, but also overall maintenance is improved and becomes more cost efficient. Currently, rotorcraft transmissions are overhauled at prescribed intervals. The transmissions are overhauled long before the calculated life of any of the critical components. Implementation of a reliable on-board condition monitoring system can increase the time between overhauls, or on-condition maintenance, without sacrificing safety by continuously monitoring the state and wear condition of critical components. The reduction in the frequency of overhauls not only decreases maintenance costs, but also decreases the probability of replacing good components with defective ones.

1.2 OVERVIEW OF TRANSMISSION CONDITION MONITORING METHODS

There are currently two basic methods of monitoring the condition of drive train components. The first uses a debris monitoring device that detects the size and rate of wear particles in the transmission lubricant as an indicator of severe wear and incipient failure. The second method is based upon vibration data obtained using one or more sensors mounted on the transmission case.

Most debris monitoring devices use magnetically captured debris to detect surface fatigue failures in critical gearbox oil wetted components such as gears and bearings. Some of the debris monitoring devices classify the captured particles by rough sizes, and keep account of the rate of capture and total debris count. This provides an indication as to the damage severity of the failing component(s). One problem with these devices is their limited ability to detect gear failures, since in most cases these-failures do not produce large amounts of metallic debris far enough in advance to provide sufficient warning time.

The use of vibration analysis methods for condition monitoring can be further classified into time domain and frequency domain methods. Time domain methods use statistical analysis techniques on direct or filtered time signals to detect parametric or pattern changes as transmission components wear. Statistical methods such as standard deviation and kurtosis are used to qualify general wear from tooth specific damage, respectively. Frequency domain methods use the Fast Fourier Transform (FFT) to convert the time signal into its' corresponding frequency components. Vibration energy at specific frequencies (i.e. primary, harmonics, sidebands, etc.) can be used to monitor geartrain component failures. Both methods use time synchronous averaging to cancel out all vibration that is non-periodic with the shaft frequency being used as the synchronous signal.

CHAPTER II
THEORY AND TECHNIQUES

An understanding of the theory behind the diagnostic techniques investigated along with some basic digital signal processing theory was needed to successfully carry out this analysis. A review of this study is presented in this chapter to give the reader sufficient background into the methods used.

2.0 DIGITAL SIGNAL PROCESSING TECHNIQUES

An important part of the experimental portion of this study was the conversion of the analog signals recorded into digitized data. Digitizing the data allowed the techniques being investigated to be applied to the data efficiently and easily on a standard personal computer. Along with the analog to digital conversion, the digital Fourier transform was used to convert digitized time data to frequency data. Because of the significance of these and other digital signal processing techniques used to the overall analysis, some digital signal analysis theory will be presented below.

The goal of the analog to digital conversion process is to obtain this conversion while maintaining sufficient accuracy in frequency, magnitude, and phase information. Two basic concepts responsible for the accuracy of the conversion are sampling and quantization. Sampling is the rate of time signal digitization, or the timing between the digital pieces of the time record. Quantization is related to converting the analog amplitude value to a digital value. Of the two concepts, sampling is usually the more critical because it effects frequency as well as amplitude accuracies.

All analog to digital (ADC) conversion devices sample at constant increments of time. Two theories, Shannon's Sampling Theory and Rayleigh's criterion, relate the sampling process to the limits of the information obtainable with minimum errors. Shannon's sampling theory, also known as the Nyquist criterion, states that the frequency the ADC device samples must be greater than two times the maximum frequency of interest. This theory outlines the highest frequency detectable in a signal, with minimum errors, given a specific sampling rate. Raleigh's criterion is related to the ability to resolve closely spaced frequency components. For a given time record of length T (seconds), the minimum resolution frequency, or the lowest frequency component measurable, is given by the following equation.

$$f(min) = \frac{1}{T} \tag{1}$$

The errors associated with sampling processes can be grouped into two categories, variance and bias. Variance is due primarily to random deviations of the sampled signal from the mean, or expected value. These random deviations are often caused by noise in the signal and measurement equipment. The easiest way of reducing variance errors is by time synchronous averaging. With this method the signal is averaged in the time domain with each record starting at the same point in a cycle, as determined by a synchronous signal. The portions of the signal not coherent with the synchronous time period, such as random noise and signals not periodic within this period, are averaged out. Ideally the number of averages improves the signal to noise ratio by the following equation.

$$S/N \text{ (after Nt averages)} = (\sqrt{Nt})*(S/N)(\text{original}) \tag{2}$$

where : S/N = signal to noise ratio

Bias errors cannot be minimized through averaging techniques. Limitations of the equipment or techniques used are the prime contributors of bias errors. Aliasing, a common bias error, results from the limitation of using finite information to describe an infinite process. An example of aliasing can be seen in in Figure 2.1. The solid line plot represents the actual signal. Because the sampling rate was conducted at a frequency lower than the frequency of interest, the digital representation of the signal, the dashed line plot, incorrectly implies a low frequency signal. To guard against aliasing problems, Shannon's sampling theory along with anti-aliasing filters, or low pass filters, should be utilized with any ADC device. The anti-aliasing filters serve to assure that any frequencies higher than the frequency of interest are removed from the signal prior to the ADC process.

One of the most powerful tools used in signal analysis is the Fourier transform. The basic theory behind the Fourier transform is that any continuous time signal can be represented by a series of sine and cosine functions of various amplitudes, frequencies, and phase relationships. Use of the Fourier transform produces no new information, it just transforms the data from one independent variable to another. In most instances time domain data is transformed to the frequency domain. Determining the frequency content of a time based signal is especially useful when analyzing mechanical systems with rotating components. The Fourier transform in the classical case is given in the following equations.

$$F(w) = \int_{-\infty}^{\infty} f(t)\exp(-jwt)\, dt \qquad \text{(forward transform)}$$

$$f(t) = \int_{-\infty}^{\infty} F(w)\exp(jwt)\, dt \qquad \text{(inverse transform)} \qquad (3)$$

where : f(t)= function in the time domain
F(w)= function in the frequency domain

Because the limits of integration of the classical form of the Fourier transform are from negative to positive infinity, the Discrete Fourier Transform (DFT) must be used with experimental data. Equations for the DFT are given below.

$$\bar{F}(m) = 1/N \sum_{n=0}^{N-1} f(n)\exp(-j2\pi mn/N) \qquad \text{(forward transform)}$$

$$\bar{f}(n) = 1/N \sum_{m=0}^{N-1} F(m)\exp(j2\pi mn/N) \qquad \text{(inverse transform)} \qquad (3)$$

The DFT is based upon a set of assumptions concerning the sequence of the discrete data values collected. These assumptions are: 1) the signal must be a totally observed transient within the time period of observation, or 2) the

4

signal must be composed only of harmonics during the time period of observation. Leakage, a bias error, is a good example of the type of errors resulting if neither of the assumptions are met when applying the DFT. Figure 2.2 illustrates the resulting transform, labeled "DISCRETE FT", as compared to the true transform, labeled "EXACT FT". The time signal in this case was neither transient nor periodic within the time record, thus the energy in essence leaked out into other frequency lines not representative of the actual signal. Windowing is one method used to minimize leakage errors. For example, the Hanning window multiplies the time signal by a function that gradually reduces to zero at the end of the time period. This forces the signal to appear to be transient within the time period, thus satisfying the DFT assumptions. There are functions that naturally meet the DFT assumptions, these are called self windowing functions. These functions produce no leakage errors and thus require no windowing.

The Fast Fourier Transform (FFT) was developed to reduce the computational time of the standard DFT process. The FFT time savings results from partitioning the DFT matrix into a number of smaller individual matrices and reordering the data for more efficient computation. This results in the computational time required for the FFT to be a function of $Nlog_2N$ instead of N^2, for the DFT. Along with the time saving advantages of the FFT is the retention of the phase information, which permits the evaluation of multichannel measurements such as transfer functions, and coherence. [6]

The frequency response function is another important digital signal processing method which is used to describe the dynamic properties of a physical system. The classical definition of the frequency response function is the Fourier transform of the unit impulse response function, as shown in the following equation. [7]

$$H(f) = \int_0^\infty h(t)exp(-j2\pi ft) \, dt \tag{5}$$

where : H(f) = Frequency response function
h(t) = Unit impulse response function

The frequency response function gives a direct relationship of the output to the input of a system in the frequency domain. This relationship is especially useful when trying to determine how a signal is altered as it passes through a system.

There are several ways of estimating the frequency response function using measured quantities. The first method is simply computed by dividing the Fourier transform of the output by the Fourier transform of the input, as given in Equation 6.

$$\bar{H}yx(f) = Y(f)/X(f) \tag{6}$$

where : $\bar{H}yx$ estimates H
Y(f) and X(f) are the Fourier transforms
of the output and input, respectively.

5

To reduce the variance error in the estimate of the frequency response a number of samples must be involved, as seen in Equation 7.

$$\overline{H}yx(f) = \frac{\sum_{i=1}^{NS} Y(f)_i}{\sum_{i=1}^{NS} X(f)_i} \qquad (7)$$

The above estimates are reasonable, however, to obtain the optimum estimate of the frequency response function in the presence of noisy signals, the least squares technique is often used. This technique produces an unbiased estimate of the frequency response function even in the presence of input noise, assuming that the input signal and the input noise are not correlated. [7] The frequency response estimate in this case is given by Equation 8.

$$\overline{H}yx(f) = Gyx(f) / Gxx(f) \qquad (8)$$

$$\text{where:} \quad Gyx(f) = \sum_{i=1}^{NS} Y(f)_i \, X^*(f)_i$$

$$Gxx(f) = \sum_{i=1}^{NS} X(f)_i \, X^*(f)_i$$

In this equation Gyx represents the cross power spectrum, and Gxx represents the auto power spectrum of the input, both of which can be calculated even in the presence of noise. The phase information is preserved in the term Gyx. The cross and auto power spectrums are also used to calculate another important signal processing parameter, the coherence function.

The coherence function provides a means of determining the causality relationship between the input and output of a system. The coherence function is given in Equation 9 below.

$$\gamma^2(f) = \frac{Gxy(f) \; Gxy^*(f)}{Gxx(f) \; Gyy(f)} \qquad (9)$$

where: Gxy(f) = The cross spectrum
Gxy*(f) = The complex conjugate of the cross spectrum
Gxx(f) = The auto power spectrum of the input
Gyy(f) = The auto power spectrum of the output

The coherence function is a measure of the amount of the output signal that is directly related to the input signal at any specific frequency. If, for example, at a certain frequency the coherence function has a value of 1.0, then the output is a direct result of the input signal at that frequency. If the

coherence function has a value less than unity but greater than zero, then one
or more of the following conditions may exist, as outlined by Bendat [7]:

1) Extraneous noise is present in the measurements.
2) Resolution bias errors are present in the spectral estimates.
3) The system relating y(t) to x(t) is not linear.
4) The output y(t) is due to other inputs besides x(t).

The coherence function is normally used in conjunction with frequency response
measurements. Here the coherence function provides a measure of the quality of
the measurement by giving the relationship of the output signal to the input
impulse. Another way of representing the coherence function information is by
the signal to noise ratio. The signal to noise ratio is easily found using the
coherence function as shown in Equation 10.

$$S/N~(f) = \frac{\gamma^2(f)}{1 - \gamma^2(f)} \tag{10}$$

2.1 THEORY OF GEAR FAILURE PREDICTION METHODS

Several gear failure prediction methods were investigated and applied to
the experimental data. The basic theory behind each method is given in the
following sections.

FMO METHOD

The FMO parameter is a time domain discriminant proposed by Stewart [1]
that provides a simple method to detect major changes in the meshing pattern.
FMO is defined as the ratio of the peak-to-peak level of the signal average to
the sum of the rms levels of the meshing frequency and its harmonics, as given
in Equation 11.

$$FMO = \frac{PP}{\sum_{i=1}^{n} A(f_i)} \tag{11}$$

where: PP = peak-to-peak level of signal average
A = amplitude at mesh frequency (i=1) and
harmonics (i>1)

FMO is formulated to be a robust indicator of major faults in a gear
mesh. Major tooth faults, such as breakage, usually results in an increase in
peak-to-peak level and no appreciable change in meshing frequency levels,
which causes FMO to increase. For heavy uniform gear wear, the peak to peak
level remains somewhat constant and the meshing frequency levels tend to
decrease, causing the FMO parameter to increase. In heavy wear situations,
the gear tooth profile and surface quality degrades, causing the meshing energy
to be redistributed from the meshing frequencies to the modulating sidebands.
From the physical viewpoint, two surfaces in sliding contact produce more ran-
dom fluctuations in the signal as the amount and magnitude of their surface

7

variations increase. This explains the redistribution of energy in the frequency domain with the increasing wear. For minor tooth damage, neither peak-to-peak levels or meshing frequencies levels change an appreciable amount, thus FM0 response in this case is limited. [8]

FM4 METHOD

FM4 was developed to detect changes in the vibration pattern resulting from damage to a single tooth. FM4 analysis, proposed by Stewart [1], filters out the regular meshing components from the signal average and performs two statistical operations, standard deviation and kurtosis, on the difference signal. Equation 12 and Figures 2.3 through 2.5 illustrate the formulation of the difference signal.

$$D(t) = A(t) - R(t) \tag{12}$$

where: A(t) = original signal average
R(t) = regular meshing components of signal average
D(t) = difference signal

Figure 2.3 represents a plot of an actual signal A(t) after time synchronous averaging. Figure 2.4 represents a plot of the regular meshing components R(t) of that signal. R(t) is found by taking the FFT of the original signal, extracting the regular components and taking the inverse FFT of these components. The regular components consist of the shaft frequency and its harmonics, the primary meshing frequency and its harmonics along with their first order sidebands. The first order sidebands are generally due to runout of the gear because of machining or assembly inaccuracies [9], and thus are considered regular components. The difference signal is then found by subtracting the regular components from the original signal. Figure 2.5 shows a plot of the resulting difference signal. The FM4 analysis method is comprised of the standard deviation and kurtosis of the difference signal along with a squared representation of the difference signal. The square of the difference signal represented in Figure 2.5 is shown in Figure 2.6. As seen in this figure the square of the difference signal magnifies any abnormalities present in the difference signal.

The FM4 analysis method uses standard deviation and kurtosis to extract information from the resulting difference signal. The standard deviation of the difference signal indicates the amount of energy in the non-meshing components, where the kurtosis indicates the presence of peaks in the difference signal. The theory behind FM4 is that for a gear in good condition the difference signal would be primarily noise with a Gaussian amplitude distribution [8]. The standard deviation should be relatively constant, and a normalized kurtosis value of three would be reflected [3]. When a tooth develops a major defect, such as root cracks or severe spalling, a peak or series of peaks appear in the difference signal. The kurtosis value would thus increase to reflect these peaks. The standard deviation will increase only when the peak(s) become severe enough to bring up the rms level of the entire difference signal. It should be noted that the standard deviation will also increase with increases in uniform gear wear. This is to be expected, since the standard deviation of the difference signal is an indicator of the energy level of the non-meshing components, which increases as the gear wears. Thus both the standard deviation and the normalized kurtosis should be used in conjunction with each other to detect the onset and severity of single tooth defects.

Standard deviation is defined as the second statistical moment of an array of values about the mean of those values. It is an indicator of the variance of the values in the array. The standard deviation of the difference signal can be found using the following equation.

$$RMSDS = \left[1/N \sum_{i=1}^{N} (d_i - \bar{d})^2 \right]^{1/2} \tag{13}$$

where : RMSDS = Standard Deviation
$\bar{d}$ = Mean value of the signal

Kurtosis is defined as the fourth statistical moment of an array of values about the mean of those values. It is an indicator of the existence of major peaks in the array. The digital form of the kurtosis equation is given in Equation 14.

$$K = 1/N \sum_{i=1}^{N} (d_i - \bar{d})^4 \tag{14}$$

where: K = Kurtosis
$\bar{d}$ = Mean value of signal

This absolute kurtosis value will increase proportionally with general increases in the standard deviation. To keep the kurtosis parameter sensitive to single tooth damage only, the normalized kurtosis equation is given below.

$$NK = \frac{N \sum_{i=1}^{N} (d_i - \bar{d})^4}{\left[\sum_{i=1}^{N} (d_i - \bar{d})^2 \right]^2} \tag{15}$$

where: NK = Normalized kurtosis
$\bar{d}$ = Mean value of signal

As seen in Equation 15, the normalized kurtosis is simply the absolute kurtosis divided by the fourth power of the standard deviation, or the square of the variance. This allows the normalized kurtosis to be sensitive only to

9

peaks in the difference signal, regardless of changes in the standard deviation.

Because the normalized kurtosis values are non-dimensional, signals with different magnitudes but similar shapes will have similar values. A square wave is found to have a normalized kurtosis value of 1.0, for a sine wave the value is 1.5, and for a signal of essentially noise with a Gaussian amplitude distribution the normalized kurtosis value is found to be 3.0 [3]. Thus, a normalized kurtosis value greater than 3.0 is indicative of a peak or series of peaks existing in the signal. One pitfall with the normalized kurtosis parameter is its drastic decrease in peak sensitivity as the number of peaks of similar magnitudes increase beyond two. Thus for failures involving two or more teeth, the normalized kurtosis value may not increase far beyond 3.0, and the failure must be detected with the standard deviation level.

HILBERT TRANSFORM METHOD

A technique was developed by McFadden [2] to detect local gear defects, such as fatigue cracks, using the Hilbert transform. The basic theory behind this technique is that the sidebands around the dominant meshing frequency modulate the meshing frequency to produce the time average signal. Using the Hilbert transform, the signal can be demodulated, resulting in the corresponding amplitude and phase modulation functions. The phase modulation function is especially sensitive to fatigue cracks by indicating a phase lag at the point the cracked tooth goes into mesh [2].

The Hilbert transform is primarily used to transform a real time signal into a complex time signal with real and imaginary parts. The real part of the complex time signal is the actual time signal, and the imaginary part is the Hilbert transform of the actual time signal. This complex time signal is referred to as the analytic signal, and is given in the following equation.

$$AN(t) = A(t) + iH[A(t)] \qquad (16)$$

where: $AN(t)$ = analytic signal
$A(t)$ = original signal
$H[A(t)]$ = Hilbert transform of original signal

The Hilbert transform of a real valued time signal, $A(t)$, is defined as the convolution of the time signal with $1/\pi t$, as shown in Equation 17.

$$H[A(t)] = 1/\pi \int_{-\infty}^{\infty} A(\tau)(1/(t-\tau)) \, d\tau \qquad (17)$$

An easier way of computing the Hilbert transform is to utilize the convolution theorem, i.e. the convolution of two signals in the time domain is equivalent to the inverse Fourier transform of the product of the two signals in the frequency domain. Thus, to determine the Hilbert transform of a real-valued time signal the signal must be transformed to the frequency domain, phase shifted by -90 degrees, and transformed back to the time domain. The determination of the Hilbert transform using this method is illustrated in Equation 18.

$$H[A(t)] = F^{-1}[(-i \, sgnf) \, A(f)] \qquad (18)$$

where: $A(f)$ = Fourier transform of original signal
$sgnf$ = 1 for $f > 0$, -1 for $f < 0$
$F^{-1}[]$ = inverse Fourier transform

Once the analytic signal is found, the amplitude and phase modulation functions can be determined. The amplitude modulation function, or envelope of the signal, is the magnitude of the analytic signal, and is given in Equation 19.

$$|AN(t)| = [(A(t))^2 + (H[A(t)])^2]^{1/2} \qquad (19)$$

The phase modulation function, or instantaneous phase variation, is found by using Equation 20 below.

$$\phi(t) = \tan^{-1}[H[A(t)]/A(t)] - 2\pi f_0 t \qquad (20)$$

where: f_0 = carrier frequency

The phase modulation function, $\phi(t)$, represents the instantaneous phase angle variation with respect to the nominal gear speed [10]. The second term in Equation 20 represents a ramp function with a frequency equal to the carrier frequency, f_0, that is being modulated. This term is required to separate the instantaneous phase angle variations from the constant carrier frequency phase function.

Before creating the analytic signal, the original signal must be bandpass filtered about a dominant meshing frequency. This dominant frequency is either the primary mesh frequency or one of its harmonics, whichever appears to give the most robust group of sidebands. The width of the bandpass filter depends on the location of the meshing frequency to other meshing frequency harmonics. McFadden [2] suggests using a bandwidth giving the maximum amount of sidebands, even if they interfere with the sidebands from other harmonics. The reasoning here is to include as much of the primary modulating sidebands as possible, assuming that the interference from the other sidebands is negligible. The dominant frequency, or carrier frequency, is then removed and the resulting bandpassed sidebands are used in constructing the analytic signal and modulation functions.

As stated earlier, the phase modulation function appears to be the most sensitive of the two modulating functions to gear fatigue cracks. One particular feature of the phase modulation function is its ability to distinguish between an actual fatigue crack and a particle on the tooth. For a fatigue crack, the phase modulation function would experience a phase lag at the point the cracked tooth went into mesh. For a particle on the tooth, the phase modulation function would experience a phase lead when that tooth went into mesh [2].

11

CREST FACTOR

The crest factor, CF, is a simple measure of detecting changes in the signal pattern due to impulsive vibration sources, such as tooth breakage [3]. The crest factor is easily calculated by dividing the peak level of the signal average to the standard deviation of the signal average, as given in Equation 21.

$$CF = \frac{PL}{RMS} \qquad (21)$$

where: PL = peak level of signal
        RMS = standard deviation of signal average

Peaks in the signal will result in an increase in CF.

SIDEBAND LEVEL FACTOR

The sideband level factor, SLF, is a course indicator of single tooth damage or gear shaft damage. [8] To calculate SLF the first order sideband levels about the primary meshing frequency are divided by the standard deviation of the signal average, as seen in Equation 22.

$$SLF = \frac{FOSL}{RMS} \qquad (22)$$

where: FOSL = first order sidebands level
        RMS = standard deviation of signal

A bent or damaged shaft will result in an eccentric meshing pattern, directly reflecting an increase in the first order sidebands level, thus increasing the SLF value. It is unclear to the author how this factor is sensitive to single tooth damage.

ENERGY RATIO

The energy ratio (ER) is formulated to be a robust indicator of heavy uniform wear. This factor divides the standard deviation of the difference signal by the standard deviation of the signal composed of the regular frequency components only [3]. The difference signal and the regular components signal are the same as those defined previously in the FM4 analysis section. Equation 23 illustrates the ER factor.

$$ER = \frac{RMSDS}{RMSRC} \qquad (23)$$

where: RMSDS = standard deviation of difference signal
        RMSRC = standard deviation of regular components
                portion of the signal

12

For heavy wear, the mesh energy redistributes from the regular meshing frequency components to the modulating sidebands. This would result in an increase in the rms level of the difference signal, the numerator, and a decrease in the rms level of the regular components signal, the denominator. The net result would be an increase in the ER value in a more robust fashion than just the increase in the difference signal rms level, as calculated in the FM4 analysis.
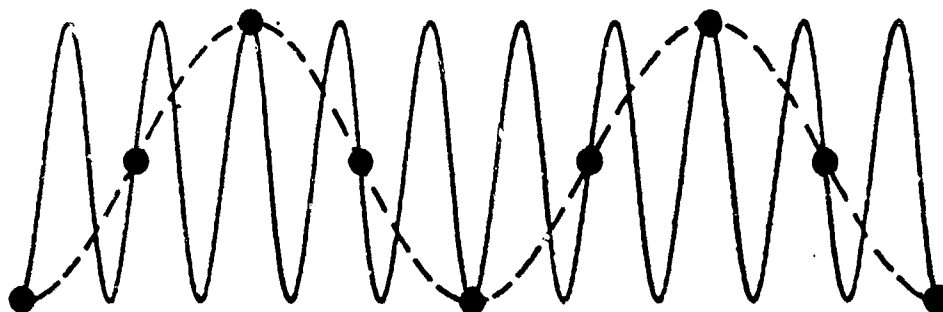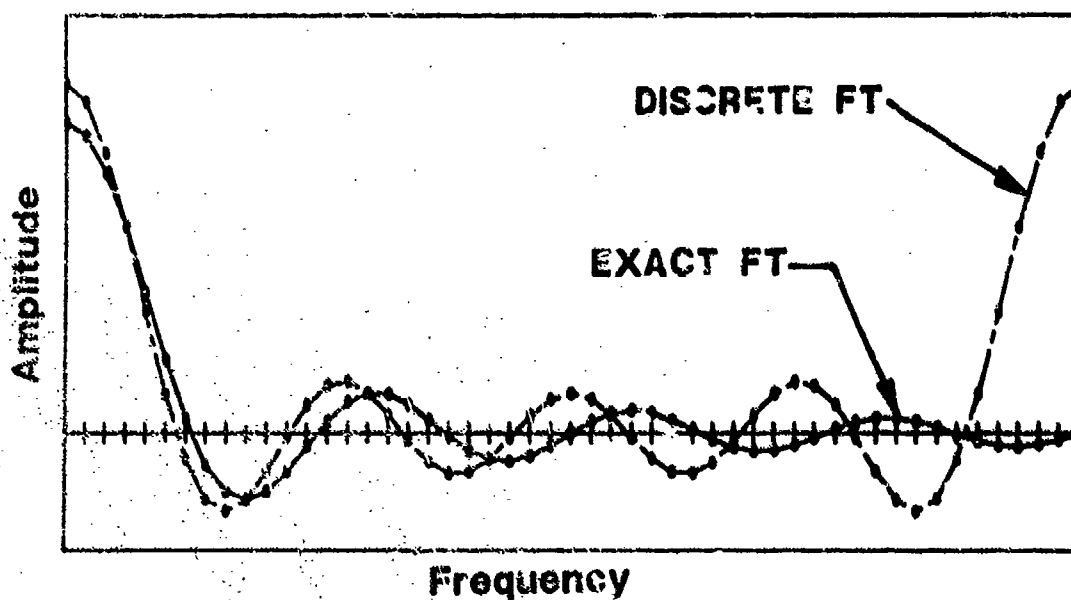
Figure 2.1 : Example of the Aliasing Problem.

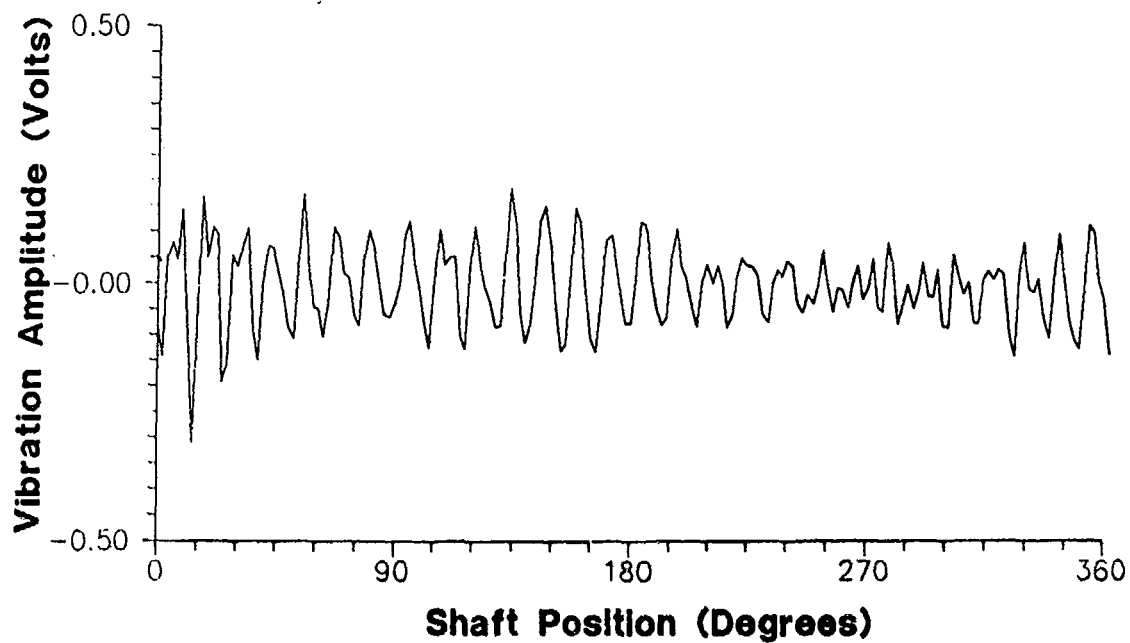Figure 2.2 : Example of Leakage Problem.

Figure 2.3 : Plot of Actual Signal Average, A(t), for One Shaft Revolution.
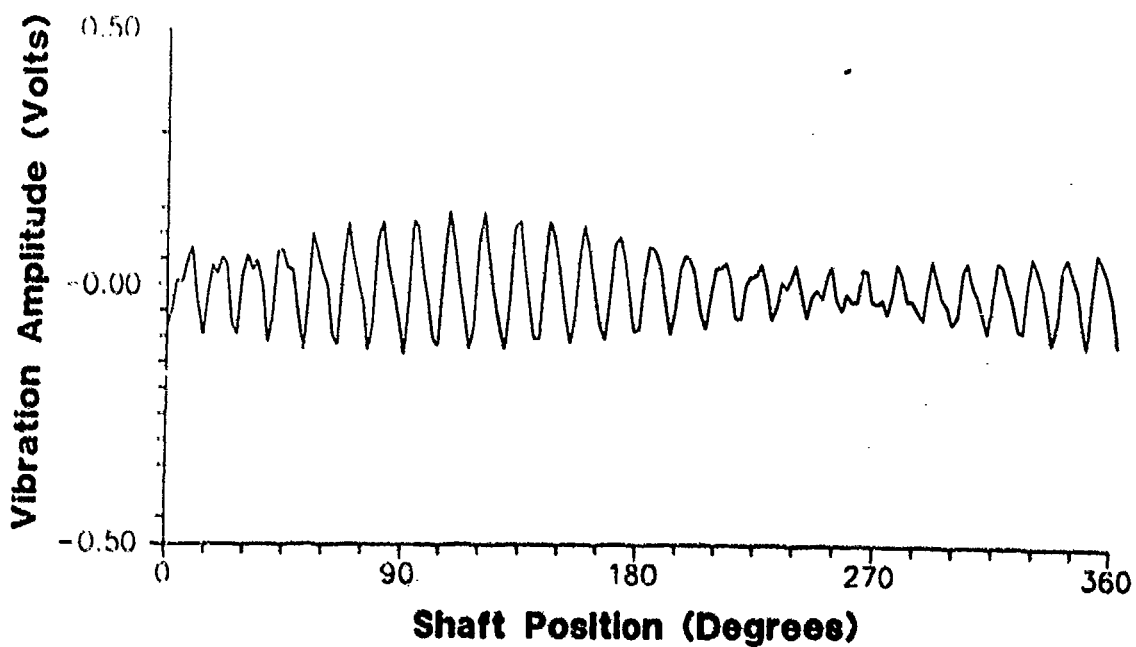

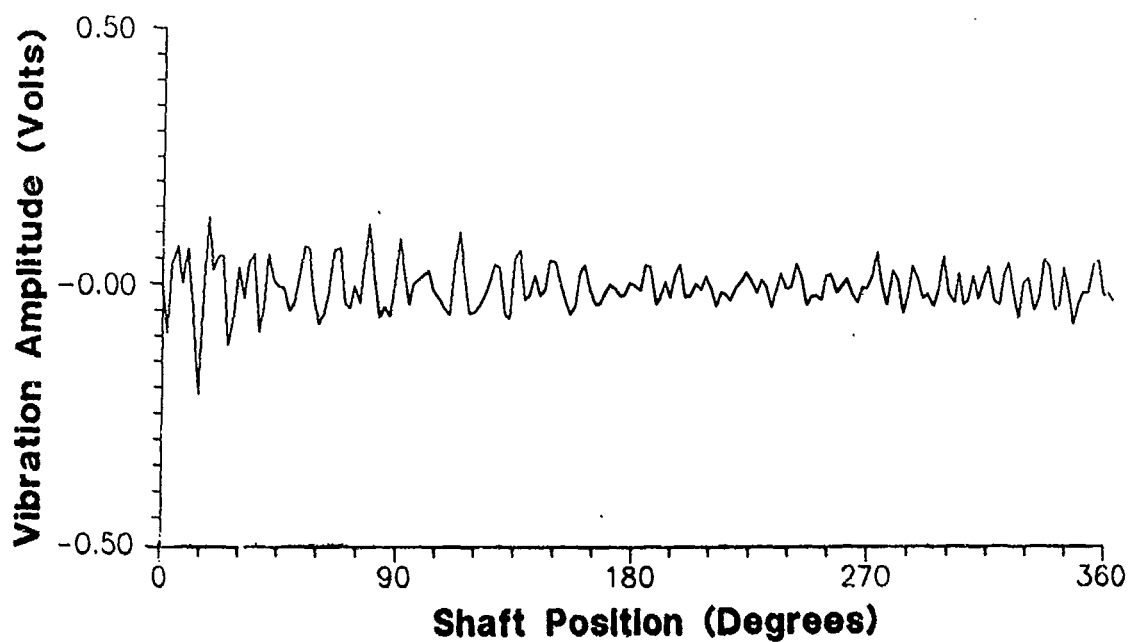Figure 2.4 : Plot of Regular Part, R(t), of Signal, for One Shaft Revolution.

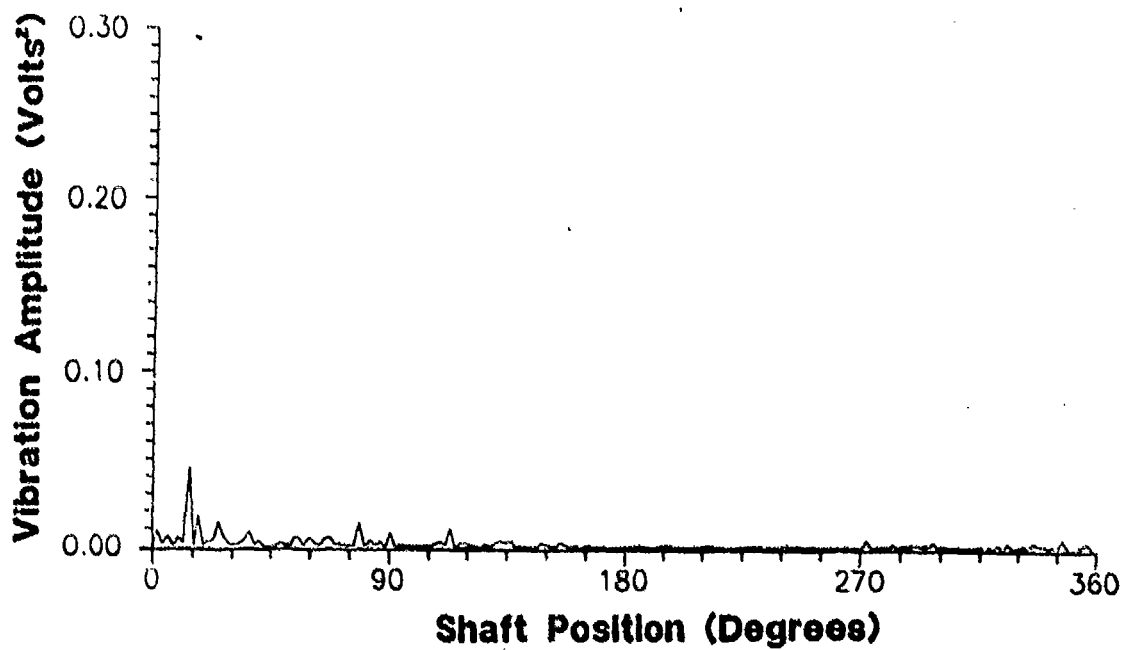Figure 2.5 :   Plot of Difference Signal, D(t), for One Shaft
Revolution.

Figure 2.6 :   Plot of Squared Difference Signal, $[D(t)]^2$,
for One Shaft Revolution

CHAPTER III
EXPERIMENTAL PROCEDURES

The experimental portion of this study was conducted on a gear fatigue testing apparatus at NASA Lewis Research Center. Some background information on the fatigue tester will be presented in this chapter along with some details on the type of gears tested and their specific modes of failure. Also discussed in this chapter is the test instrumentation used, basic test set-up, and some frequency response measurements performed on the fatigue tester.

3.0 SPUR GEAR FATIGUE APPARATUS

The spur gear fatigue test apparatus at NASA Lewis Research Center first became operational in 1972. It has supplied the means to obtain crucial data on the effects of gear materials, gear surface treatments, and lubrication types and methods on the fatigue strength of aircraft quality gears. A cut away view and schematic diagram of the fatigue rig is shown in Figure 3.1. The test rig operates on the four-square, or recirculating torque, principal. As seen in Figure 3.1, the slave gear provides the recirculating torque by virtue of the hydraulic pressure acting on the load vanes. The tooth load is controlled by varying the amount of hydraulic pressure applied. Because of this recirculating torque principal, the drive motor provides only the power required to overcome the frictional losses at the desired running speed. The fatigue rig is capable of providing 75 kW (100 hp) at the designed operating speed of 10,000 rpm.

3.1 TEST GEARS

The gears tested using the fatigue test apparatus were all the same type and were subjected to identical loading conditions. All of the gears were made of AISI 9310 steel and were manufactured to AGMA class 13, aircraft quality, tolerances. The test gears have 28 teeth, a pitch diameter of 88.9 mm (3.50 in.), a pressure angle of 20 degrees, and a tooth face width of 6.35 mm (C.25 in.). The gears were loaded to 74.6 Nm (660 in lbs), which resulted in a pitchline maximum hertz stress of 1.71 GPa (248 ksi), at an operating speed of 10,000 rpm. This represents a load of almost two times the normal design load for these gears. This testing procedure was used in order to obtain failures within a reasonable amount of test time. Table I lists the basic run parameters along with the number of hours to failure and the overall mode of failure for each run. As seen in this table, the only run parameters that differ between the runs are the surface treatment, and the type of lubricant.

Three different surface treatments were encountered in the eleven runs recorded. The gears in runs 1 through 7 all used the standard surface treatment, which is a final grinding operation to a surface finish of 356 mm rms (14 in. r.). The gears in runs 8 through 11 were shot peened and then honed. The main ason for shot peening is to create subsurface residual stresses that improve the pitting fatigue life of a gear. The gears in runs 8 through 10 used the SPH method, a high intensity shot peening method designed to produce high subsurface residual stresses. The gears in run 11 used the SPL method, a low intensity shot peening method designed to produce low subsurface residual stresses. The basic differences in life and failure modes, as seen in Table I, are primarily due to the different lubricants used.

17

TABLE I: Test Run Descriptions

RUN #	GEAR SURFACE TREATMENT	LUBRICATION	TOTAL LIFE (Hours)	BASIC FAILURE MODE
1	Standard	Type A Oil	49	Heavy Wear and Scoring
2	Standard	Type A Oil	36	Heavy Wear and Scoring
3	Standard	Type A Oil	9	Broke Tooth
4	Standard	Type A Oil	79	Heavy Wear and Scoring
5	Standard	Type A Oil	39	Heavy Wear and Scoring
6	Standard	Type A Oil	54	Heavy Wear and Scoring
7	Standard	Type A Oil	50	Broke Tooth
8	SPH	Type B Oil	520	No Failure (Single Pits)
9	SPH	Type B Oil	245	Single Pits
10	SPH	Type B Oil	339	Distributed Pits
11	SPL	Type B Oil	100	Distributed Pits

The two different oils used were classified type A oil and type B oil. The type A oil did not appear to have sufficient additives to provide a good Elasto-Hydro Dynamic (EHD) film thickness between the gear surfaces under extreme pressure. Without an adequate EHD film thickness the tooth surfaces obtain metal to metal contact, causing severe surface wear in a relatively short period of time. This is especially evident by the fact that the runs with the type A oil, runs 1 through 7, experienced heavy wear and surface scoring, and an average life of only 63 hours. Comparatively, runs 8 through 11, which used type B oil, experienced an average life of 300 hours, and subsurface fatigue failures in the form of pitting. The type B oil was a synthetic paraffinic oil with five volume percent of an extreme-pressure (EP) additive. This EP additive contains sulfur and phosphorus to enable the oil to keep an adequate EHD film thickness, minimizing metal to metal contact, even under extreme pressure.

The failure modes experienced by the various gears can be categorized into four basic damage related groups. These groups are: 1) Heavy wear and scoring, 2) Tooth breakage, 3) Single pits, and 4) Distributed pitting. The groups are based on the types and magnitude of damage found on the gears at the end of their runs. As indicated in Table I, run 8 was not classified as failed because it ran the maximum of 520 hours without exceeding the rig's vibration limit. The point of failure on the fatigue rig was determined by an overall vibration level from an accelerometer mounted on the rig. When this level reached the preset threshold, the rig shutdown and the run was classified as failed. Because the gears of run 8 experienced damage similar to another run, it is included in that run's group. A more detailed description is given in the following sections.

HEAVY WEAR AND SCORING:
Runs 1, 2, and 4 through 7 all experienced heavy wear and scoring uniformly over all the gear teeth. Figures 3.2 and 3.3 illustrate the wear patterns observed. As seen in these figures, the driven gear teeth experienced heavy wear and scoring at the tip portion of the tooth, a band of light pitting at the double to single tooth contact point, and heavy wear in the root region of the tooth. The driver gear teeth experienced similar wear patterns to the driven gear teeth, with the exception that the top portion of the tooth experienced lighter wear and scoring. Run 3 experienced the same wear patterns, although to a lesser degree due to the premature tooth failure at 9 hours into the test. The tooth surfaces appeared extremely course, especially in the regions of heavy wear and scoring.

TOOTH BREAKAGE
Runs 3 and 7 experienced tooth breakage during the fatigue test conducted. One tooth broke during run 3, causing the rig to shut down. A photograph of the fracture surface on the driven gear in run 3 is shown in figure 3.4. No detailed tooth crack propagation analysis was done on this tooth, however by visual inspection, there appeared to be only three distinct bands in the fracture area, with little evidence of fracture surface smoothing. This indicates that the time between crack formation and tooth fracture was relatively short. Run 7 also experienced tooth fracture; however, a failure in the automatic shut down mechanism did not stop the rig soon enough to prevent extensive damage to both gears. Thus no tooth fracture observations could be performed on run 7 gears.

19

SINGLE PITS

Runs 8 and 9 experienced similar damage in the form of single pits. Figures 3.5 and 3.6 illustrate the wear pattern found on the gears in run 8 at the end of the run. As seen in these figures all but one of the teeth on the driver and driven gear appear to have no sign of wear or pitting. A moderate pit appears on one tooth on the driver gear, and a larger pit appears on one tooth of the driven gear. Figures 3.7 and 3.8 illustrate the condition of the gears in run 9 at the point of failure. As seen in these figures, run 9 appears to have a similar failure pattern as found in run 8, with one exception. The large pit on the driven gear in run 9, although roughly the same size as the large pit in run 8, has it's major axis orientated across the gear tooth rather than along the tooth surface, as found in run 8. The defects found on the gears in runs 8 and 9 are characterized as single tooth defects.

DISTRIBUTED PITTING

Runs 10 and 11 experienced similar damage in the form of distributed pitting. Figures 3.9 and 3.10 illustrate the wear pattern present on the gear teeth in run 10. As seen in these figures, the driver gear exhibits a wear pattern of pitting bands with various intensities over 60 percent of the teeth. The driven gear displayed a similar pattern over a smaller region of teeth. Figures 3.11 and 3.12 illustrate the wear pattern present on the gear teeth of the gears used in run 11. As seen in these figures, the distributed pitting bands appear in a similar fashion to those in run 10, although to a lesser extent.

3.2 INSTRUMENTATION SET-UP

Figure 3.13 illustrates the test instrumentation set-up used in this study. As seen in this figure, two accelerometers, PCB Model 303A, were mounted on the rig close to the test gear mesh. The vibration signal from these accelerometers were recorded on a high precision tape recorder, Sangamo Weston Sabre VII, along with a once per revolution signal and a time code signal. A one minute signature was collected every three hours by using a timer to control recording time. The once per revolution signal was provided by a photon sensor that produced a narrow time pulse (.202 msec) for each revolution of the shaft. This signal was used for time synchronous averaging, and for determining the actual rotational speed. The time code signal was used during tape playback to distinguish between the separate data points, and to provide the exact time and day for each data point recorded.

After the runs were recorded, the data was then analyzed by replaying the tape into a single channel dynamic signal analyzer, with a dynamic range of 80 dB, and transferring it to a personal computer. The raw data was digitized and averaged by the analyzer and sent via a general purpose interface bus to an IBM compatible personal computer. The PC used a standard IEEE-488 interface board to control the analyzer and download the digitized data to DOS files on the PC's disc drive. The data transferred was the averaged amplitude and phase portions of the Fourier transform. The data was then analyzed by using several FORTRAN programs, each based on the various prediction techniques investigated.

The primary mesh frequency was an important factor in choosing and setting the test instrumentation. For the 28 teeth test gears operating at 10,000 rpm, the primary and first harmonic of the mesh frequency occurs at approximately 4700 Hz and 9400 Hz, respectively. The accelerometers were chosen with a frequency range of 0 to 10,000 Hz to capture the mesh frequencies. The recorder tape speed was set at 762 mm/sec (30 in/sec) with wideband group I FM recording electronics to give a recording frequency range of 0 to 20 000 Hz, with a

20

dynamic range of 50 dB. FM recording was used to give good amplitude stability, independent of the storage characteristics of the recording tape. Using a tape reel with a 2800 m length (9200 ft), one reel translated to 184 hours of coverage, or 7.7 days. This was considered a reasonable time interval, since some of the tests ran continuously for nearly 21 days. The analyzer was set up to time average the signal over 40 averages for each data point, using the shaft synchronous signal as the input trigger. The FFT was performed over the range 0 to 12,500 Hz.

During the first stages of the data analysis process, it was discovered that the side accelerometer provided the same information as the top accelerometer. In fact, the meshing frequency components in the side accelerometer signal were not as dominant as in the top accelerometer signal. This is probably due to the fact that the top accelerometer is orientated to sense the vertical vibrations of the box. This is coincident with the direction of the primary component of the tooth mesh loads, resulting from the side by side arrangement of the test gears. Thus, the vibration data from the top accelerometer was used primarily in this analysis, with the side accelerometer data used as a backup.

3.3 FREQUENCY RESPONSE MEASUREMENTS OF FATIGUE RIG

During the initial stages of the data analysis, it was discovered that the recorded time signals contained frequency data not coherent with the gear meshing frequencies. Figures 3.14 through 3.17 illustrate the presence of the extraneous frequencies as run 7 progressed from initiation to failure. This phenomenon was found in all of the runs recorded. As seen in these figures, certain frequencies, not coincident with the gear mesh frequencies or associated sidebands, increase drastically through the run cycle. The primary mesh frequency, highlighted by an arrow in the figures, is in most cases lower in magnitude than the extraneous frequencies. The amplitudes near 3000 and 6000 Hz appear to be the most dominant. If the gear failure prediction techniques were applied to the signals given in Figures 3.14 through 3.17, results not indicative of the actual gear condition would dominate. Therefore, it was necessary to investigate these extraneous frequency components and determine their origin. If these components could be attributed to a known source, they then could be removed from the signal with confidence.

A number of possible sources of the extraneous frequency components were investigated. Because the signal is synchronous time averaged with the gear shaft rotation, the only possible periodic sources coincident with the shaft speed are the roller bearings, ball bearings, and the slave gear. The location of these components are given in Figure 3.1. Based on the assumptions of a single defect and that the rolling elements remain in rolling contact, bearing defect frequencies were calculated using existing equations. [11] These frequencies covered outer race, inner race, and rolling element defects, and fell within the 64 to 1400 Hz range. These explain some lower frequency components, but they were too low for the dominant frequencies in question. The slave gear primary mesh frequency was found to be 6084 Hz, which is near some of the extraneous frequencies, but it was not exactly coincident. The next step in identifying the frequencies in question was to determine the modal parameters of the rig using frequency response measurements.

Frequency response measurements performed on the fatigue rig illustrated how the dynamics of a transfer path can critically alter a signal. The frequency response measurements were taken at two locations on the box with the reference point being the top accelerometer location, as illustrated in Figure 3.18. For these tests, the impact method was used. A modal hammer with

21

a steel tip and force transducer was used as the input to the system, with the top accelerometer serving as the output signal. The force transducer and accelerometer were input into a two channel dynamic signal analyzer capable of calculating the frequency response function. Twenty averages were taken for each measurement. The FFT of the input impulse is given in Figure 3.19. As seen in this figure, the impulse adequately excites the frequencies in question.

Results from the frequency response measurements directly correlated the unexplained frequency components to the path modes. The frequency response measurement of the path from the top of the bearing cover to the top accelerometer location is given in Figure 3.20. The coherence function for this measurement, shown in Figure 3.21, indicates the output is almost totally a function of the input up to 10,000 Hz. Figures 3.22 and 3.23 give the frequency response measurement and its' coherence for the path from the gear shaft to the top accelerometer location. As seen in Figures 3.20 and 3.22, the vibration path from the gear to the top accelerometer drastically alters the signal due to the natural frequencies inherent in the box. As the gears experience wear, the meshing energy redistributes from the primary meshing frequencies to a wide range of frequencies in the frequency spectrum. When these frequencies become coincident with the natural frequencies associated with the transfer path the corresponding amplitudes increase. This phenomenon is clearly illustrated in the 3000 Hz region and in the region within the 5000 to 8000 Hz band in Figures 3.14 through 3.17. The frequencies in these regions are coincident with the natural frequencies associated with the transfer path, as evident in Figures 3.22 and 3.23.

Most of the frequencies in question were found to be a direct result of the structural dynamics of the transfer path and as such are not desired as inputs for the various failure prediction techniques. Therefore these frequencies were removed from the processed signals by filtering techniques. The functions illustrated in Figures 3.20 and 3.22 were used to determine the frequencies to remove. Careful attention was placed on eliminating only those frequencies known to be dominant, and to allow frequencies adjacent to the mesh frequencies to be passed. Fortunately, the primary mesh frequency region had no dominant natural frequencies present; however some of the upper sidebands were eliminated with the filtering. All of the analysis methods were applied to the filtered signal. It is acknowledged that some of the desired signal was eliminated with the filtering; however, it is assumed that the errors associated with the filtering process are less than those associated with leaving the dynamic effects of the transfer path in the signal. The frequency bands most commonly filtered out were between 400 and 1500 Hz, 2400 and 3700 Hz, and 5200 and 8400 Hz.
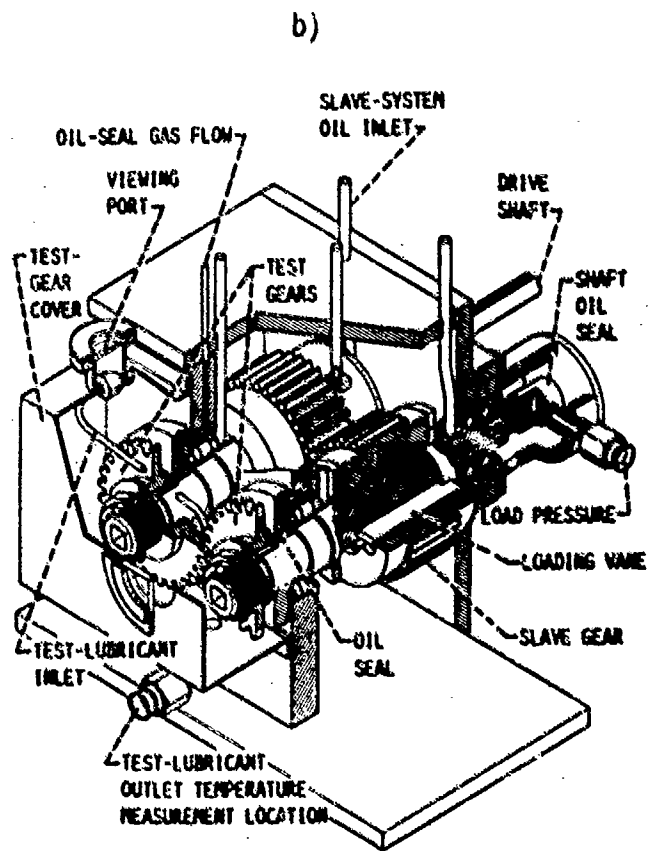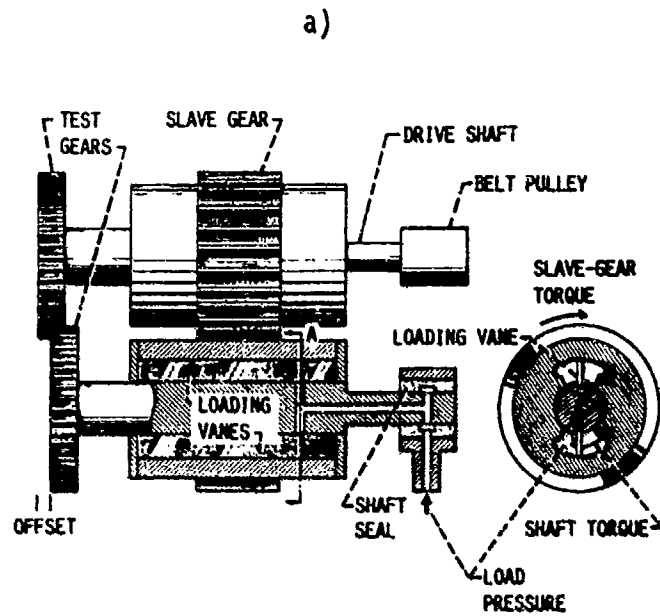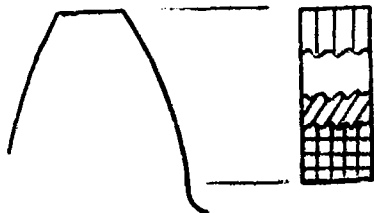
a)

b)

Figure 3.1 : Gear Fatigue Test Apparatus.
a) Schematic Diagram.
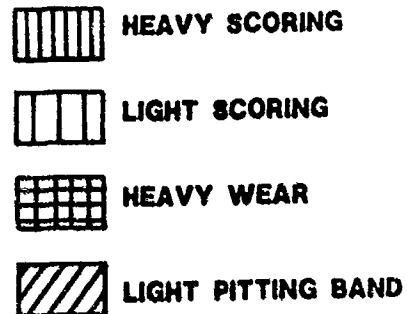b) Cutaway View.

23

DRIVER GEAR

Uniform Damage

Tooth Specific Damage

None.

DRIVEN GEAR
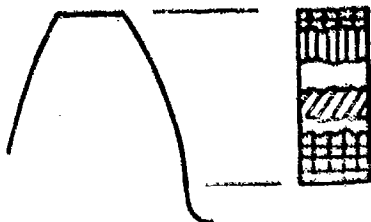
Uniform Damage

**All Dimensions
in mm**

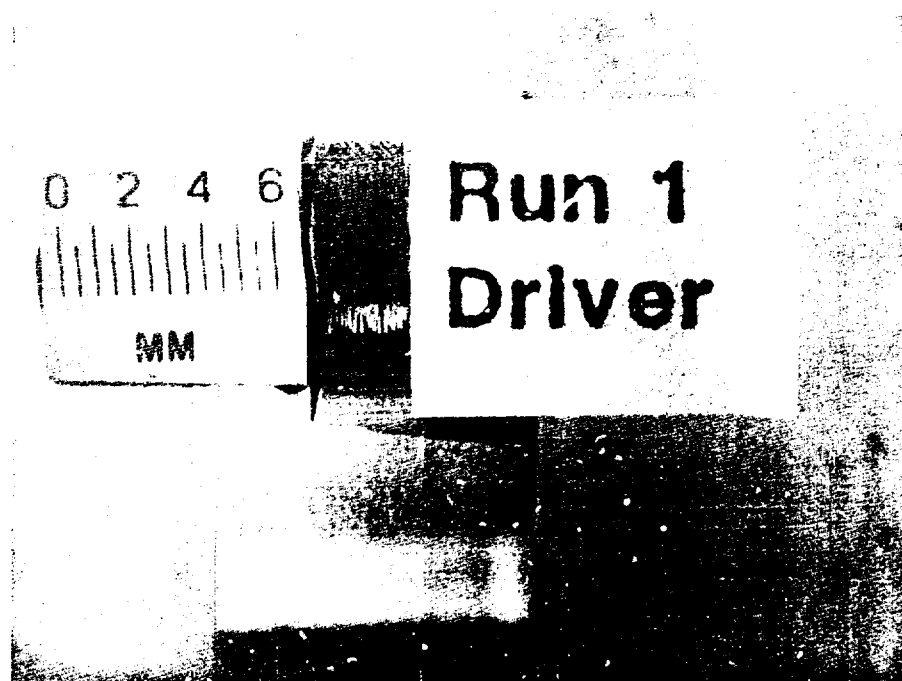**Tooth Specific Damage**

None

Figure 3.2 : Illustration of Tooth Damage Found on Gears in Runs 1, 2, and 4 through 6.

a) driver gear teeth

b) driven gear teeth

Figure 3.5   Photographs of uniform damage found
on gears in Run 1
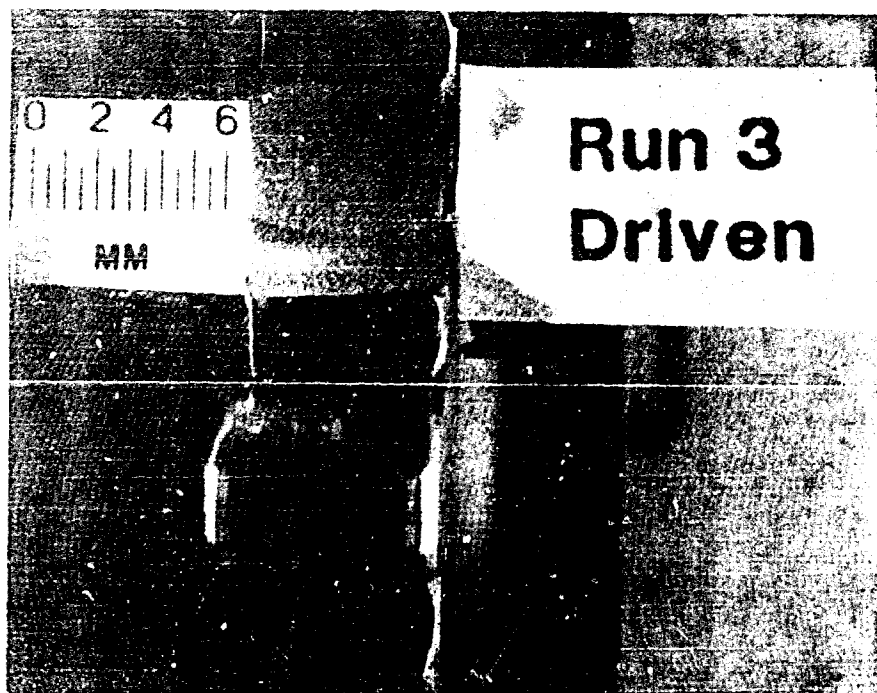
Figure 3.4 : Photograph of tooth fracture area on
driven gear in Run 3

DRIVER GEAR

Uniform Damage
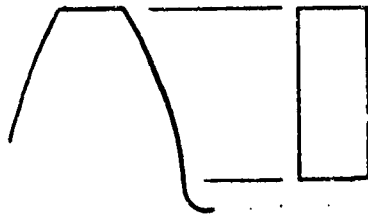
Tooth Specific Damage

KEY

HEAVY PIT
(Depth > .2 mm)

MODERATE PITTING BAND
(.1 mm < Depth < .2 mm)

LIGHT PITTING BAND
(Depth < .1 mm)

HEAVY WEAR

MODERATE WEAR

DRIVEN GEAR

Uniform Damage

**All Dimensions
In mm**

Tooth Specific Damage

.8

2.0

Figure 3.5 : Illustration of Tooth Damage Found on Gears in Run 8.
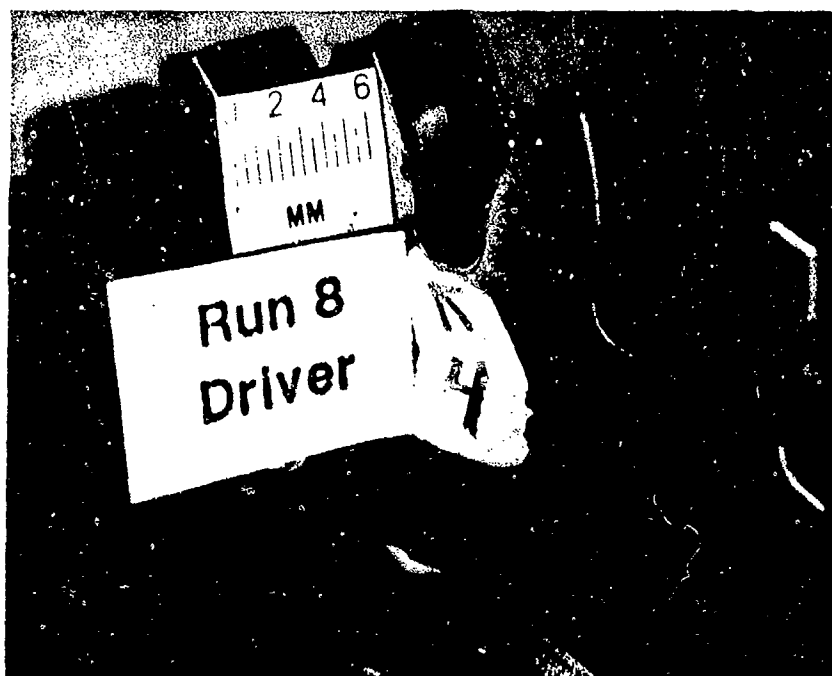
a) driver gear tooth

b) driven gear tooth

Figure 3.6 : Photographs of tooth damage found
on gears in Run 8

DRIVER GEAR

Uniform Damage
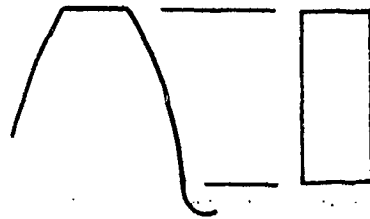
KEY

HEAVY PIT
(Depth > .2 mm)

MODERATE PITTING BAND
(.1 mm < Depth < .2 mm)

LIGHT PITTING BAND
(Depth < .1 mm)

HEAVY WEAR

MODERATE WEAR

Tooth Specific Damage

DRIVEN GEAR

Uniform Damage

All Dimensions
In mm

Tooth Specific Damage

2.2
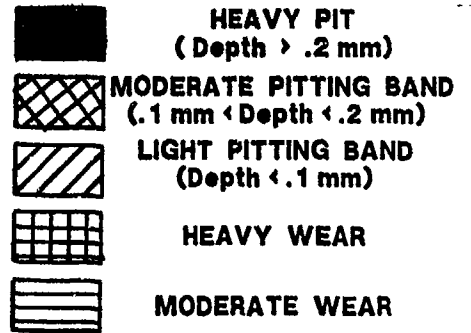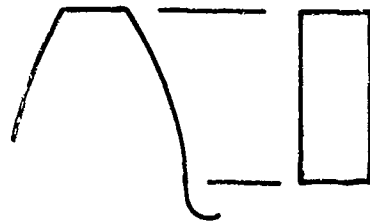
Figure 3.7 :   Illustration of Tooth Damage Found on Gears in Run 9.

a) driver gear tooth
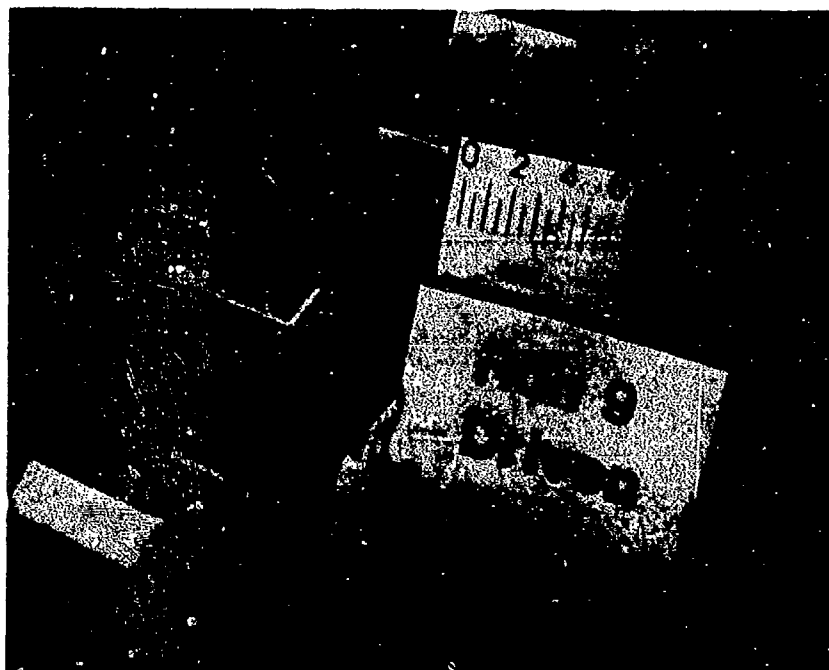
b) driven gear tooth
Figure 3.8 : Photographs of tooth damage found
on gears in Run 9

DRIVER GEAR

Uniform Damage

KEY

■	HEAVY PIT (Depth > .2 mm)
▨	MODERATE PITTING BAND (.1 mm < Depth < .2 mm)
▧	LIGHT PITTING BAND (Depth < .1 mm)
▦	HEAVY WEAR
▤	MODERATE WEAR

Tooth Specific Damage

8   9   11   12   13-15   16, 19-25

.5
2.5

DRIVEN GEAR

Uniform Damage

All Dimensions In mm

Tooth Specific Damage

9   10   11,12   13   14   16

.7   2.0

.7
1.5
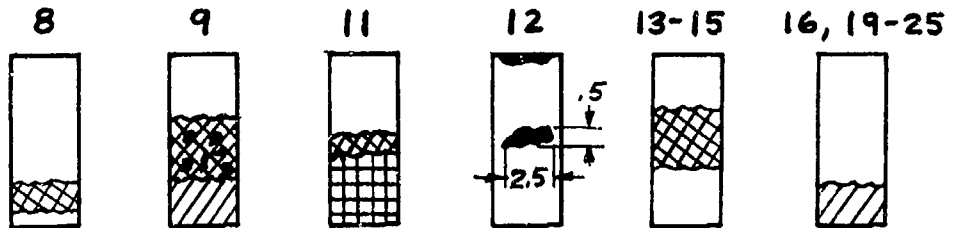
Figure 3.9 :   Illustration of Tooth Damage Found on Gears in Run 10.
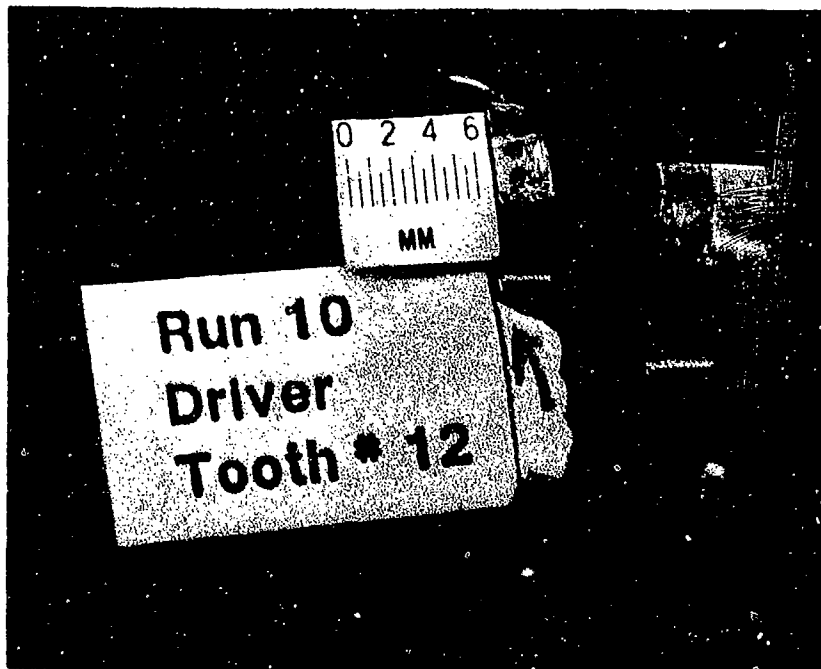
a) Tooth # 12, driver gear
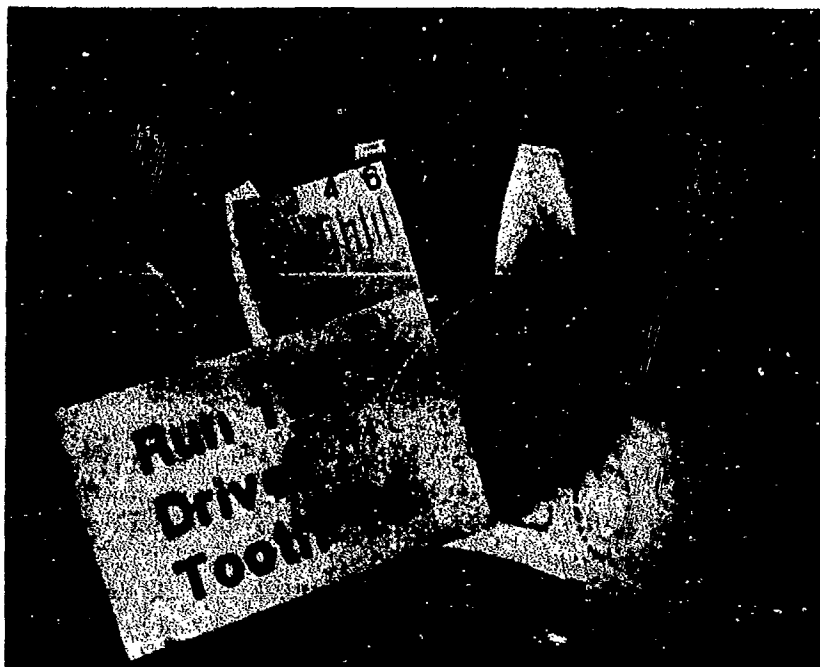
b) Tooth # 8, driver gear
Figure 3.10 : Photographs of tooth damage found
on gears in Run 10

c) Tooth # 13, driven gear

d) Tooth # 10, driven gear
Figure 3.10 : Concluded.

DRIVER GEAR

Uniform Damage

KEY

■	HEAVY PIT (Depth > .2 mm)
⊠	MODERATE PITTING BAND (.1 mm < Depth < .2 mm)
▨	LIGHT PITTING BAND (Depth < .1 mm)
▦	HEAVY WEAR
▤	MODERATE WEAR

Tooth Specific Damage

14   15   16   17,18   19,20   21-24

.8
.8

DRIVEN GEAR

Uniform Damage

**All Dimensions
In mm**

Tooth Specific Damage

2,3   4-6   7   8

#4 →
ONLY

.4 →
1.8
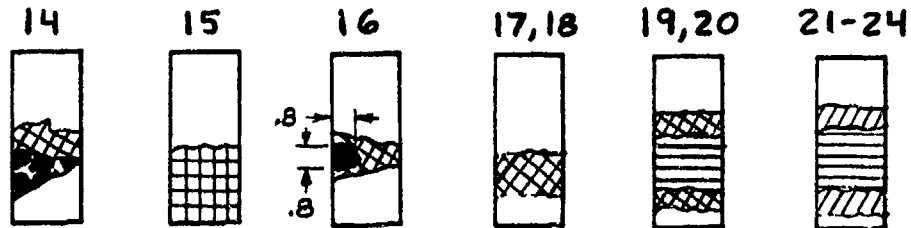
Figure 3.11:   Illustration of Tooth Damage Found on Gears in Run 11.

a) Tooth # 14, driver gear

b) Tooth # 16, driver gear
Figure 3.12 : Photographs of tooth damage found
on gears in Run 11

c) Tooth # 8, driven gear
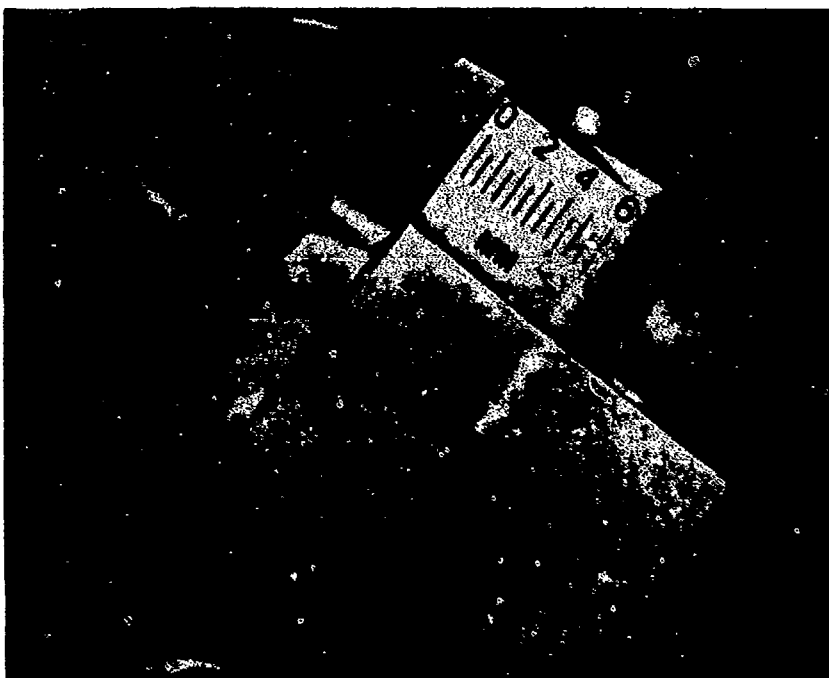
d) Tooth # 4, driven gear
Figure 3.12 : Concluded.
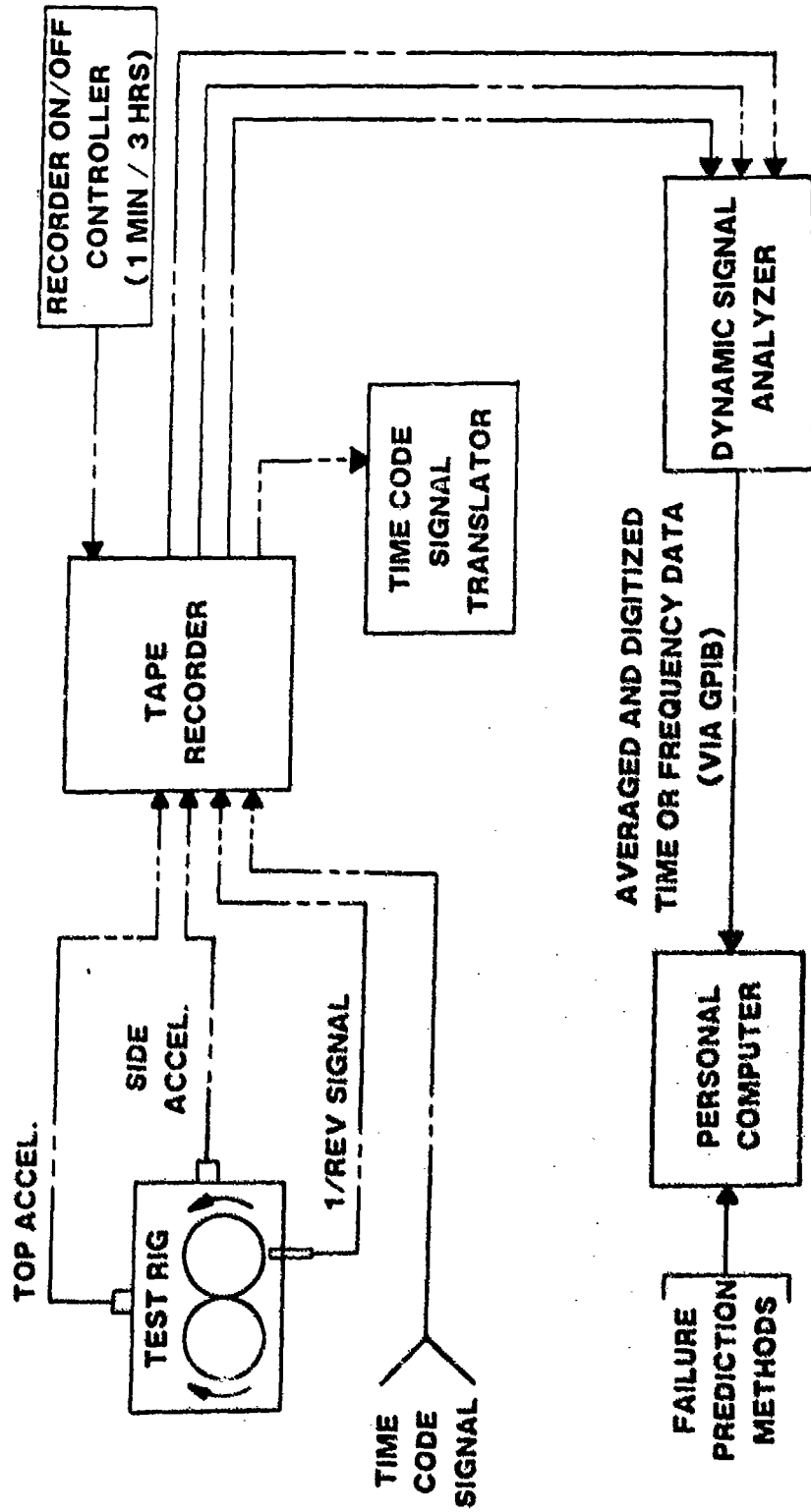
Figure 3.13: Illustration of Test Set-up.

37
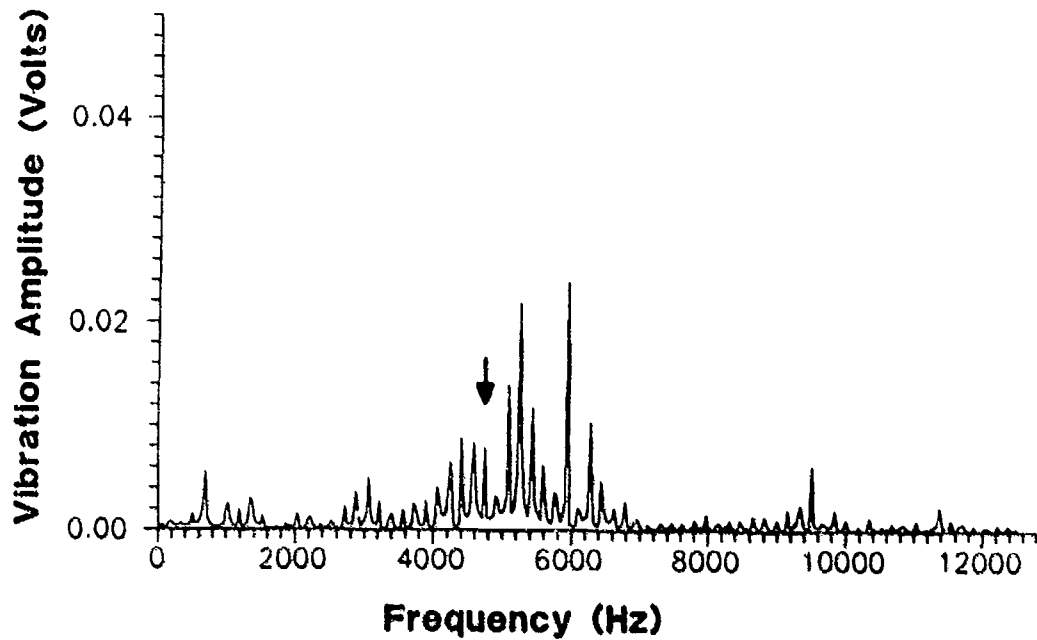
Figure 3.14 : Frequency Spectrum of Run 7 at Start of Run.
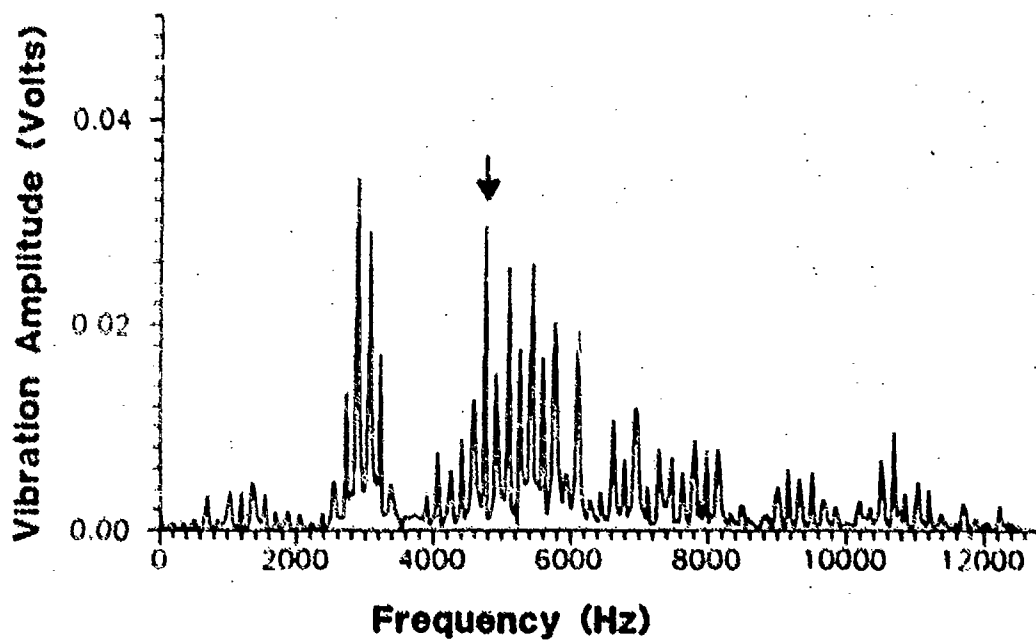
Figure 3.15 : Frequency Spectrum of Run 7 After 32 Hours of Running.
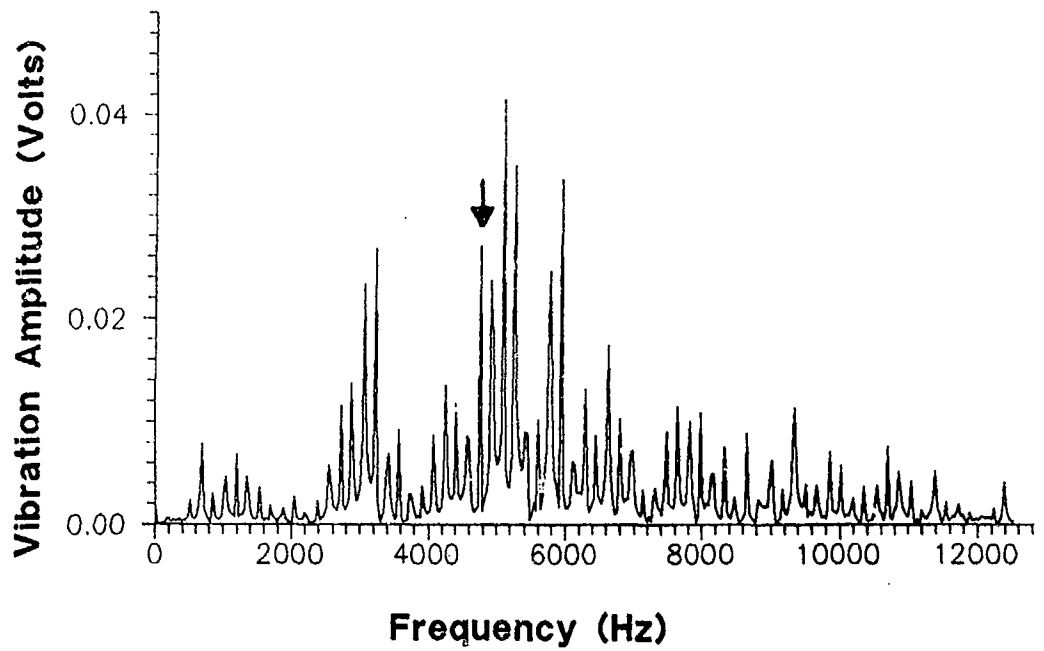
Figure 3.16 :   Frequency Spectrum of Run 7 After 44 Hours of Running.
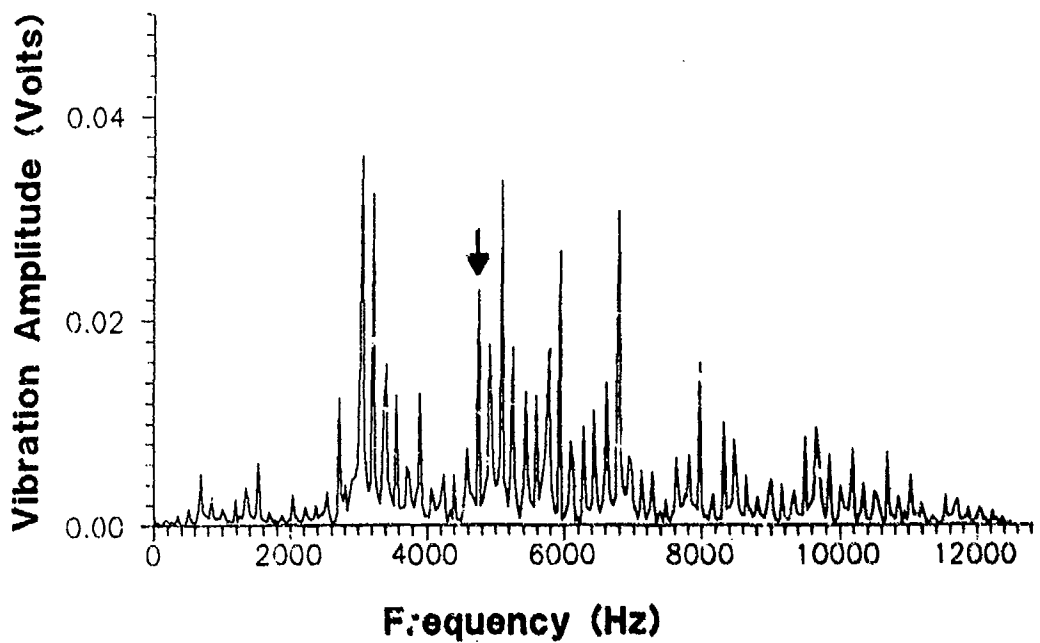
Figure 3.17 :   Frequency Spectrum of Run 7 After 50 Hours of Running.

Test	Modal Hammer Location	Accelerometer Location
Test 1	B	A
Test 2	C	A
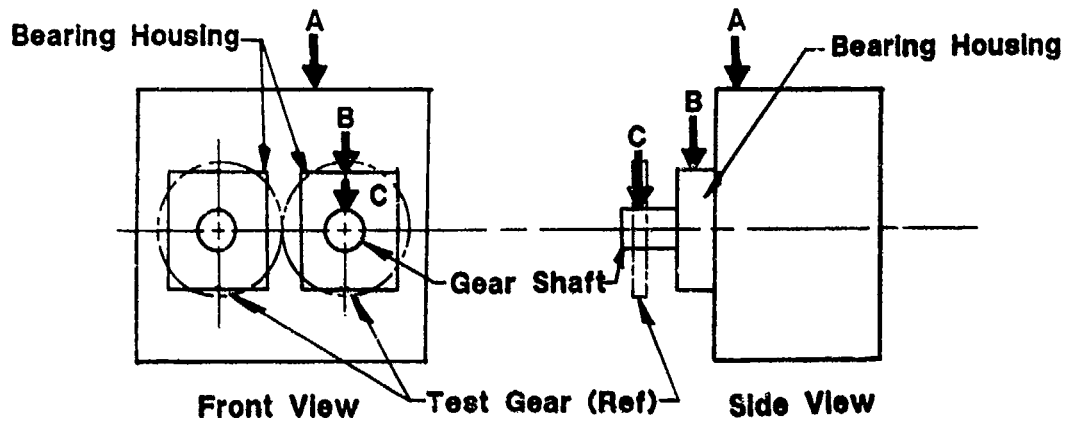
Figure 3.18 : Illustration of Frequency Response Measurement
Locations.
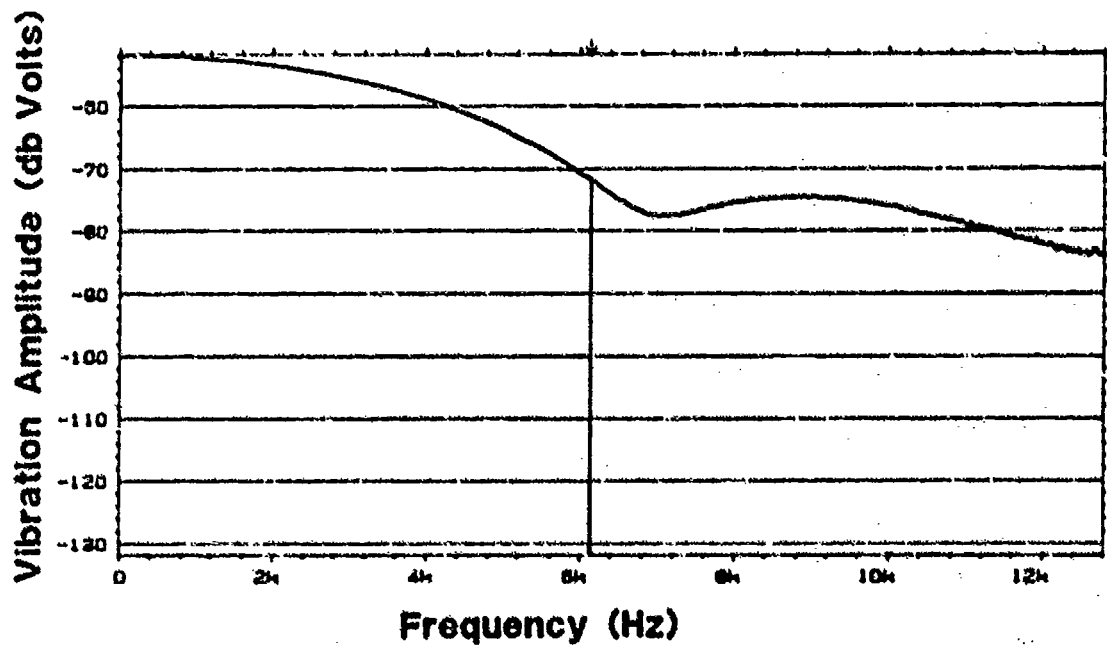
Figure 3.19 : Power Spectrum of Input to Frequency Response
Measurements.

40
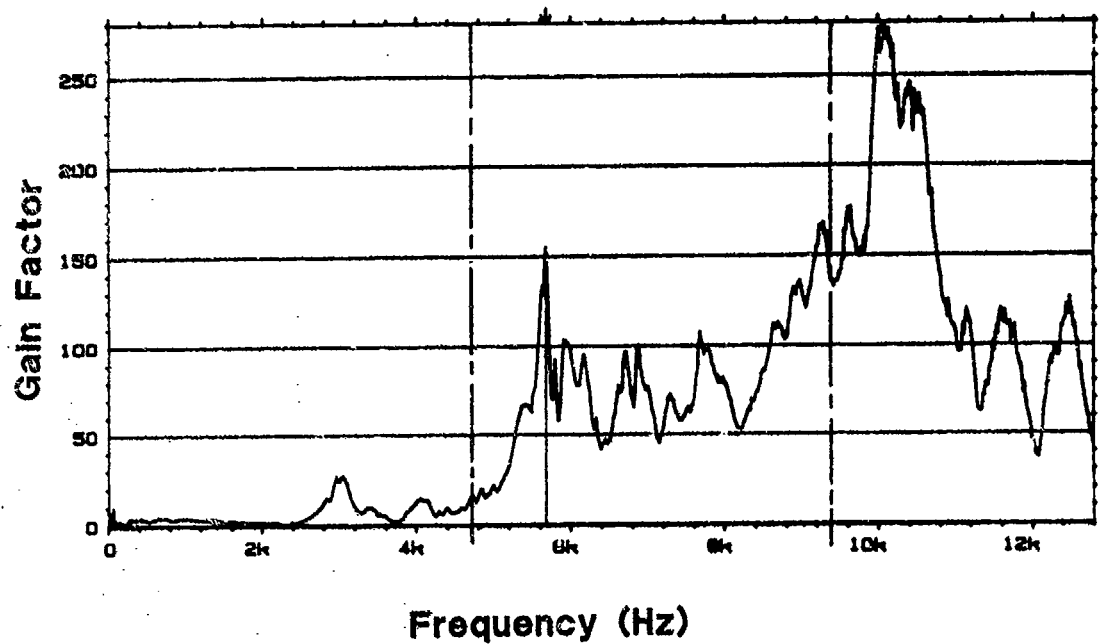
Figure 3.20 : Magnitude of Frequency Response Function, Test 1,
Between the Top Accelerometer Location and the Top of
the Bearing Housing.
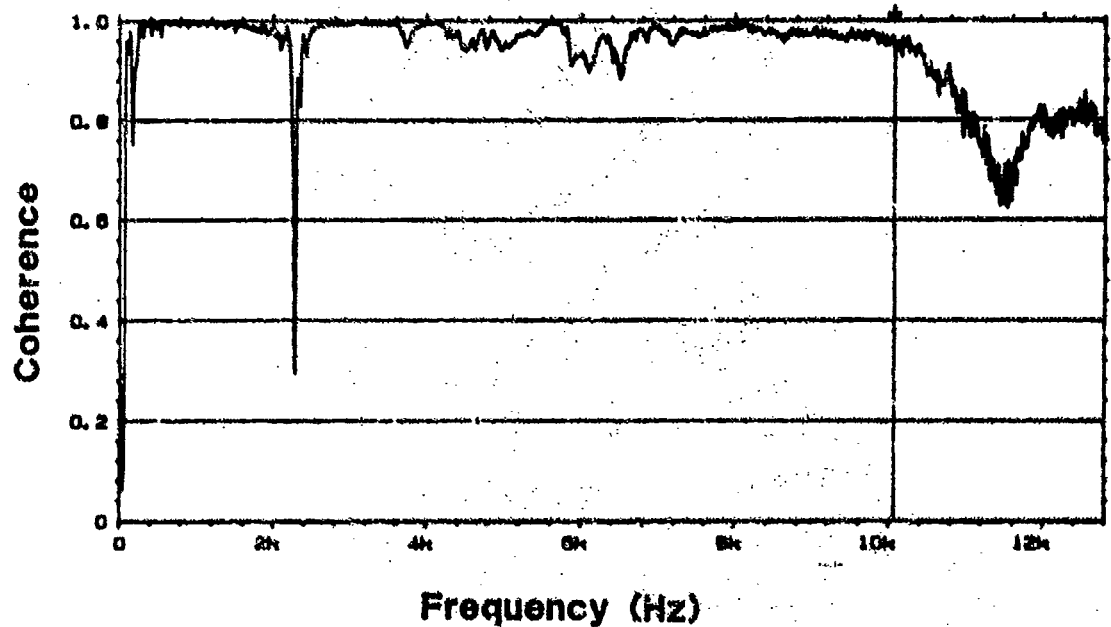
Figure 3.21 : Coherence Function of Test 1 Measurements, Between the
Top Accelerometer Location and the Top of the Bearing
Housing.
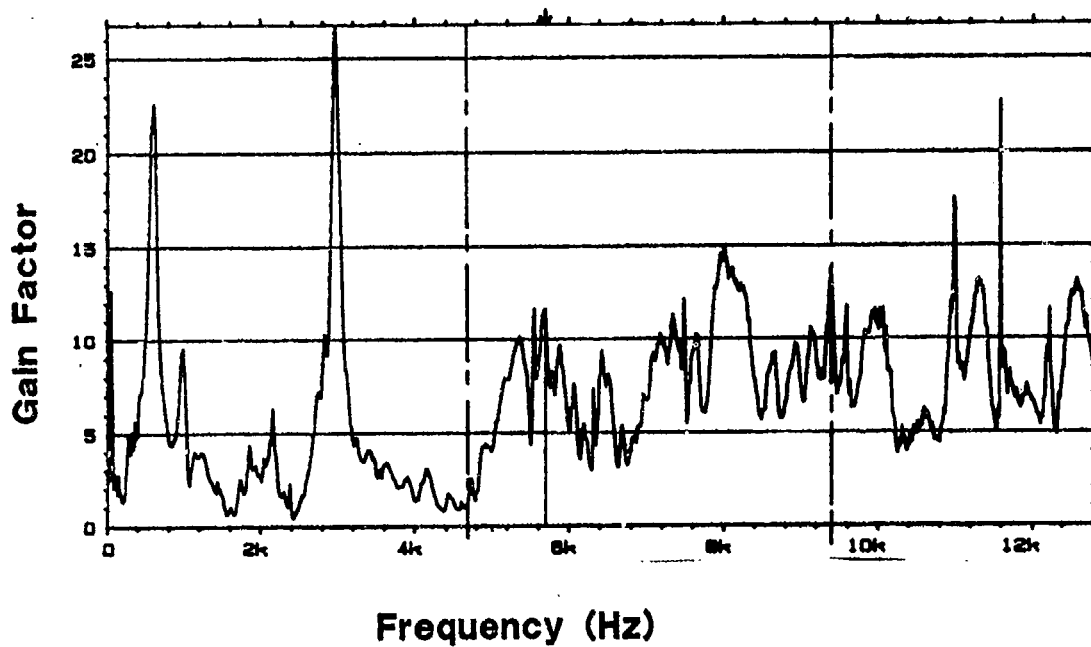
Frequency (Hz)

Figure 3.22 : Magnitude of Frequency Response Function, Test 2,
Between the Top Accelerometer Location and the Top of
the Gear Shaft.

Frequency (Hz)
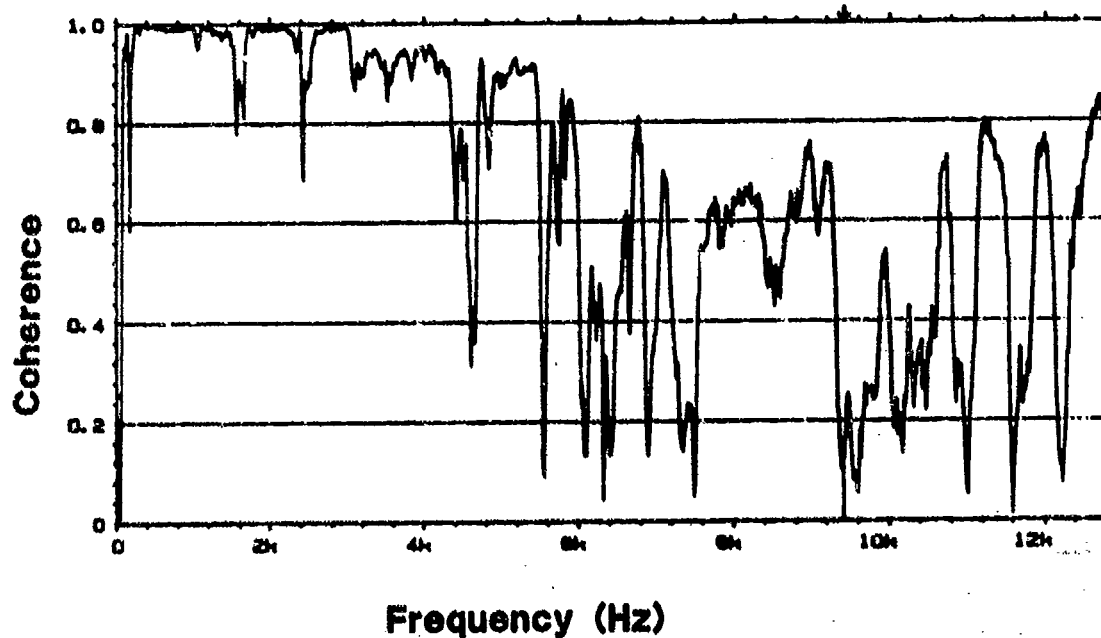
Figure 3.23 : Coherence Function of Test 2 Measurements, Between the
Top Accelerometer Location and the Top of the Gear
Shaft.

CHAPTER IV
APPLICATION AND RESULTS

The main portion of this study was the application of the various gear fault methods to experimental data. Chapter 4 briefly explains the various computer programs developed that apply each of the techniques. Also, this chapter presents and discusses the results of these techniques.

4.0 PROGRAMS DEVELOPED

To apply the various predictive techniques to the experimental data, several computer programs were developed. The programs are written in FORTRAN, and listed in the appendices. For those methods requiring Fourier analysis, the standard FFT algorithm developed by Cooley and Tukey [12] is included in each routine. The computer programs use the data files created using the dynamic signal analyzer. The results of the programs are stored in data files that can be plotted using commercially available routines.

The programs use the various equations and theories presented in Chapter II. Program EFMO.FOR, listed in Appendix A, calculates the FMO parameter for each time data point in the run. Program TFM4.FOR, listed in Appendix B, applies the FM4 techniques to the data by calculating the normalized kurtosis and standard deviation values of the difference file for each time data point. Program HILB.FOR, listed in Appendix C, uses the Hilbert transform technique to calculate the instantaneous phase variations as a function of shaft position for each time data point. Program PARAM.FOR, listed in Appendix D, calculates the crest factor, sideband level factor, and energy ratio for each time data point.

The computer programs were verified by inputting known functions. As an example of this, the kurtosis and standard deviation routines in program TFM4.FOR were verified by inputting a sine wave and square wave, and comparing the results with exact solutions. Table II illustrates the results of this verification test. The square wave did not provide as high a correlation as the sine wave, mainly because the input square wave contained some irregularities.

TABLE II: Program TFM4.FOR routines verification

Routine - Input	Measured value	Actual Value	% Difference
Standard Deviation			
- Sine wave	1.3472	1.3435	0.28 %
- Square Wave	1.9180	1.9000	0.95 %
Normalized Kurtosis			
- Sine Wave	1.4896	1.5000	0.69 %
- Square Wave	1.0404	1.0000	4.04 %

4.1 RESULTS

FMO METHOD

The FMO method did very well at detecting a majority of the heavy wear and scoring damage experienced by runs 1, 2, and 4 through 6, as it was designed to do. Figures 4.1 through 4.5 plot the three parameters: a) FMO, b) Peak-to-peak level (the FMO numerator), and c) Sum of mesh amplitudes (the FMO denominator), for these runs. As seen in these figures, all of the runs, except run 1, exhibit an increase in the FMO parameter, plot a, with increasing run time. These same runs also show a decrease in the primary meshing frequency and second harmonic amplitude sum, plot c, with increasing run time. It is interesting to note that in Figure 4.3, run 4, the FMO plot indicates heavy damage at 49 hours into the test, due to a decrease in meshing frequency amplitudes, whereas the peak-to-peak level, plot b, starts increasing at 55 hours and peaks at 64 hours. Run 1 did not provide good FMO trends even though the gear experienced similar damage.

FMO is designed to detect major tooth faults such as the breakage experienced during runs 3 and 7. Because no data was collected at the time of breakage, or immediately after it occurred, FMO was unable to be applied to these runs.

FMO was applied to runs 8 and 9, which experienced single tooth pits, even though FMO is not designed to detect single tooth faults. As seen in Figure 4.6, run 8 shows a gradual overall increase in FMO values with run time, and a gradual overall decrease in meshing frequency amplitudes. This trend in run 8 could be attributed to its long run time of 520 hours, which may have resulted in uniform wear not observable by visual inspection. Run 9 showed no logical trend with FMO.

FMO was also applied to runs 10 and 11, where the gears experienced distributed pitting damage. As seen in Figures 4.7 and 4.8, the FMO values for both runs increase near the end of the run time. The meshing frequency amplitudes show an overall decrease with increasing run time, indicating the existence of heavy wear. Since FMO does not respond to specific tooth damage, it is reasonable to assume that the pitting occurred over enough teeth to act as a uniform wear phenomenon, and thus was capable of being detected by FMO. It is interesting to note that for run 10, Figure 4.7, the FMO value increased sharply at the 220 hours point. At this same point in time, the meshing frequencies amplitude sum decreased sharply, possibly indicating the time when most of the major distributed pitting happened. The peak-to-peak level at this period contained no major fluctuation, only a gradual increase in level.

FM4 METHOD

The normalized kurtosis parameter was unable to detect the single tooth faults found in the test gears. Runs 8 and 9 experienced specific faults in the form of one large and one small pit. As seen in Figures 4.9 and 4.10, these defects had limited effect on the kurtosis parameter. The fatigue cracks that resulted in broken teeth in runs 3 and 7 were also undetected by the kurtosis parameter, as seen in Figure 4.11 for run 7. The normalized kurtosis values for the two data points of run 3, not plotted, were 2.98 and 3.04. It should be noted that the data points collected at the end of runs 3 and 7 were taken 3 and 2 1/2 hours, respectively, prior to the point of tooth fracture. Only run 11 had limited success using the normalized kurtosis parameter. As seen in Figure 4.12, a normalized kurtosis value of 5.3 was registered at 88 hours of operation; however, the value decreased to approximately 3.0 at 96 hours. One explanation for this trend is that only one large pit was

present at the 88 hour mark. As more pits formed, the number of peaks increased causing the normalized kurtosis value to decrease.

The standard deviation parameter, although used in FM4 for single tooth failure detection, proved to be a good indicator of heavy wear. Runs 1, 2 and 4 through 6 all experienced heavy wear and scoring. The standard deviation plots for these runs, given in Figures 4.13 through 4.17, all show clear trends of increasing values near the end of each run with only minor fluctuations. The standard deviation plot of run 1, Figure 4.13, indicates a definite trend as compared to the FM0 plot of run 1, which did not respond to the heavy wear.

Plots of the squared difference signal of FM4 provided some general information on the wear condition of the tooth surfaces. The plots of the squared difference signal are presented as a function of gear rotation. Two plots are given in each figure. The top graph (a) represents the data collected at the beginning of the run and the bottom graph (b) represents the data collected at the end of the run. The runs that experienced heavy wear and scoring show definite increases in the difference signal between the start and end plots throughout the gear rotation. An example of this is given in Figure 4.18. The specific pits of runs 8 and 9 were not seen in their squared difference signal plots. The wear pattern on the driver gear in run 10 is reflected in the squared difference signal given in Figure 4.19. Run 11 experienced similar wear as run 10; however, the wear pattern was not easily detected in its squared difference signal plot.

HILBERT TRANSFORM METHOD

The Hilbert transform method was primarily developed to detect fatigue cracks using the phase modulation function described in Section 2.1. Runs 3 and 7 are the only runs that experienced tooth fracture due to probable fatigue cracks. Figure 4.20 plots the phase modulation function for the two data time intervals of run 3. Several phase shifts can be seen in the first plot, 2 hours into the run; however, they are not reflected in the second plot representing the last data point. Nothing in the last data point plot indicates the presence of a fatigue crack, i.e. no large phase lags present. Figure 4.21 plots the phase modulation function for the last two data time intervals of run 7. The only possible indication of a fatigue crack starting is the phase lag at approximately half way into the shaft rotation, near the 180 degrees point. The phase lag starts during the second to last time interval, 47 hours into the run, and grows to the size seen in the last interval, 50 hours into the run. More data after this last data point is required to claim with any certainty that this phase lag represents an actual fatigue crack. Again it must be noted that the last data points for runs 3 and 7 were taken 3 and 2 1/2 hours, respectively, before tooth fracture.

CREST FACTOR AND SIDEBAND LEVEL FACTOR

Both the crest factor and sideband level factor are designed to respond to signals with impulsive vibration sources, specifically tooth breakage. Runs 3 and 7 were the only runs that experienced tooth fracture. The crest factor and sideband level factor for run 7 are plotted in Figure 4.22. Run 3 was not plotted, since it had only two time intervals recorded before fracture occurred. As seen in Figure 4.22, neither the crest factor (plot a) or the sideband level factor (plot b) display any indication that a tooth fracture was going to occur. These parameters may be sensitive to tooth breakage only after it has happened. Unfortunately, no data was collected during or after the fracture occurred.

ENERGY RATIO

The energy ratio is designed to be a robust indicator of heavy wear. Runs 1, 2, and 4 through 6 experienced heavy wear and scoring. The energy ratio graphs of these runs are given in Figures 4.23 through 4.27. As seen in these figures, the energy ratio does not provide as good an indication of wear as the FMO and the standard deviation methods. The energy ratio graphs for runs 10 and 11 are given in Figure 4.28 and 4.29, respectively. Of these two runs, only run 10 had an increase in its' energy ratio parameter.
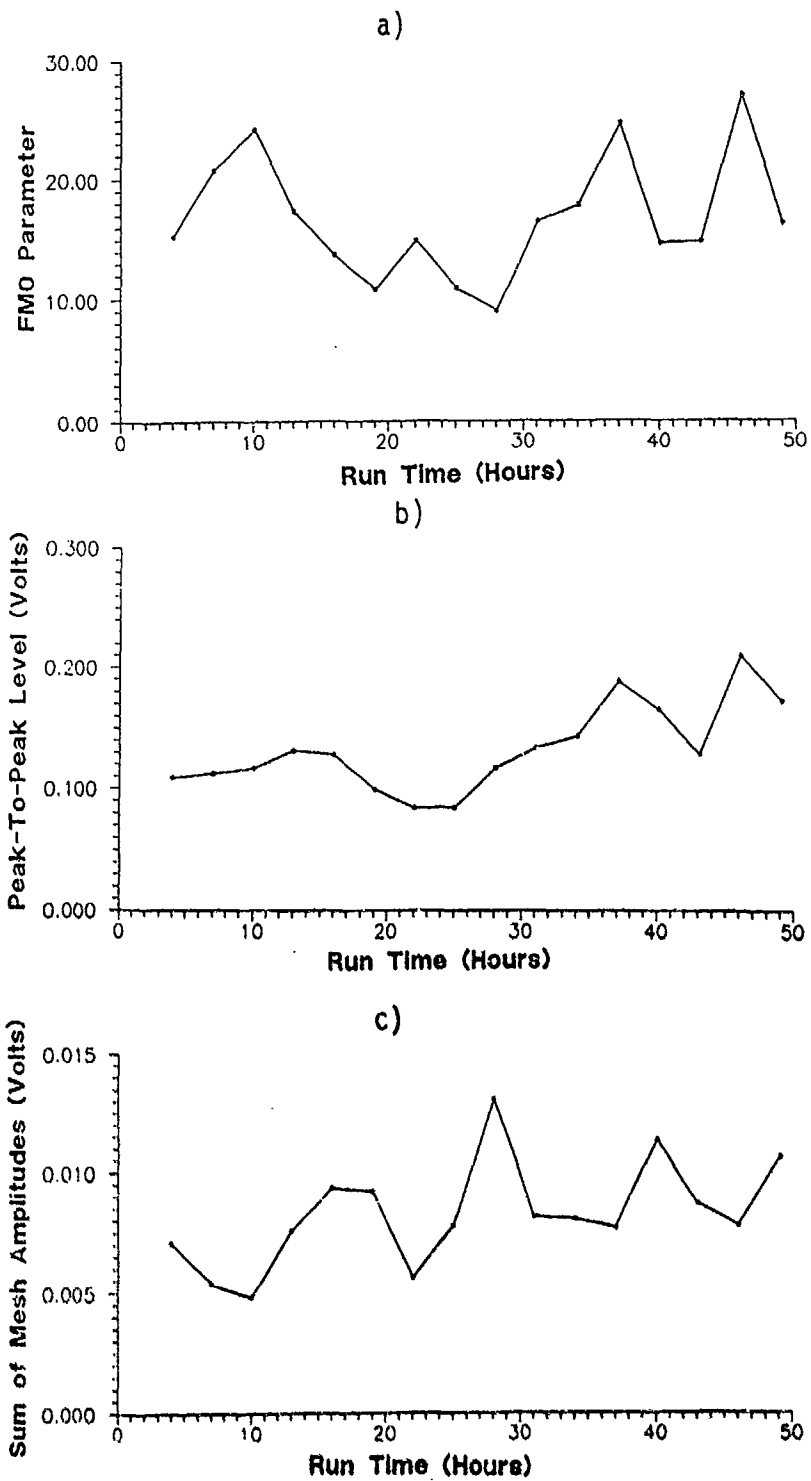
Figure 4.1 : Plot of FMO Parameters for Run 1.
a) FMO Parameter.
b) Numerator of FMO.
c) Denominator of FMO.
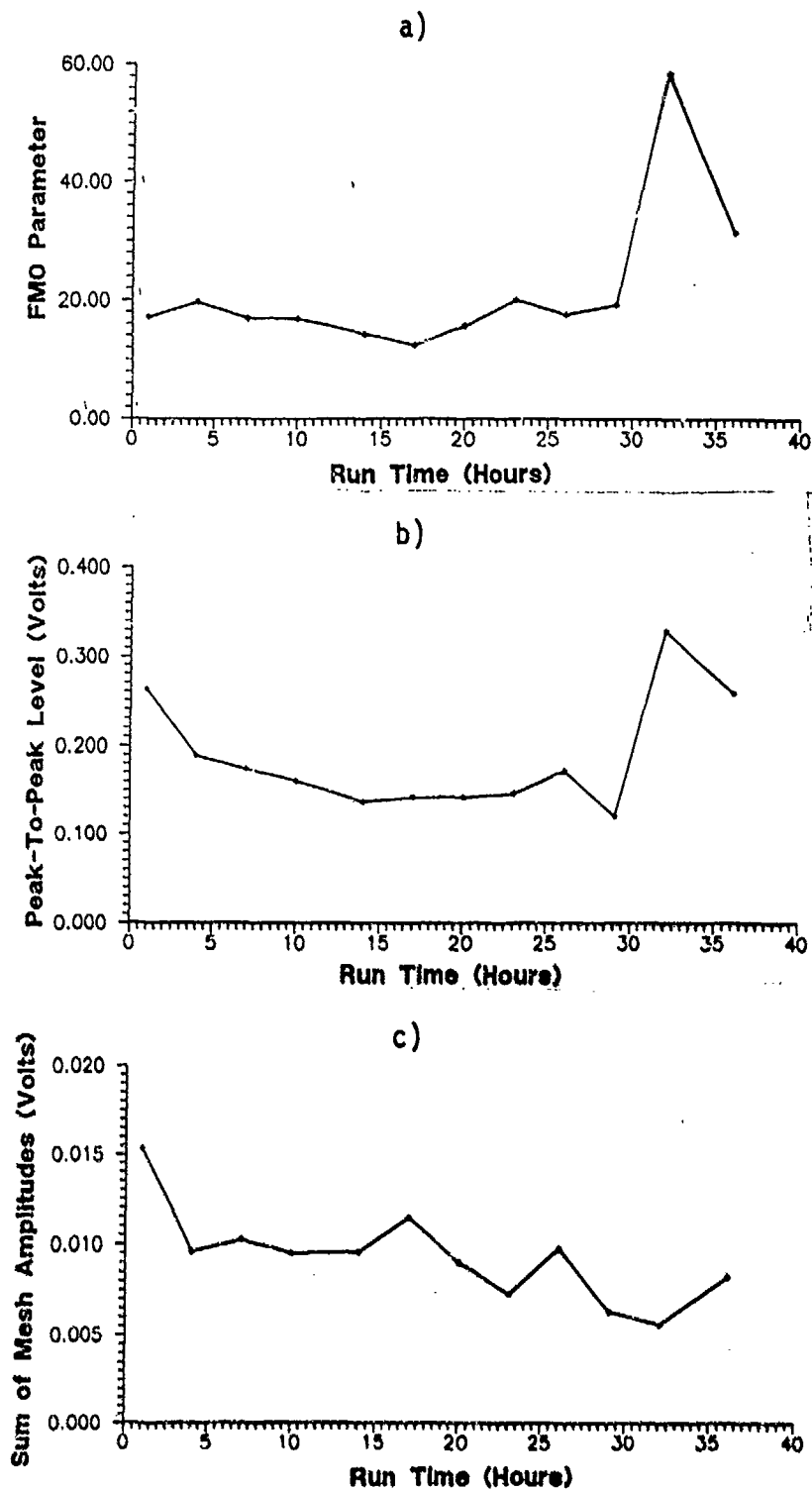
Figure 4.2 :   Plot of FMO Parameters for Run 2.
          a) FMO Parameter.
          b) Numerator of FMO.
          c) Denominator of FMO.

48
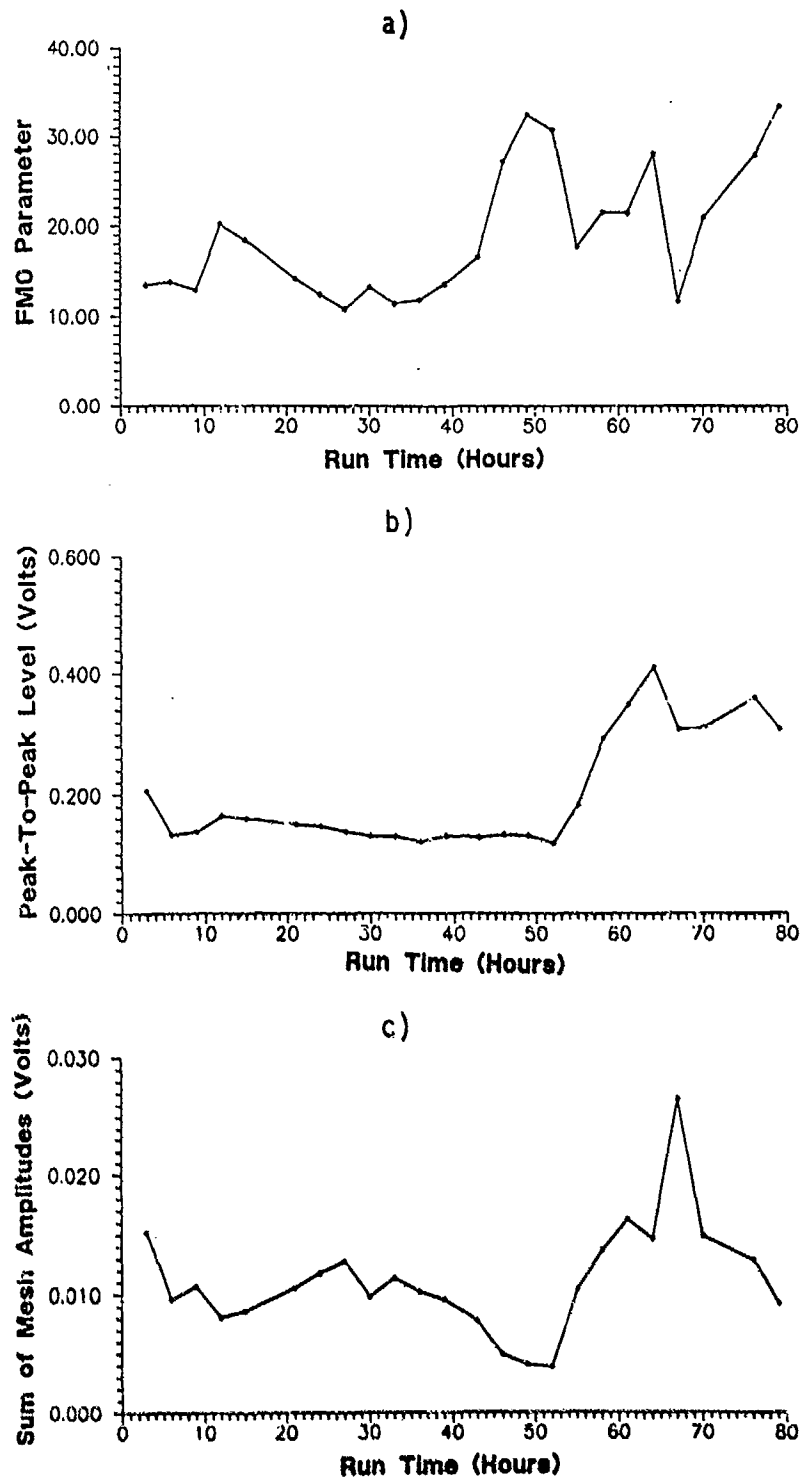
Figure 4.3 : Plot of FMO Parameters for Run 4.
          a) FMO Parameter.
          b) Numerator of FMO.
          c) Denominator of FMO.

49

a)

b)

c)
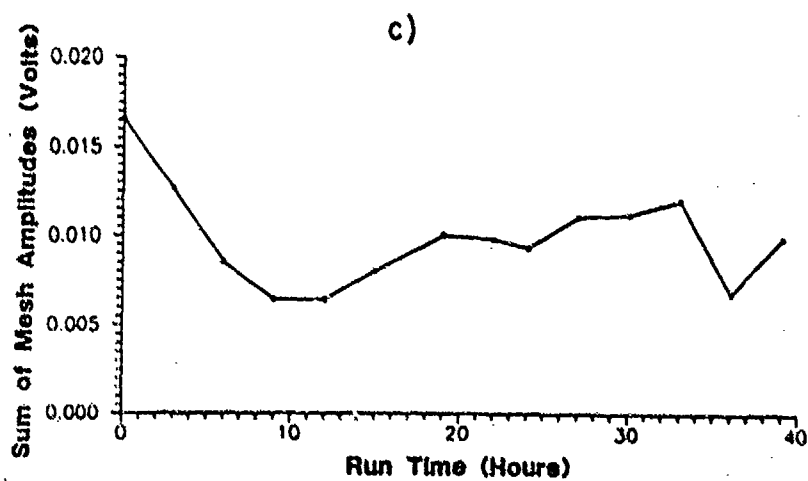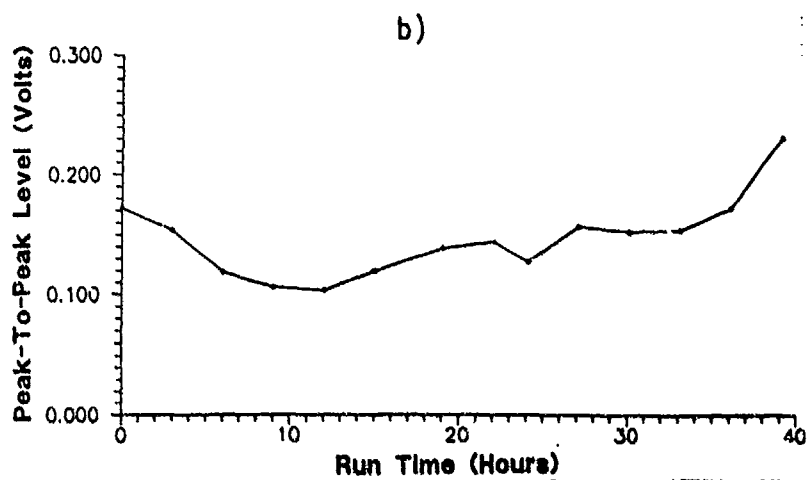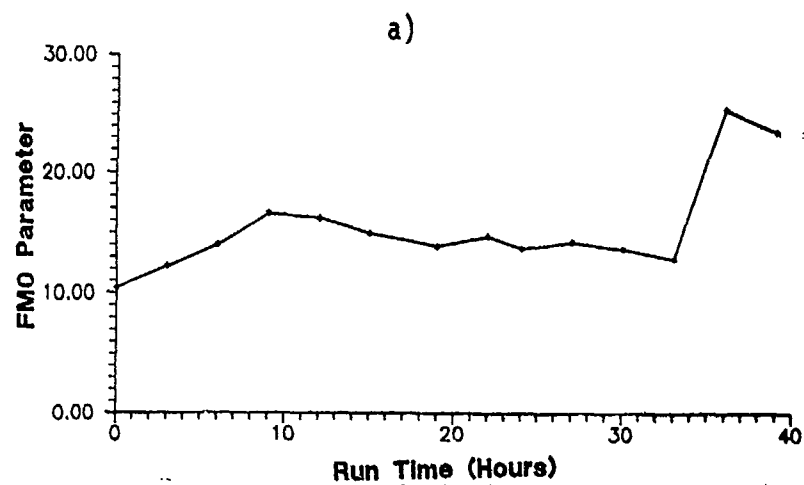
Figure 4.4 :   Plot of FMO Parameters for Run 5.
a) FMO Parameter.
b) Numerator of FMO.
c) Denominator of FMO.
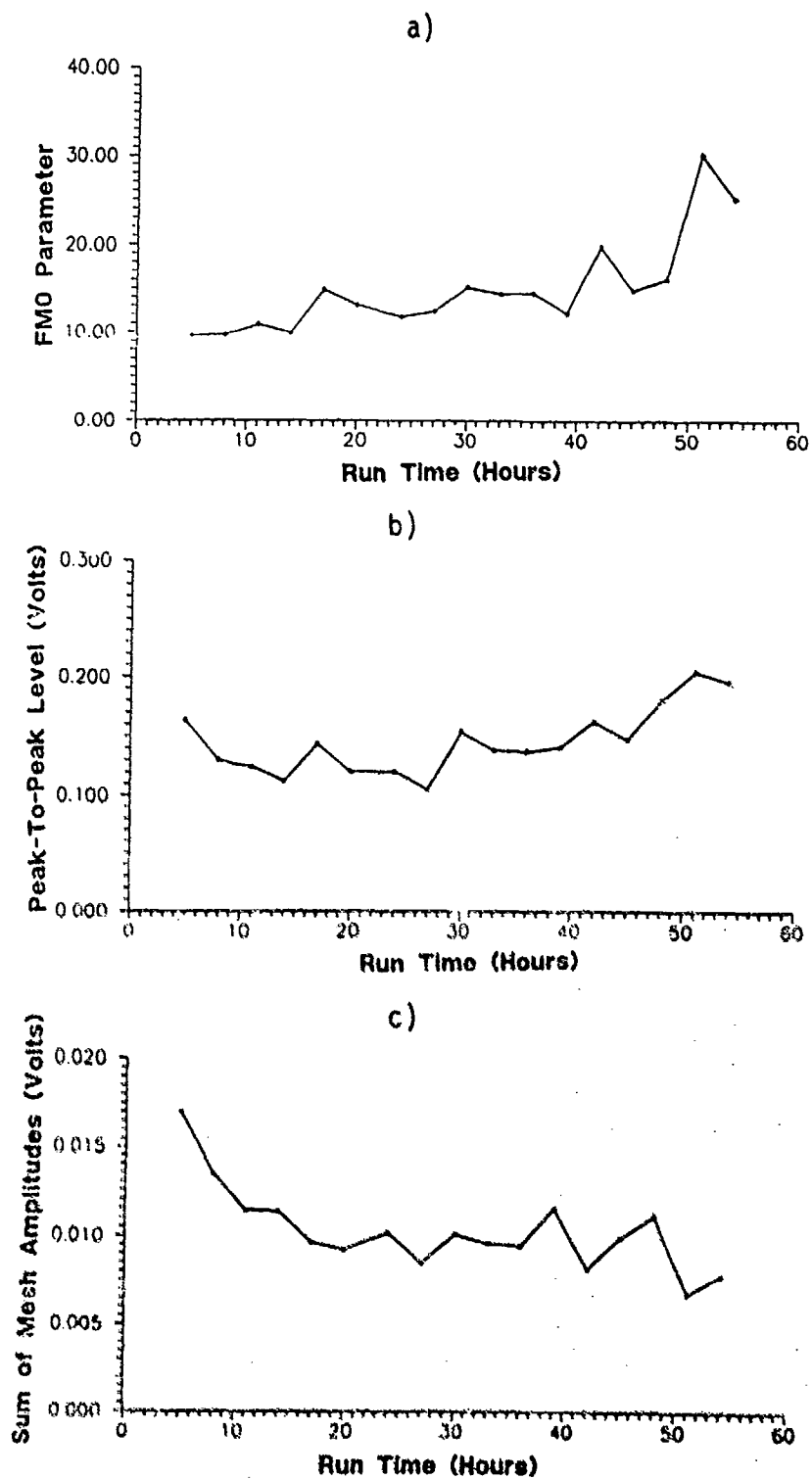
Figure 4.5 :   Plot of FMO Parameters for Run 6.
            a) FMO Parameter.
            b) Numerator of FMO.
            c) Denominator of FMO.
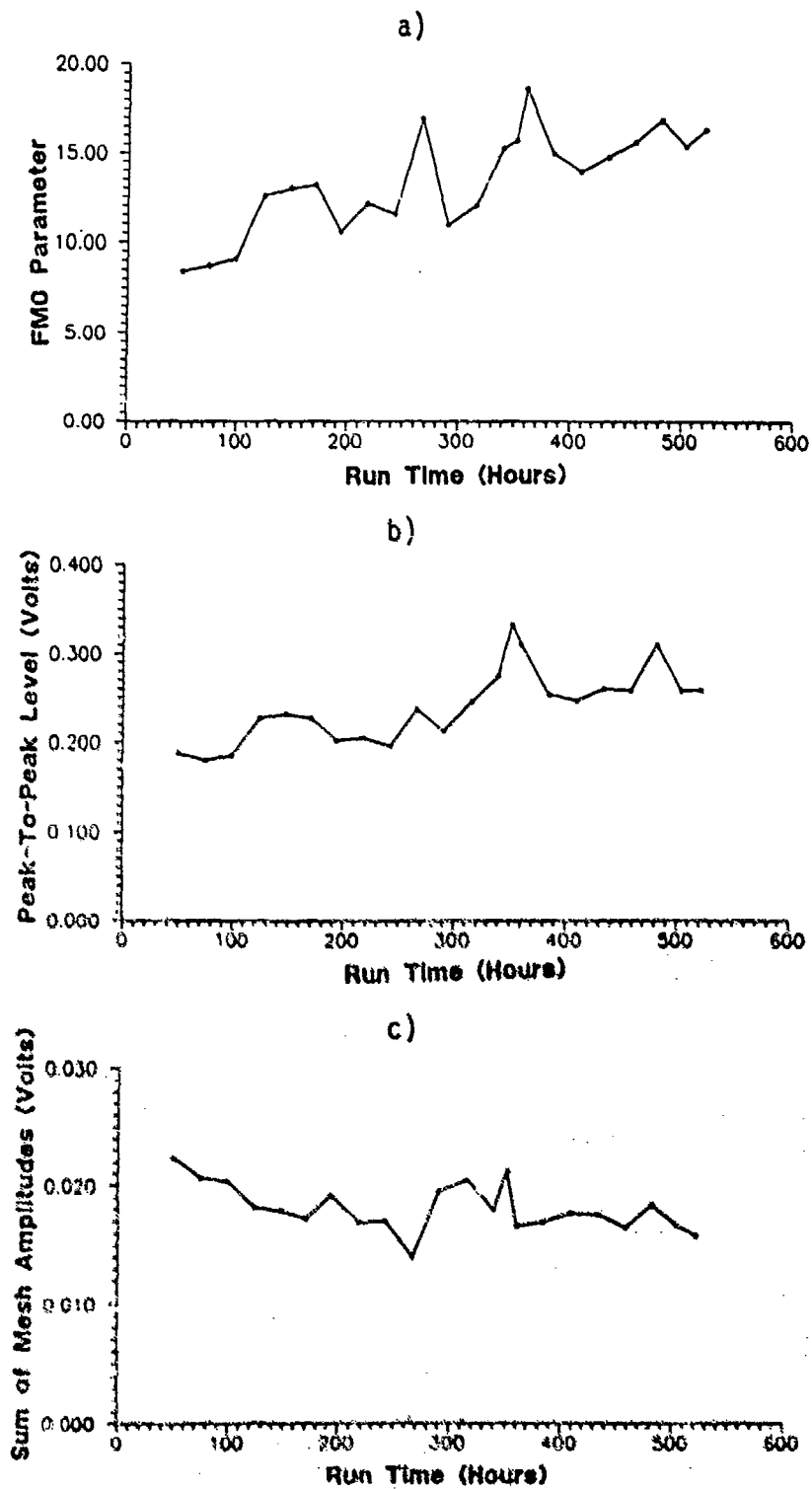
Figure 4.6 : Plot of FMO Parameters for Run 8.
a) FMO Parameter.
b) Numerator of FMO.
c) Denominator of FMO.

52

a)

b)

c)
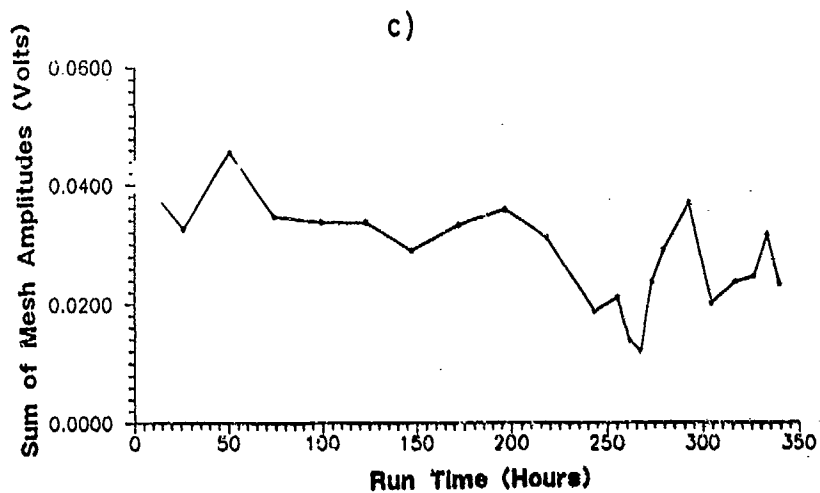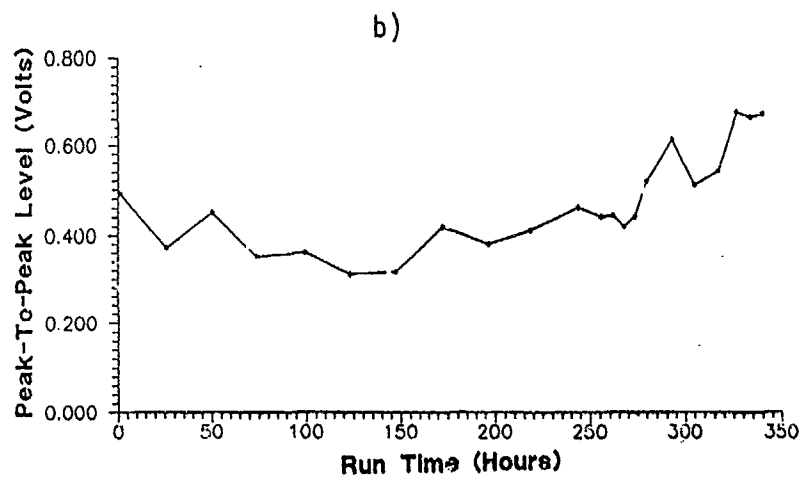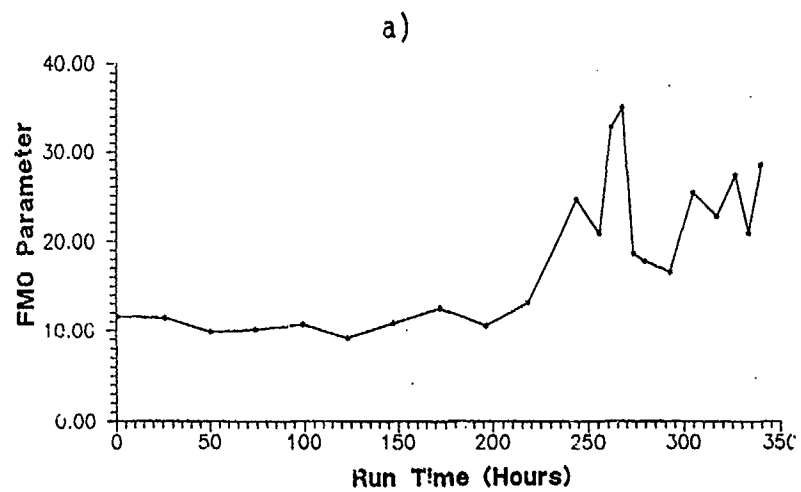
Figure 4.7 : Plot of FMO Parameters for Run 10.
a) FMO Parameter.
b) Numerator of FMO.
c) Denominator of FMO.
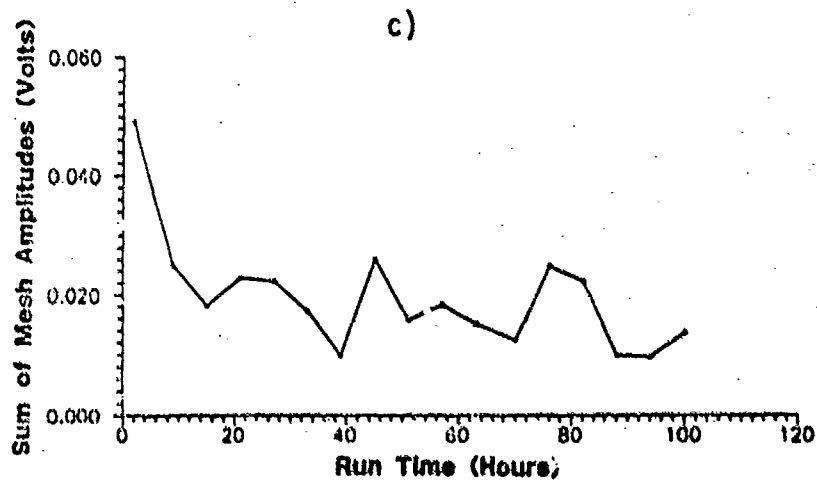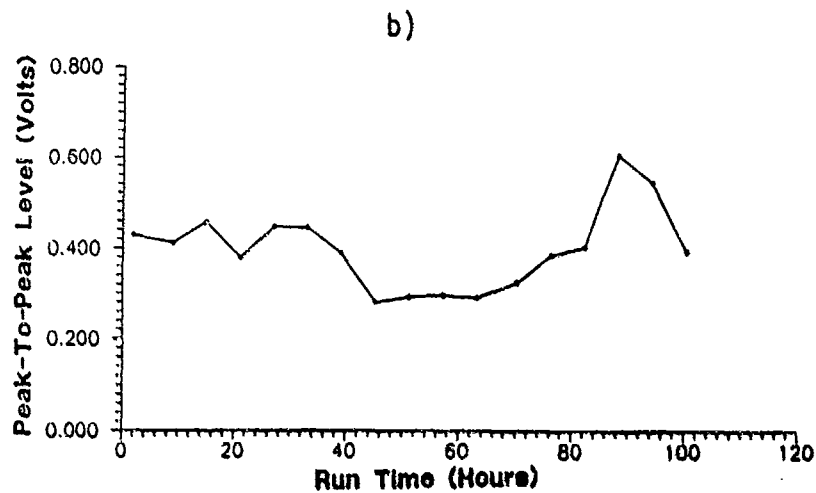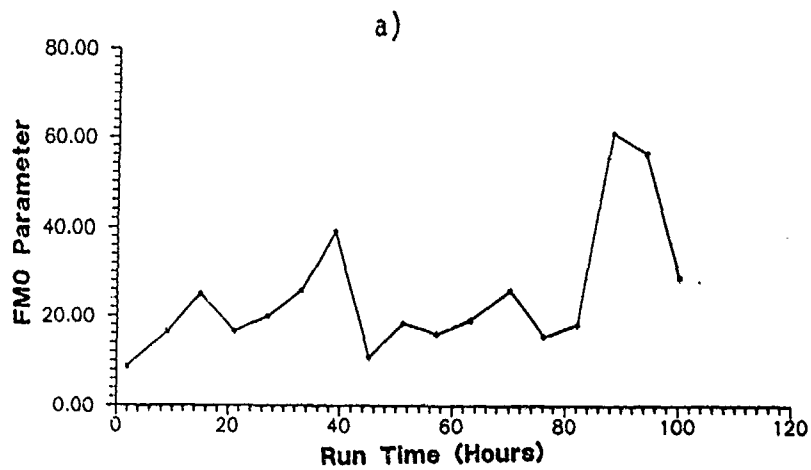
Figure 4.8 : Plot of FMO Parameters for Run 11.
a) FMO Parameter.
b) Numerator of FMO.
c) Denominator of FMO.

54
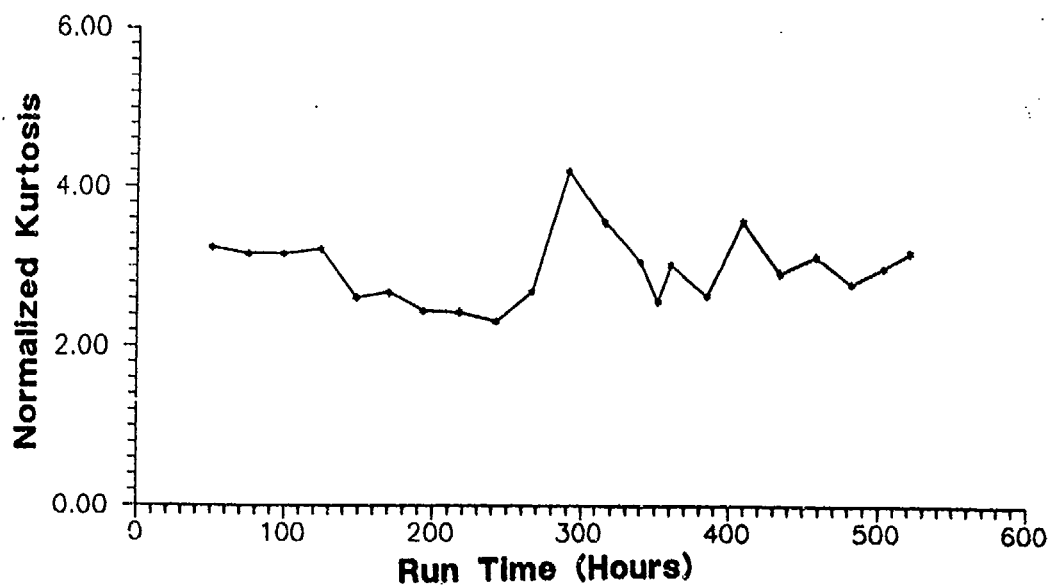
Figure 4.9 :   Plot of Normalized Kurtosis (FM4) for Run 8.
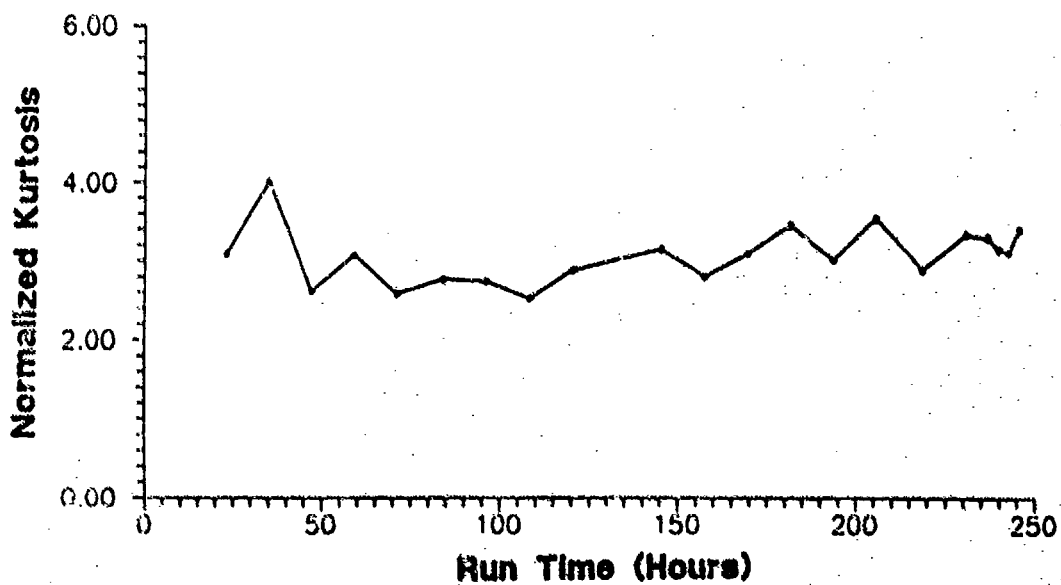
Figure 4.10 :   Plot of Normalized Kurtosis (FM4) for Run 9.
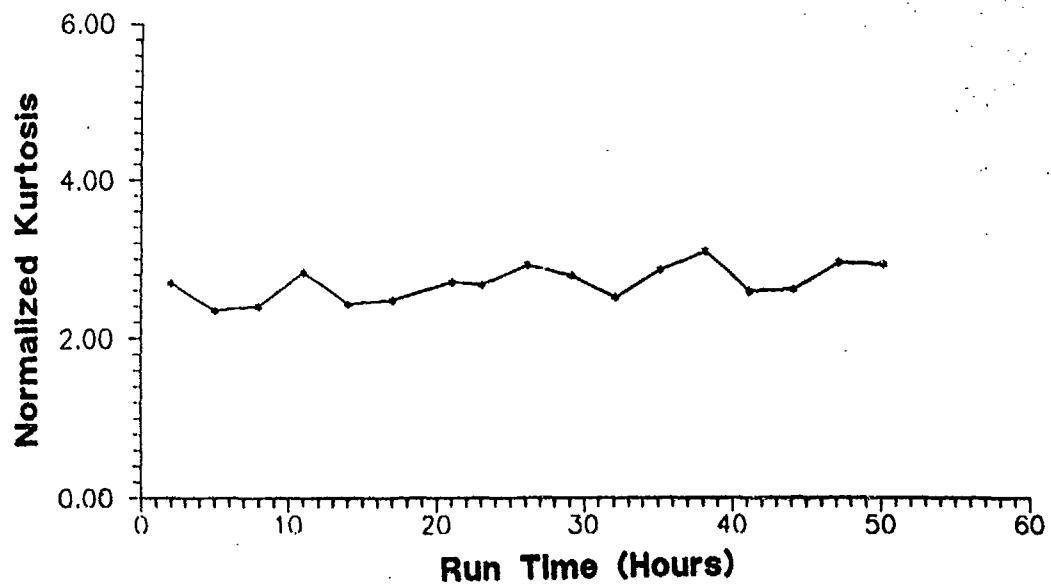
Figure 4.11 : Plot of Normalized Kurtosis (FM4) for Run 7.
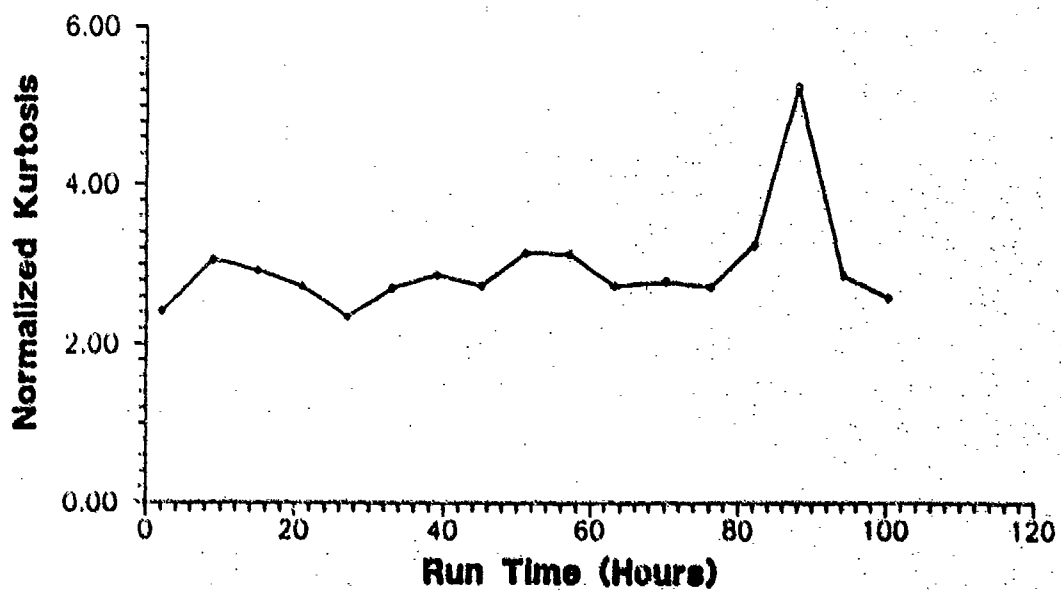
Figure 4.12 : Plot of Normalized Kurtosis (FM4) for Run 11.
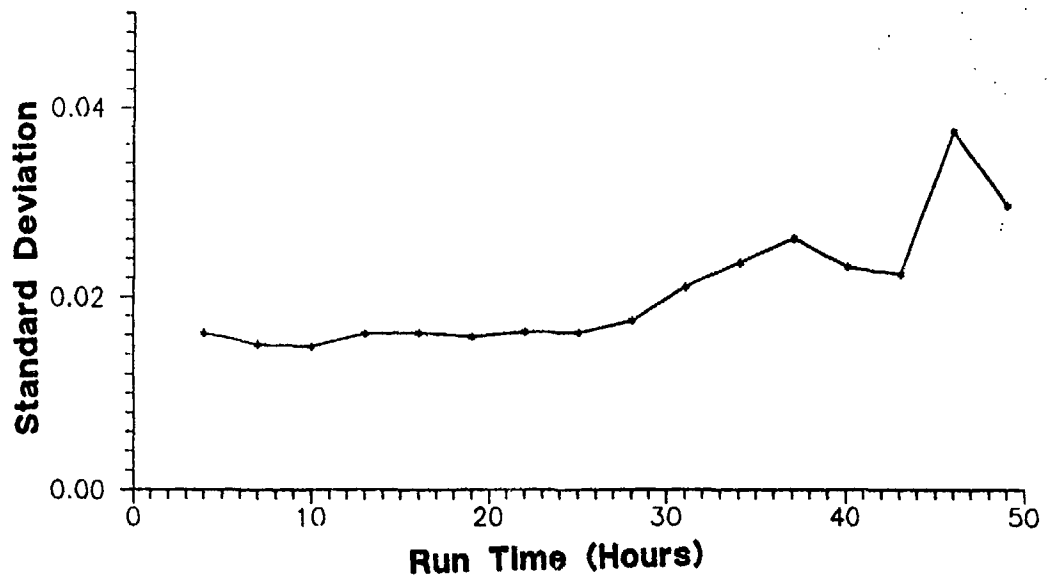
Figure 4.13 :   Plot of Standard Deviation of Difference Signal (FM4) for Run 1.
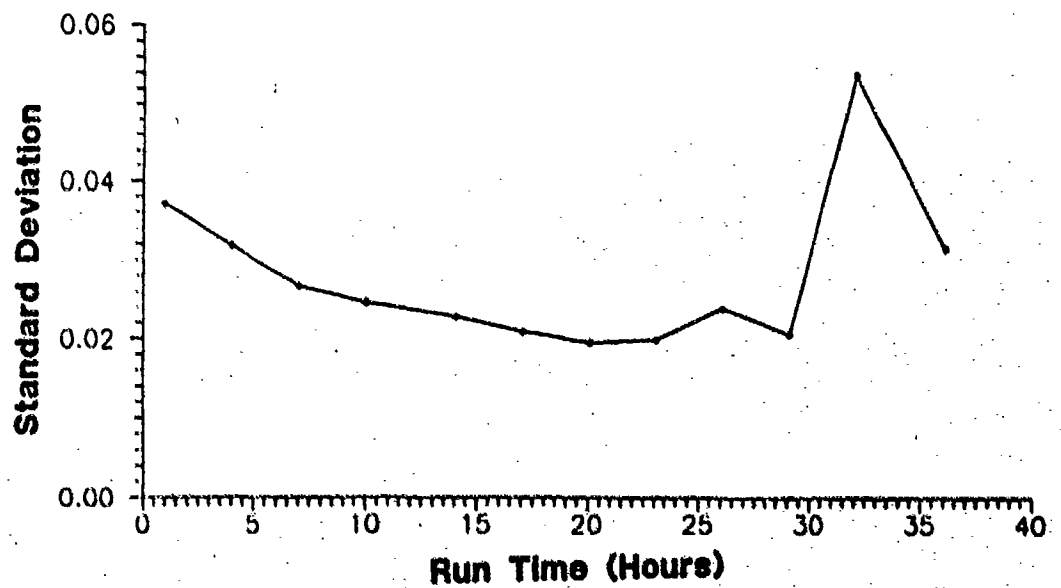
Figure 4.14 :   Plot of Standard Deviation of Difference Signal (FM4) for Run 2.
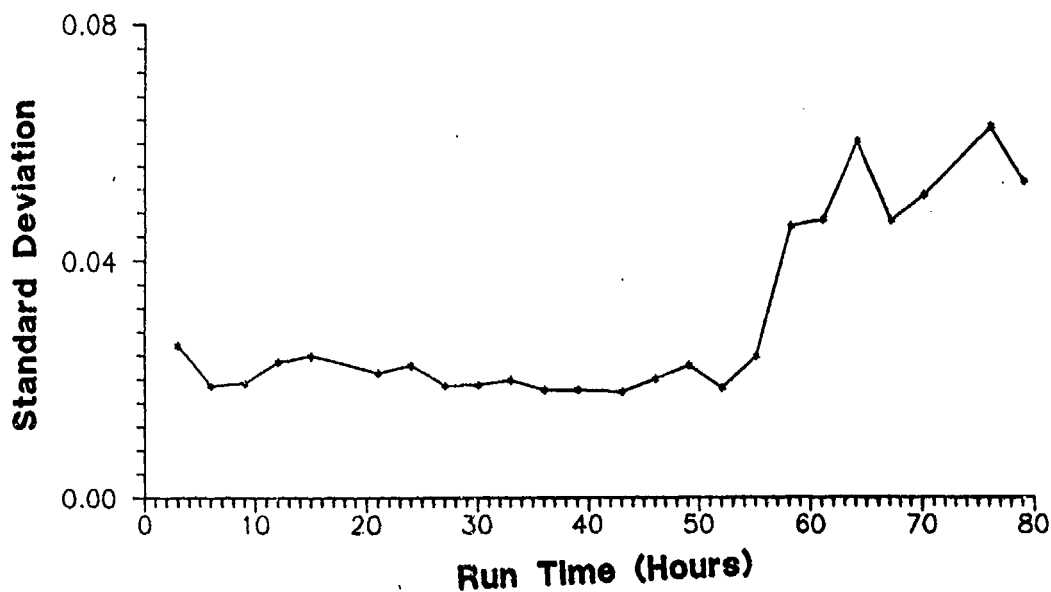
Figure 4.15 : Plot of Standard Deviation of Difference Signal (FM4)
for Run 4.
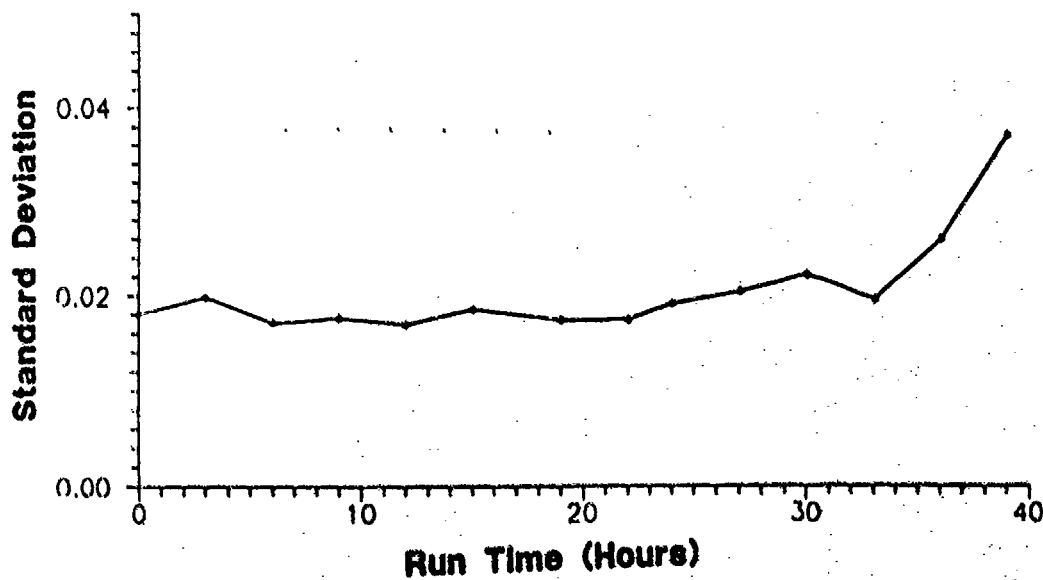
Figure 4.16 : Plot of Standard Deviation of Difference Signal (FM4)
for Run 5.
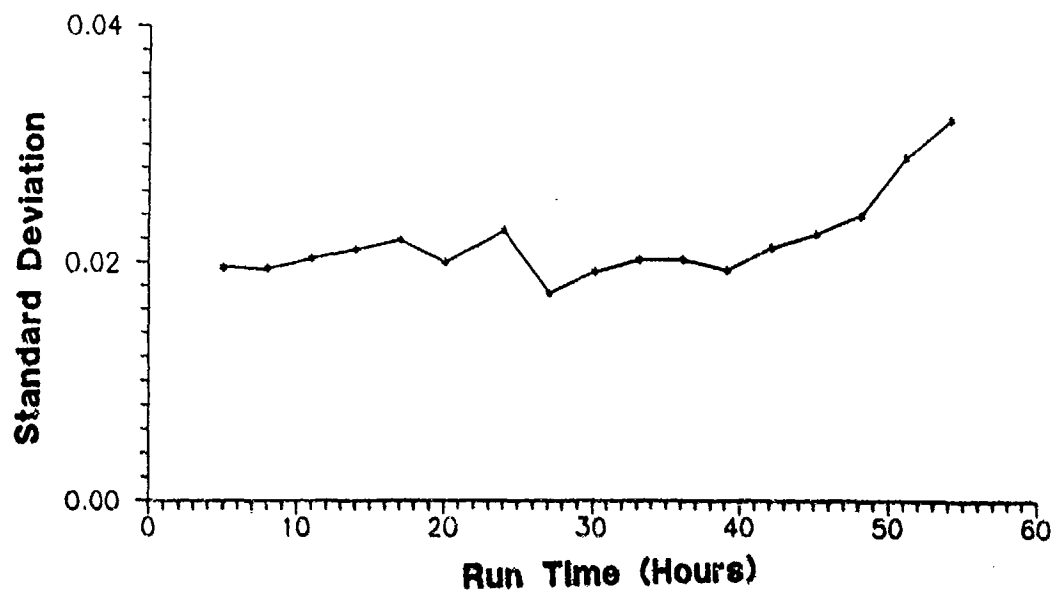
Figure 4.17 :   Plot of Standard Deviation of Difference Signal (FM4) for Run 6.

a)
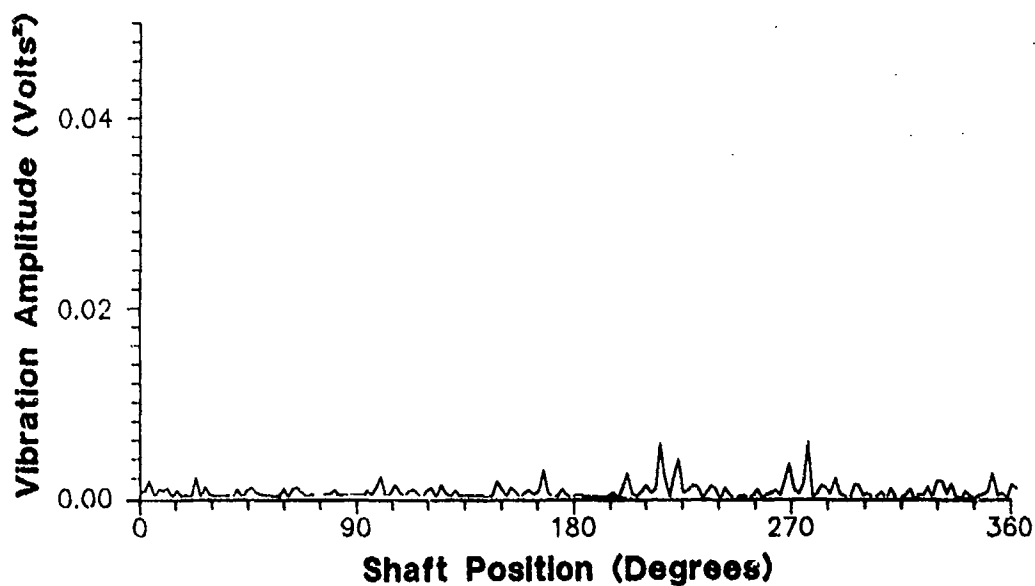
b)
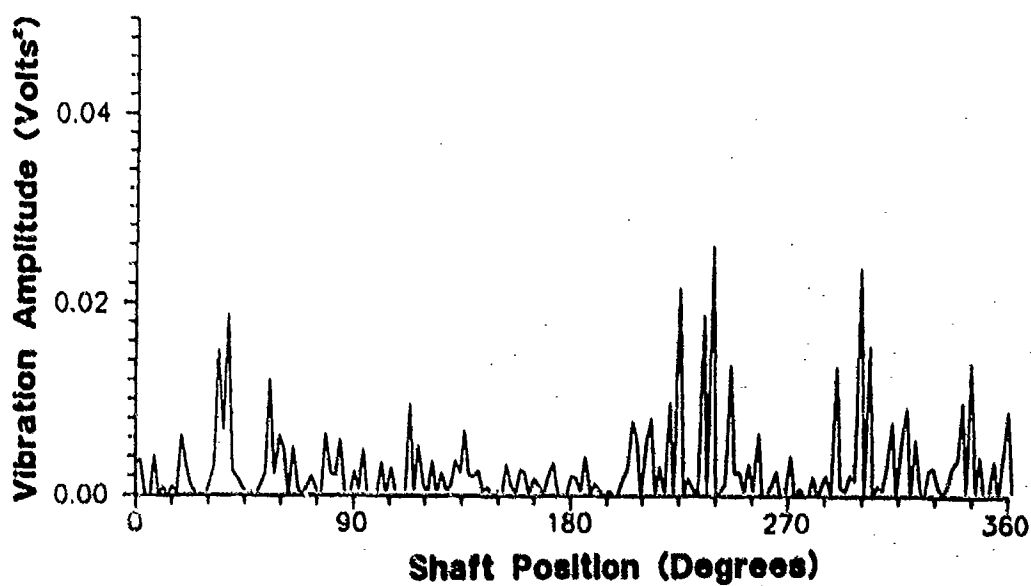
Figure 4.18 : Plot of Squared Difference Signal For Run 4.
a) At Start of Run.
b) At End of Run.

a)
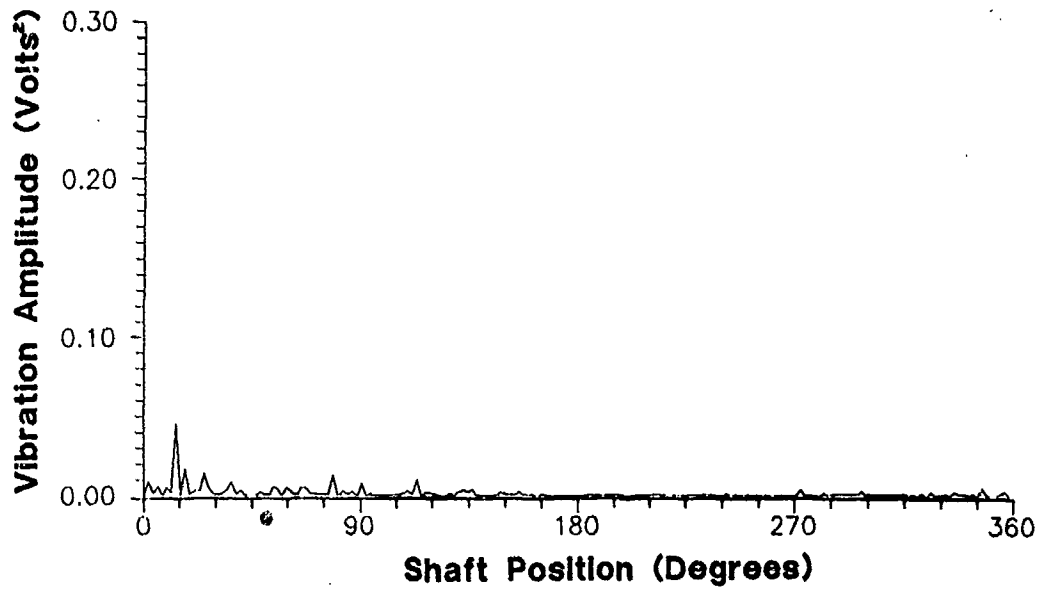
b)
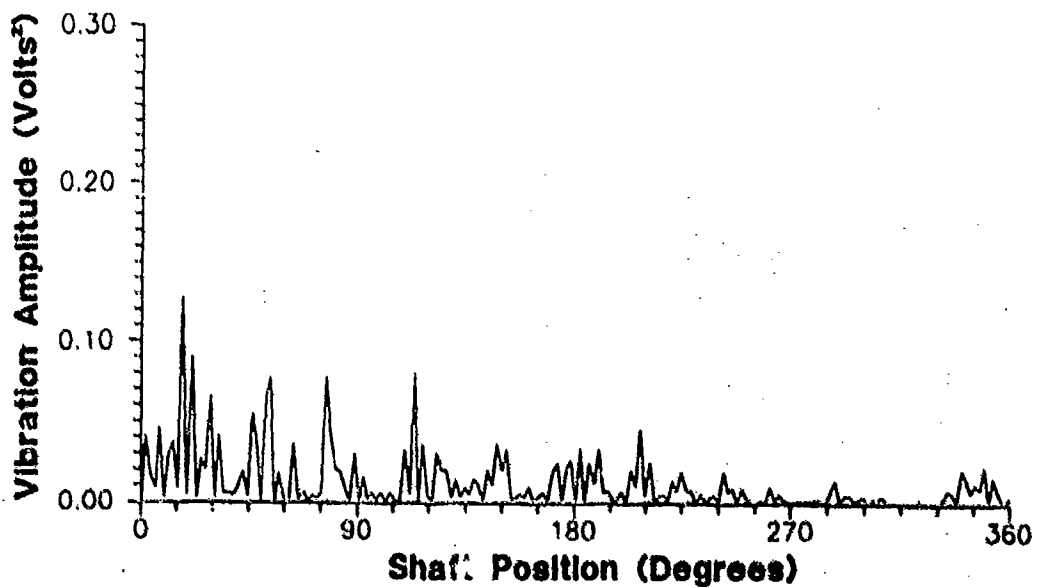
Figure 4.19 : Plot of Squared Difference Signal For Run 10.
a) At Start of Run.
b) At End of Run.

a)

b)
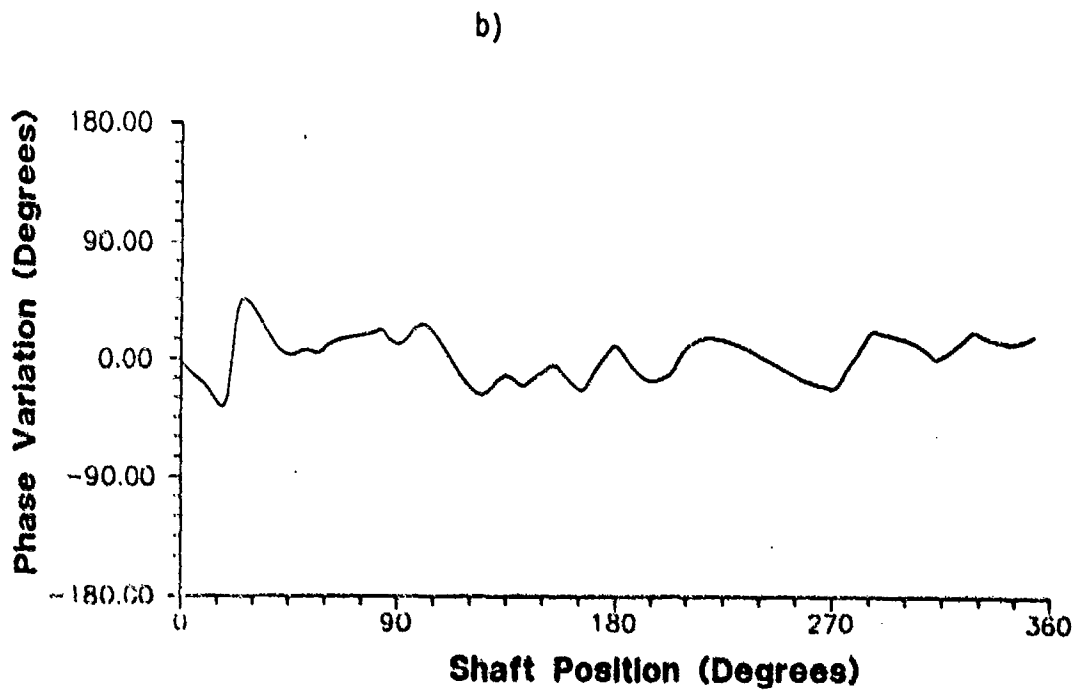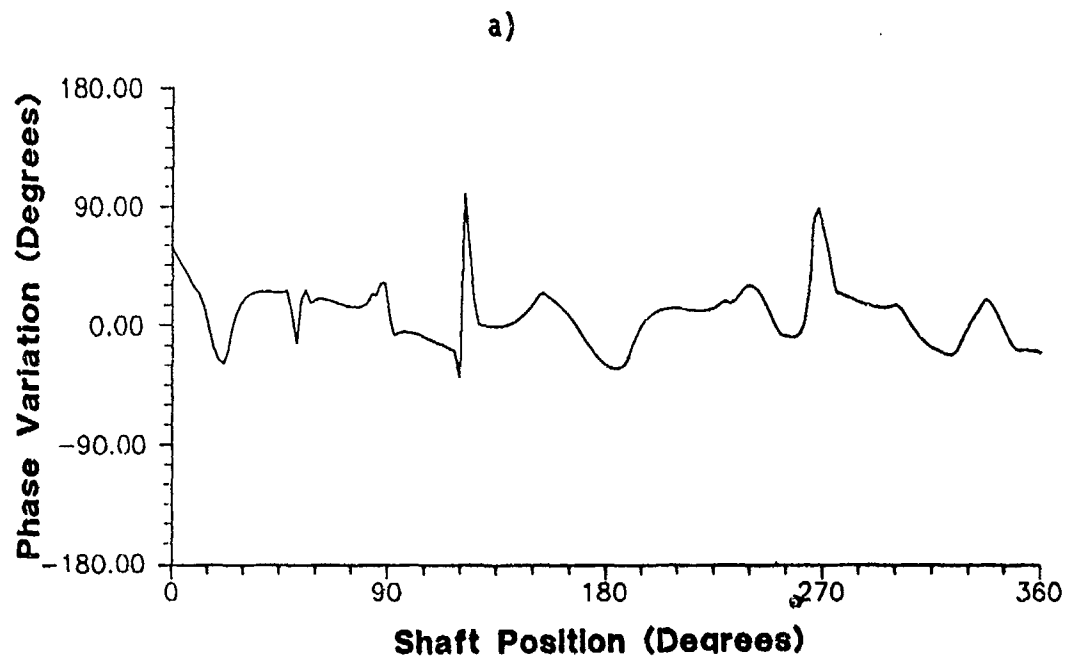
Figure 4.20 : Plot of Phase Modulation Function for Run 3.
a) At a Run Time of 2 Hours.
b) At a Run Time of 5 Hours.

62

a)
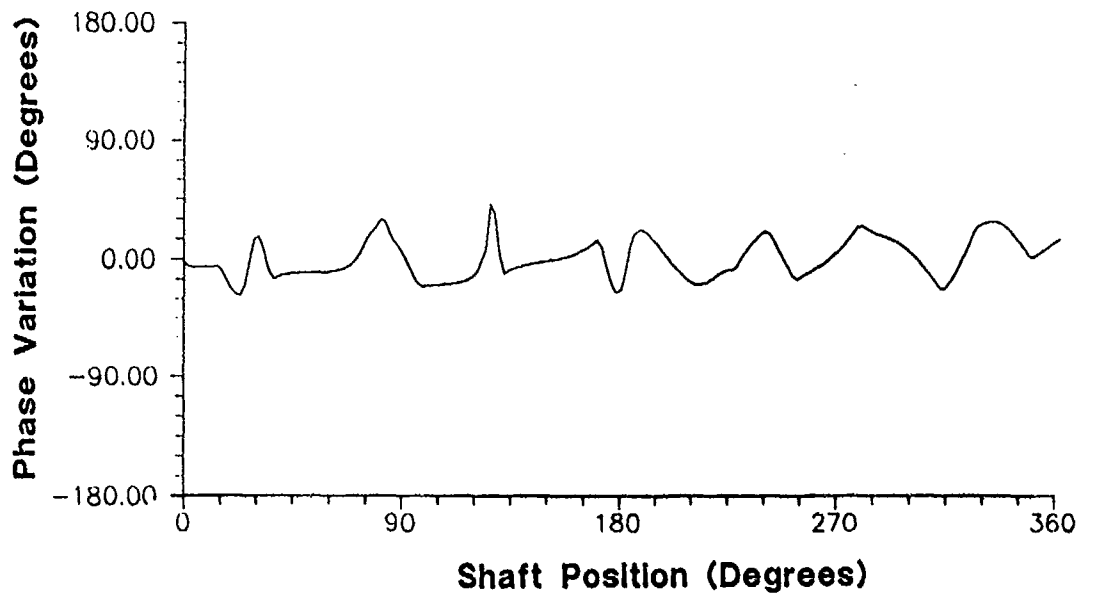
b)
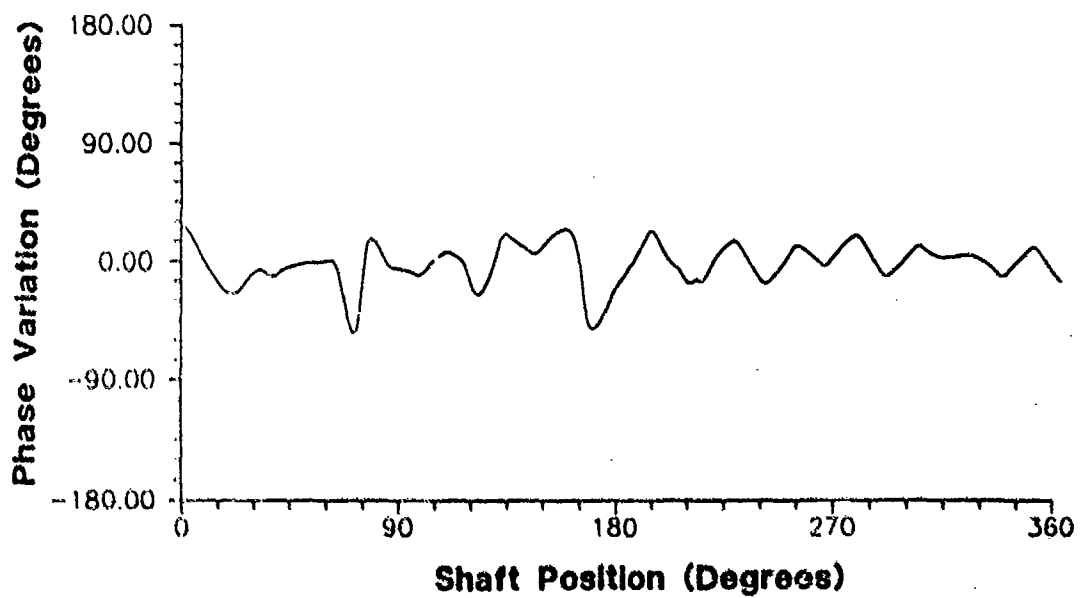
Figure 4.21 : Plot of Phase Modulation Function for Run 7.
a) At a Run Time of 47 Hours.
b) At a Run Time of 50 Hours.

63

a)

b)
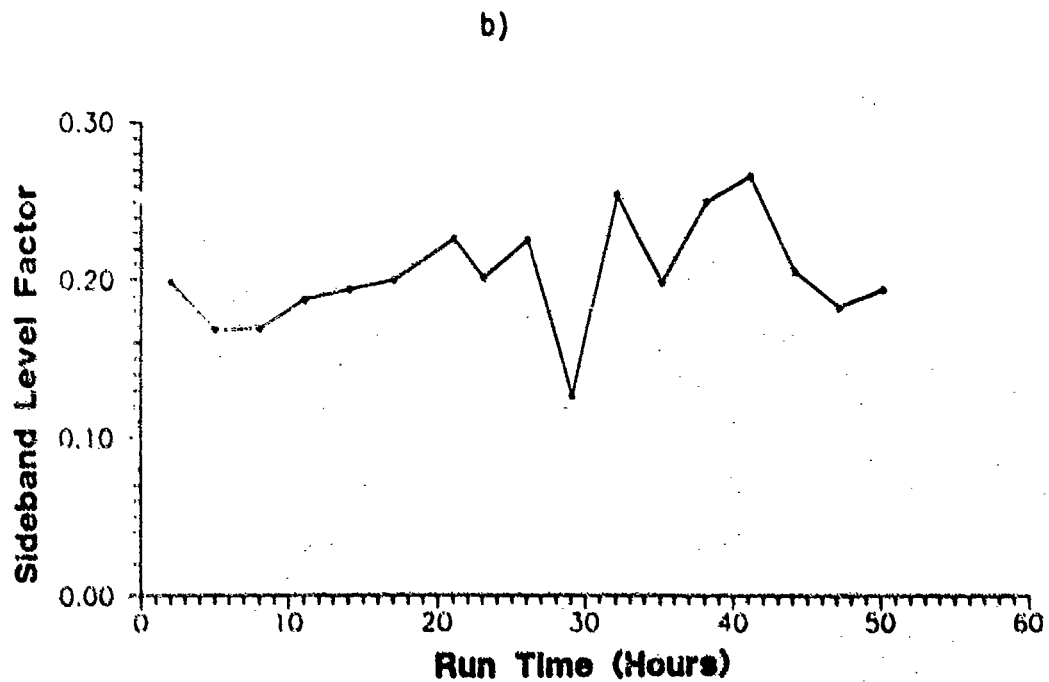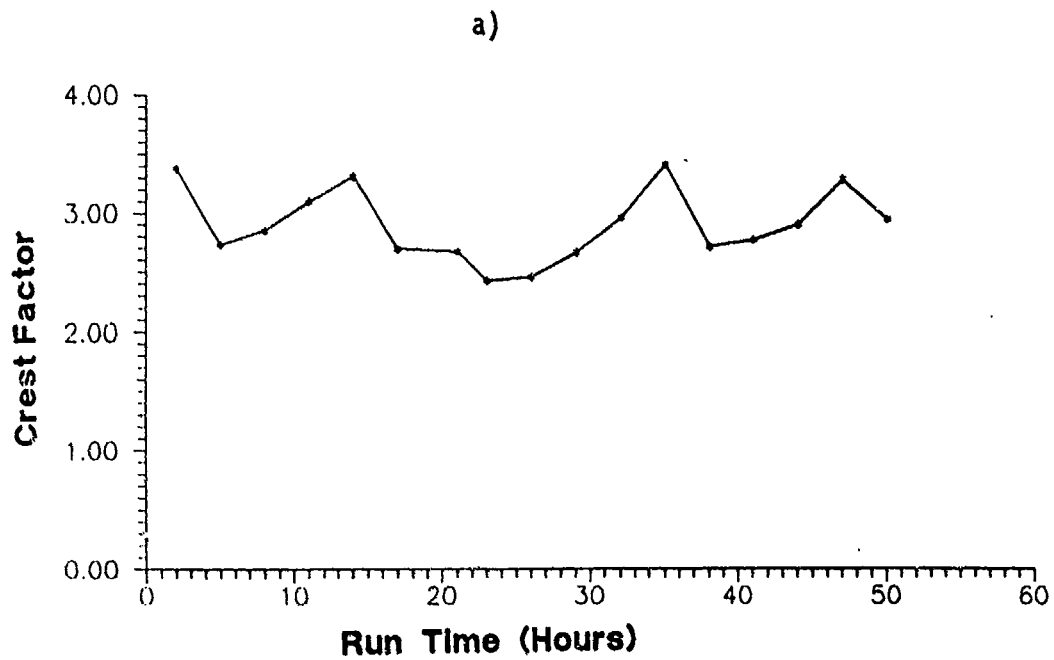
Figure 4.22 : Plot of Crest Factor and Sideband Level for Run 7.
a) Crest Factor.
b) Sideband Level Factor.
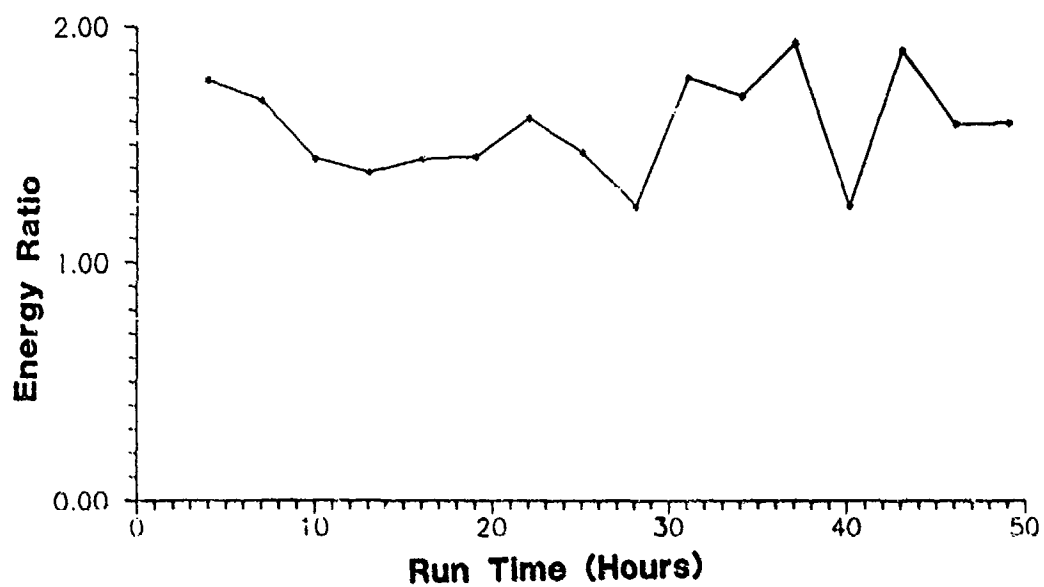
Figure 4.23 :   Energy Ratio Plot for Run 1.
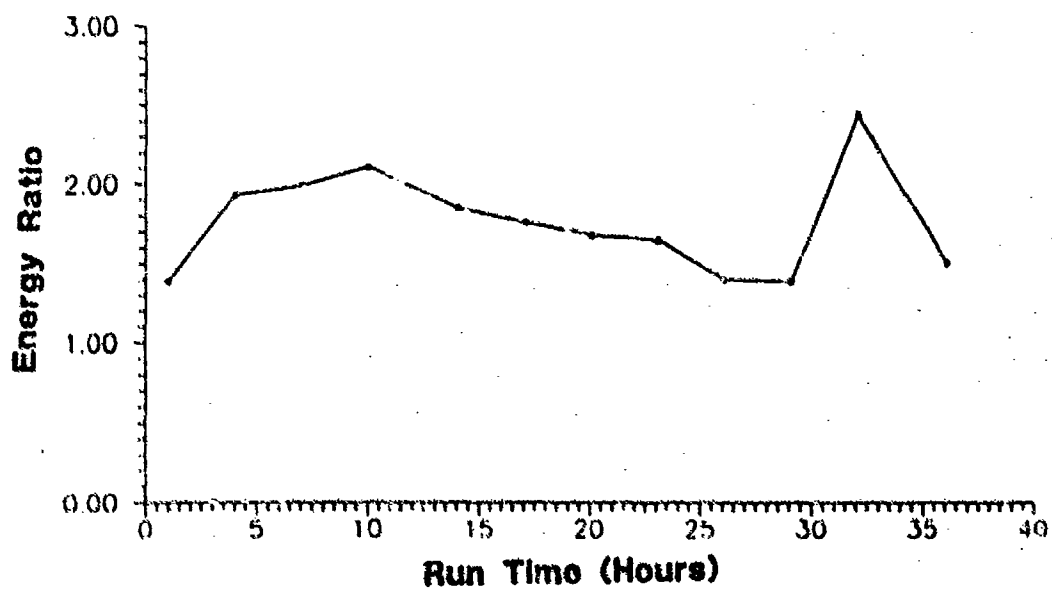
Figure 4.24 :   Energy Ratio Plot for Run 2.
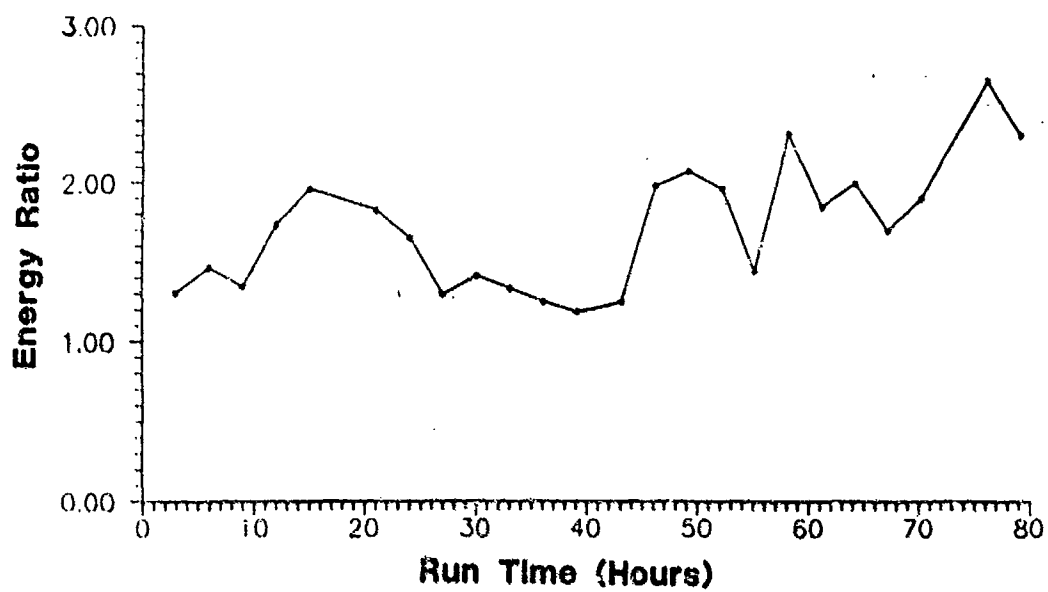
Figure. 4.25 :   Energy Ratio Plot for Run 4.
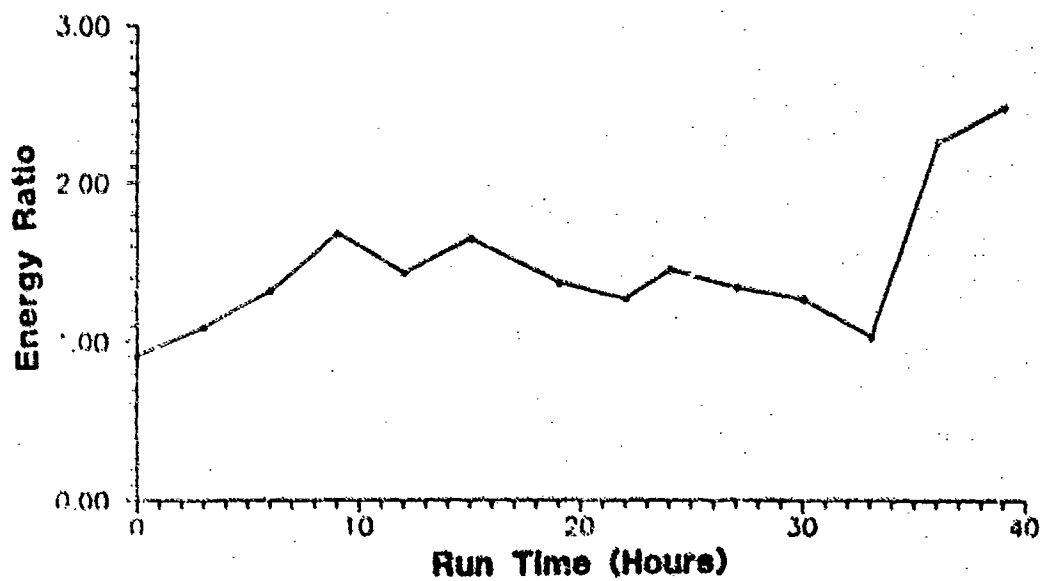
Figure 4.26 :   Energy Ratio Plot for Run 5.
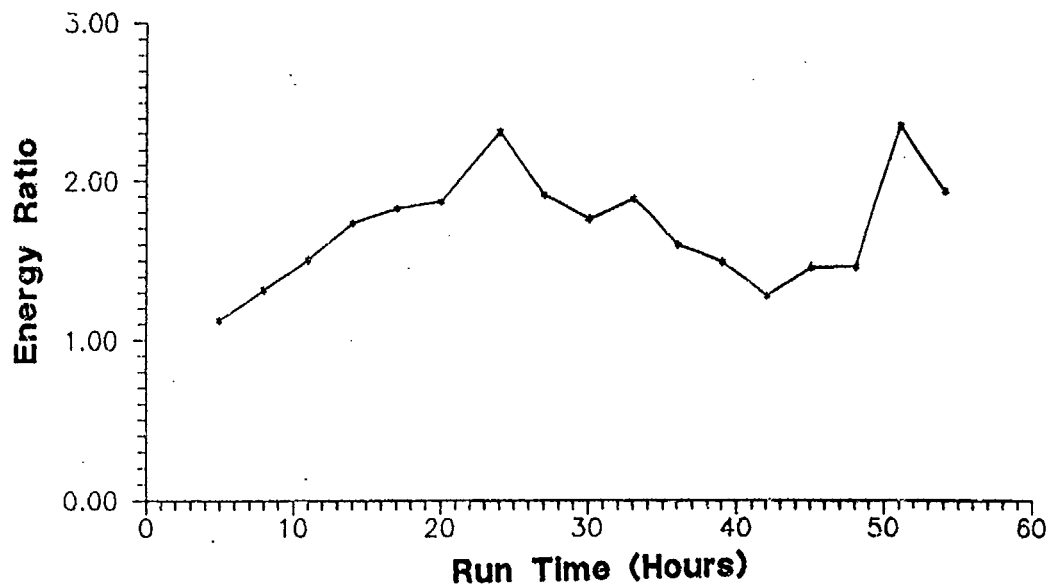
Figure 4.27 :   Energy Ratio Plot for Run 6.
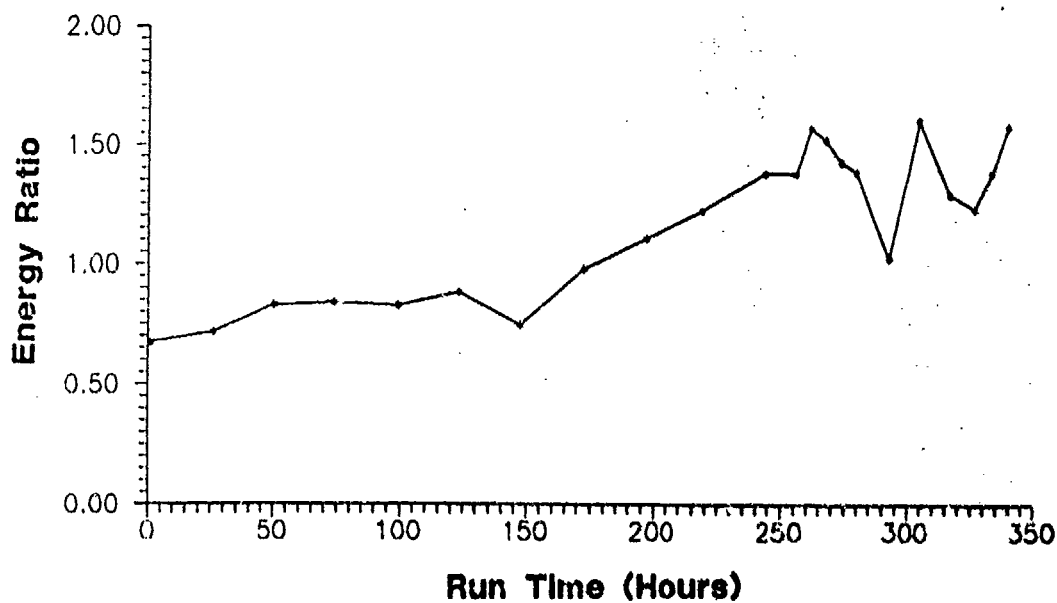
Figure 4.28 :   Energy Ratio Plot for Run 10.

67
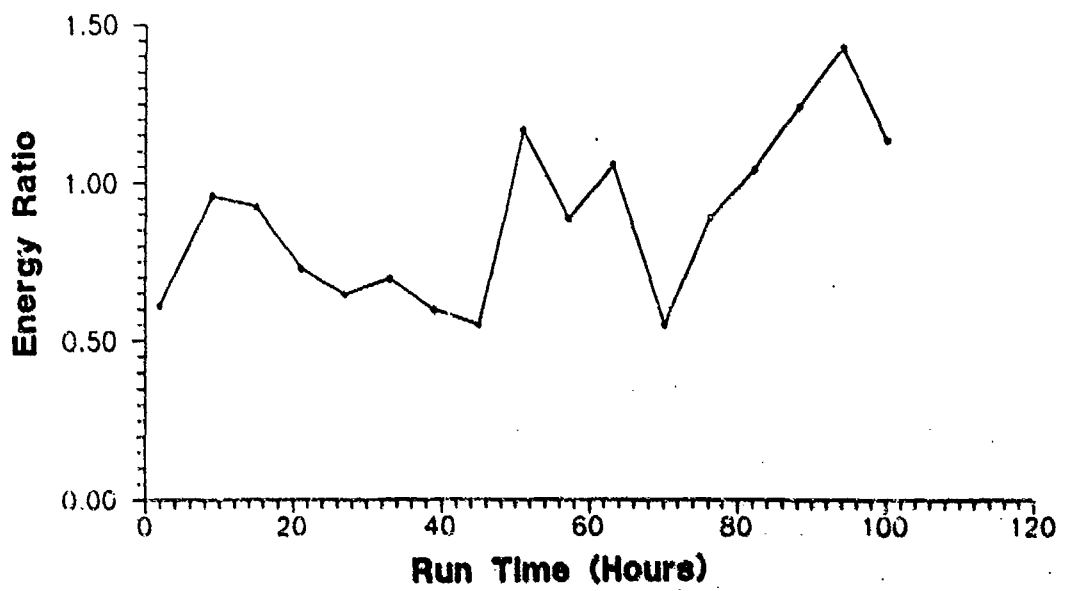
Figure 4.29 : Energy Ratio Plot for Run 11.

CHAPTER V
CONCLUSIONS AND RECOMMENDATIONS

The type and extent of the damage found on the eleven test gears can be classified into four major failure modes. The first mode can be described as heavy wear and scoring (runs 1,2 and 4 through 6). The second mode is tooth breakage (runs 3 and 7). The third failure mode is a result of single pits (runs 8 and 9). And the last mode is described as distributed pitting (runs 10 and 11). These classifications will be used to evaluate the overall performance of the various methods.

HEAVY WEAR AND SCORING

The FM0 parameter and the standard deviation of the difference signal from FM4 did very well at detecting this heavy wear condition. Results from both techniques support the theory that as a gear wears the meshing energy redistributes from the meshing frequencies to its sidebands and beyond.

The energy ratio method does not predict wear as well as the FM0 and the standard deviation methods. The most probable reason for this is in the denominator of the energy ratio. The denominator is the standard deviation of the regular signal, or the meshing frequencies and their first order sidebands. The first order sidebands should not be considered part of the regular signal for this parameter. This is because they increase in amplitude similar to the higher order sidebands as the gear wears.

An enhanced method using a combination of these techniques could prove to be a reliable uniform gear wear detection technique. One such method could use the standard deviation of the difference signal divided by the sum of the amplitudes of the meshing frequencies (primary and first harmonic). Because wear becomes detectable in the overall vibration level only when it reaches a critical stage, a robust wear indication parameter would be highly useful.

TOOTH BREAKAGE

The fatigue cracks that resulted in the broken teeth in runs 3 and 7 were not detected by any of the methods. The normalized kurtosis parameter of FM4, the phase modulation function from the Hilbert transform technique, the crest factor, and the sideband level factor are all conditioned to react to tooth cracks to varying degrees; however, none detected any fault prior to tooth fracture. The most probable reason for this can be due to the high speed and high loading conditions the test gears are subjected to. With these operating conditions, the time elapsed between initiation of the fatigue crack and eventual tooth fracture is probably orders of magnitude lower than the three hour data interval time. Since the last time records collected from runs 3 and 7 were 3 and 2 1/2 hours before actual tooth fracture, respectively, data necessary to indicate the fatigue cracks were missed.

SINGLE PITS (TOOTH SPECIFIC FAULTS)

The single pits were not detected by the normalized kurtosis in the FM4 technique. The normalized kurtosis of the difference signal is designed to detect tooth specific faults; however, no indication of these defects were recorded with this parameter. Although they physically appear large, they may have not affected the signal to the point detectable by FM4.

DISTRIBUTED PITTING

The distributed pitting damage was detected with the the FM0 parameter. It is theorized that the pitting happened over enough of the teeth to act as a

69

uniform wear phenomenon, thus becoming detectable to FM0. The square of the difference signal from the FM4 method did appear to reflect the actual wear pattern on some of the runs.

RECOMMENDATIONS

It is recommended that any future tests of this nature be implemented on an on-line basis for three major reasons. The first stems from the fact that a passive system cannot call attention to events which happen faster than the time between the data time intervals. A continuous, or on-line, system can monitor the test and record data as fast as the electronics will allow when certain parameters signal a significant event in progress. This may be the only way to provide data on the fatigue cracks that lead to tooth fracture on this rig. Another major reason is that in an on-line system it is possible to have the system stop the rig when a parameter detects a fault. The fault can be analyzed to determine its extent and nature at the exact time it is detected. This would provide an excellent means of verifying and linking certain parameters with certain faults as they naturally happen. The final advantage of an on-line system is the ability of storing data in digital form, eliminating the FM recorder. In this test, because the dynamic range of the recorder was only 50 dB, some of the lower energy components of the signal were lost. Using the analyzer to digitize and store the data directly would increase the dynamic range to 80 dB, thereby capturing more of the lower energy signals.

It is also recommended that frequency response measurements be performed between the gear shaft and the proposed measurement sites. The dynamics of the transfer path in this study were found to significantly affect the output signal, especially as the gear began to wear. An understanding of the structural dynamics associated with the transfer path is required to apply prediction techniques only to the portion of the signal reflecting the actual gear mesh dynamics.

ACKNOWLEDGEMENTS

```
0001   C****************************************************************C
0002   C                                                              C
0003   C                                                              C
0004   C     PROGRAM: EFMO.FOR     CREATED: 05-05-89   REVISED: XX-XX-XXXX C
0005   C                                                              C
0006   C     PROGRAMMER: J.J. ZAKRAJSEK                               C
0007   C                                                              C
0008   C     THIS PROGRAM COMPUTES AN ENHANCED VERSION OF THE COURSE FAULT C
0009   C     DETECTION PARAMETER (EFMO). IT IS THE BASIC FMO PARAMETER,  C
0010   C     AS PROPOSED BY STEWART IN HIS 1977 PAPER, HOWEVER, THE PEAK  C
0011   C     TO PEAK VALUE USED IN EFMO IS THE PEAK TO PEAK OF THE      C
0012   C     RECONSTRUCTED TIME SIGNAL AFTER BAND WIDTH FILTERING IS    C
0013   C     PERFORMED. THE RECONSTRUCTED TIME SIGNAL USED IS THE "FTIME" C
0014   C     FILE CREATED AFTER A-B-C FILTERING DURING FM4 CALCULATIONS IN C
0015   C     PROGRAM TFM4.FOR. THE AMPLITUDES AT THE MESH FREQUENCY AND ITS C
0016   C     HARMONIC ARE RETRIEVED FROM PREVIOUS FMO CALCULATIONS.     C
0017   C                                                              C
0018   C                                                              C
0019   C****************************************************************C
0020   C
0021         DIMENSION TIME(50),ECFDP(50),PKTPK(50),ASUM(50),FSIG(220)
0022         CHARACTER*22 FMOF,EFMOF,LIST2,FTIMEF
0023   C
0024   C ENTER INITIAL DATA AND FILE NAMES
0025   C
0026         PRINT *, 'ENTER NUMBER OF DATA POINTS'
0027         READ(*,*) K
0028         PRINT *, 'ENTER OUTPUT DATA FILE NAME (\TXXE*FMO.DAT)'
0029         PRINT *, '( * - FILTER CONFIG USED IN RECONSTRUCTED FILTER)'
0030         READ (* (A22)') EFMOF
0031         OPEN(7,FILE=EFMOF,IOSTAT=IOERR)
0032         IF (IOERR .GT. 0) GOTO 999
0033         PRINT *, 'ENTER FILE NAMES ARRAY FILE (\TXXLIST2.FIL)'
0034         READ(*,'(A22)') LIST2
0035         OPEN(8,FILE=LIST2,IOSTAT=IOERR)
0036         IF(IOERR .GT. 0) GOTO 999
0037         PRINT *, 'ENTER PREVIOUS TFMO FILE (\TXXFMO.DAT)'
0038         READ(*,'(A22)') FMOF
0039         OPEN(9,FILE=FMOF,IOSTAT=IOERR)
0040         IF(IOERR .GT. 0) GOTO 999
0041         PRINT *, 'ENTER NUMBER OF TIME DATA POINTS PER CYCLE (INTEGER)'
0042         READ(*,*) NCYC
0043   C
0044   C START TIME LOOPING, PROCESSING DATA AT EACH TIME INTERVAL
0045   C
0046         DO 300, J=1,K
0047         PRINT *, 'ACCESSING AND PROCESSING DATA FILE NO:',J
0048         READ(8,800) FTIMEF
0049     800 FORMAT(A18)
0050         READ(9,900) TIME(J),ASUM(J)
0051     900 FORMAT(F8.2,44X,F12.8)
0052         OPEN(4,FILE=FTIMEF,IOSTAT=IOERR)
0053         IF (IOERR .GT. 0) GOTO 999
0054   C
0055   C READ IN AND FIND THE MAX AND MIN VALUES OF THE FILTERED TIME RECORD
```

71

```
0056   C
0057           AMAX = 0.0
0058           BMAX = 0.0
0059           DO 100, I=1,NCYC
0060           READ(4,400) FSIG(I)
0061   400     FORMAT(20X,F16.8)
0062           IF( FSIG(I) .GT. AMAX ) THEN
0063           AMAX = FSIG(I)
0064           ENDIF
0065           IF( FSIG(I) .LT. BMAX ) THEN
0066           BMAX = FSIG(I)
0067           ENDIF
0068   100     CONTINUE
0069   C
0070   C DETERMINE PK TO PK OF FILTERED SIGNAL, AND ENHANCED FMO VALUE
0071   C
0072           PKTPK(J) = AMAX - BMAX
0073           ECFDP(J) = PKTPK(J)/ASUM(J)
0074   C
0075   C CLOSE LOOP DEPENDANT FILE, AND WRITE CALAULTED DATA
0076   C
0077           CLOSE(4,IOSTAT=IOERR)
0078           IF (IOERR .GT. 0) GOTO 999
0079           WRITE (7,700) TIME(J),ECFDP(J),PKTPK(J)
0080   700     FORMAT(F8.2,F10.4,F10.4)
0081   300     CONTINUE
0082   C
0083           PRINT *, 'EFMO VALUES STORED IN FILE;',EFMOF
0084           STOP
0085   999     PRINT *, 'ERROR NO.',IOERR
0086           END
```

```
0001   C************************************************************************C
0002   C                                                                      C
0003   C                                                                      C
0004   C       PROGRAM:  TFM4.FOR                     REVISION:      NEW       C
0005   C                                              REVISION DATE: NEW       C
0006   C       PROGRAMMER: J.J. Zakrajsek             DATE CREATED: 04-13-89   C
0007   C                                                                      C
0008   C       THIS PROGRAM COMPUTES THE FAULT DETECTION PARAMETERS AND THE   C
0009   C       RELATED MATHEMATICS FOR THE FM4 DIAGNOSTIC THEORY PROPOSED     C
0010   C       IN STEWART'S 1977 PAPER " SOME USEFULL DATA ANALYSIS           C
0011   C       TECHNIQUES FOR GEARBOX DIAGNOSTICS." THESE INCLUDE PARAMETERS  C
0012   C       SUCH AS STANDARD DEVIATION AND KURTOSIS.                       C
0013   C                                                                      C
0014   C                                                                      C
0015   C************************************************************************C
0016   C
0017         DIMENSION TIME(50),DYO(220),DSYO(220),RMAG(401)
0018         DIMENSION FREQ(401),FMAGRMS(401),FMAG(401),PHAS(401),FFMAG(401)
0019         DIMENSION TO(1024),YO(1024),FYO(1024),RFYO(1024)
0020         CHARACTER*22 TIMEF,FM4F,LIST1,LIST2,AMPLF,PHASEF,ATIME
0021         CHARACTER*18 FTIME,RTIME,NTIME,STIME
0022         COMPLEX X(1024)
0023   C
0024   C ENTER GENERAL PARAMETERS AND FILE NAMES
0025   C
0026         PRINT *, 'ENTER NUMBER OF DATA POINTS (INTEGER)'
0027         READ(*,*) K
0028         PRINT *, 'ENTER MESHING FREQUENCY, (XXXX.XX)'
0029         READ(*,*) PRIM
0030         PRINT *, 'ENTER ROTATIONAL SPEED IN REV/SEC (Hz)'
0031         READ(*,*) SPD
0032         PRINT *, 'ENTER NUMBER OF TIME DATA POINTS PER CYCLE'
0033         PRINT *, '( INTEGER, 220 MAXIMUM )'
0034         READ (*,*) NCYC
0035   C
0036   C DEFINITION OF OPTIONAL FILTER BANDS A, B, AND C
0037   C
0038         PRINT *, '3 BAND WIDTH DIGITAL FILTERS CAN BE SELECTED.'
0039         PRINT *, 'DATA EXISTING WITHIN THE THREE BANDS WILL BE FILTERED'
0040         PRINT *, 'OUT OF THE ANALYSIS BEFORE IT BEGINS FM4 CALCULATIONS'
0041         PRINT *, '       '
0042         PRINT *, 'TO USE FILTERS ENTER  (1)'
0043         PRINT *, 'TO SKIP FILTERS ENTER (0)'
0044   C
0045         READ (*,*) NN
0046         IF (NN .LT. 1) GOTO 123
0047   C
0048         PRINT *, 'ENTER STARTING FREQUENCY OF FILTER A'
0049         READ(*,*) AFILTS
0050         PRINT *, '************** ENTER END FREQUENCY OF FILTER A'
0051         READ(*,*) AFILTE
0052         PRINT *, 'ENTER STARTING FREQUENCY OF FILTER B'
0053         READ(*,*) BFILTS
0054         PRINT *, '************** ENTER END FREQUENCY OF FILTER B'
0055         READ(*,*) BFILTE
```

```
0056          PRINT *, 'ENTER STARTING FREQUENCY OF FILTER C'
0057          READ(*,*) CFILTS
0058          PRINT *, '************** ENTER END FREQUENCY OF FILTER C'
0059          READ(*,*) CFILTE
0060    123   CONTINUE
0061  C
0062  C INPUT PRIMARY FILE NAMES FILES
0063  C
0064          PRINT *, 'ENTER  TXXTIME.FIL  INPUT FILE NAME'
0065          READ(*,'(A22)') TIMEF
0066          PRINT *, 'ENTER  TXXFM4*.FIL  OUTPUT FILE NAME'
0067          PRINT *, '( * - FILTERS A-B-C VERSION)'
0068          READ(*,'(A22)') FM4F
0069          PRINT *, 'ENTER  TXXLIST1.FIL  INPUT FILES FILENAME'
0070          READ(*,'(A22)') LIST1
0071          PRINT *, 'ENTER  TXXLIST2.FIL  OUTPUT FILES FILENAME'
0072          READ(*,'(A22)') LIST2
0073  C
0074  C OPEN PRIMARY FILES
0075  C
0076          OPEN(1,FILE=TIMEF,IOSTAT=IOERR)
0077          IF(IOERR .GT. 0) GOTO 999
0078          OPEN(2,FILE=FM4F,IOSTAT=IOERR)
0079          IF(IOERR .GT. 0) GOTO 999
0080          OPEN(3,FILE=LIST1,IOSTAT=IOERR)
0081          IF(IOERR .GT. 0) GOTO 999
0082          OPEN(4,FILE=LIST2,IOSTAT=IOERR)
0083          IF(IOERR .GT. 0) GOTO 999
0084  C
0085  C STARTING POINT OF FM4 ANALYSIS LOOP FOR EACH DATA POINT
0086  C
0087          DO 111, J=1,K
0088          PRINT *, 'PROCESSING DATA POINT NO. :',J
0089          READ(1,100) TIME(J)
0090    100   FORMAT(F10.2)
0091          READ(3,300) AMPLF,PHASEF,ATIME
0092    300   FORMAT(A22,A22,A22)
0093          READ(4,400) FTIME,RTIME,NTIME,STIME
0094    400   FORMAT(A18,A18,A18,A18)
0095  C
0096  C OPEN LOOP DEPENDANT FILES
0097  C
0098          OPEN(5,FILE=AMPLF,IOSTAT=IOERR)
0099          IF(IOERR .GT. 0) GOTO 999
0100          OPEN(6,FILE=PHASEF,IOSTAT=IOERR)
0101          IF(IOERR .GT. 0) GOTO 999
0102          OPEN(7,FILE=ATIME,IOSTAT=IOERR)
0103          IF(IOERR .GT. 0) GOTO 999
0104          OPEN(8,FILE=FTIME,IOSTAT=IOERR)
0105          IF(IOERR .GT. 0) GOTO 999
0106          OPEN(9,FILE=RTIME,IOSTAT=IOERR)
0107          IF(IOERR .GT. 0) GOTO 999
0108          OPEN(10,FILE=NTIME,IOSTAT=IOERR)
0109          IF(IOERR .GT. 0) GOTO 999
0110          OPEN(11,FILE=STIME,IOSTAT=IOERR)
```

```
0111              IF(IOERR .GT. 0) GOTO 999
0112     C
0113     C READ IN PHASE AND FREQUENCY FILES
0114     C
0115              DO 222, I=1,401
0116              READ(5,500) FREQ(I),FMAGRMS(I)
0117       500 FORMAT(4X,F12.3,20X,F16.8)
0118              FMAG(I) = FMAGRMS(I) * (2.**.5)
0119              READ(6,600) PHAS(I)
0120       600 FORMAT(20X,F12.3)
0121       222 CONTINUE
0122     C
0123     C PERFORM IFFT ON ORIGINAL SIGNAL
0124     C
0125              CALL IFOUR(FREQ,FMAG,PHAS,TO,YO)
0126     C
0127     C PRINT TO FILE, 2 CYCLES OF ORIGINAL TIME SIGNAL.
0128     C
0129              NCYC2 = NCYC + NCYC
0130              DO 333, I=1,NCYC2
0131              WRITE(7,700) TO(I),YO(I)
0132       700 FORMAT(F16.8,4X,F16.8)
0133       333 CONTINUE
0134     C
0135     C PERFORM FILTERING USING FILTERS A, B, C
0136     C
0137              IF(NN .LT. 1) GOTO 234
0138              CALL FILTER(FREQ,FMAG,FFMAG,AFILTS,AFILTE,BFILTS,BFILTE,
0139           *CFILTS,CFILTE)
0140     C
0141     C PERFORM IFFT ON FILTERED SIGNAL
0142     C
0143              CALL IFOUR(FREQ,FFMAG,PHAS,TO,FYO)
0144       234 CONTINUE
0145              IF(NN .LT. 1) THEN
0146              DO 345, I=1,401
0147              FFMAG(I) = FMAG(I)
0148       345 CONTINUE
0149              DO 456, I=1,NCYC2
0150              FYO(I) = YO(I)
0151       456 CONTINUE
0152              ENDIF
0153     C
0154     C PERFORM FILTERING TO FM4 SPECIFICATIONS
0155     C
0156              CALL FFM4(FREQ,FFMAG,PRIM,SPD,RMAG)
0157     C
0158     C PERFORM IFFT ON FM4 FILTERED SIGNAL
0159     C (USES ABC FILTERED SIGNAL AS BASIS)
0160     C
0161              CALL IFOUR(FREQ,RMAG,PHAS,TO,RFYO)
0162     C
0163     C DETERMINE DIFFERENCE SIGNAL ( ORIGINAL - REGULAR COMPONENTS)
0164     C
0165              DO 444, I=1,NCYC
```

```
0166          DYO(I) = FYO(I) - RFYO(I)
0167     444 CONTINUE
0168   C
0169   C DETERMINE SQUARED DIFFERENCE SIGNAL
0170   C
0171          DO 555, I=1,NCYC
0172          DSYO(I) = DYO(I)**2.
0173     555 CONTINUE
0174   C
0175   C DETERMINE AVERAGE VALUE OF DIFFERENCE SIGNAL
0176   C
0177          DSUM = 0.0
0178          DO 666, I=1,NCYC
0179          DSUM = DSUM + DYO(I)
0180     666 CONTINUE
0181          DBAR = DSUM/FLOAT(NCYC)
0182   C
0183   C DETERMINE STANDARD DEVIATION OF NET SIGNAL
0184   C
0185          CALL STDEV(DYO,NCYC,DBAR,SDEV)
0186   C
0187   C DETERMINE NORMALIZED KURTOSIS OF NET SIGNAL
0188   C
0189          CALL KURTOS(DYO,NCYC,DBAR,RKURT)
0190   C
0191   C WRITE RESULTS TO FILES
0192   C
0193          DO 777, I=1,NCYC
0194          WRITE(8,700) TO(I),FYO(I)
0195     777 CONTINUE
0196   C
0197          DO 778, I=1,NCYC
0198          WRITE(9,700) TO(I),RFYO(I)
0199     778 CONTINUE
0200   C
0201          DO 779, I=1,NCYC
0202          WRITE(10,700) TO(I),DYO(I)
0203     779 CONTINUE
0204   C
0205          DO 780, I=1,NCYC
0206          WRITE(11,700) TO(I),DSYO(I)
0207     780 CONTINUE
0208   C
0209          WRITE(2,200) TIME(J),SDEV,RKURT
0210     200 FORMAT(F10.2,F12.6,F12.6)
0211   C
0212   C CLOSE LOOP DEPENDANT FILES
0213   C
0214          CLOSE(5,IOSTAT=IOERR)
0215          IF(IOERR .GT. 0) GOTO 999
0216          CLOSE(6,IOSTAT=IOERR)
0217          IF(IOERR .GT. 0) GOTO 999
0218          CLOSE(7,IOSTAT=IOERR)
0219          IF(IOERR .GT. 0) GOTO 999
0220          CLOSE(8,IOSTAT=IOERR)
```

```
0221            IF(IOERR .GT. 0) GOTO 999
0222            CLOSE(9,IOSTAT-IOERR)
0223            IF(IOERR .GT. 0) GOTO 999
0224            CLOSE(10,IOSTAT-IOERR)
0225            IF(IOERR .GT. 0) GOTO 999
0226            CLOSE(11,IOSTAT-IOERR)
0227            IF(IOERR .GT. 0) GOTO 999
0228    C
0229    C CLOSE LOOP, MOVE TO NEXT DATA POINT
0230    C
0231      111 CONTINUE
0232    C
0233    C
0234            PRINT *, 'FM4 VALUES STORED IN FILE :',FM4F
0235            STOP
0236      999 PRINT *, 'ERROR NO. ',IOERR
0237            END
0238    C
0239    C
0240    C END OF MAIN PROGRAM
0241    C
0242    C
0243    C**********************************************************************C
0244    C                                                                      C
0245    C       ROUTINE: IFOUR                                                 C
0246    C                                                                      C
0247    C       THIS SUBROUTINE PERFORMS AN INVERSE DISCRETE FOURIER           C
0248    C       TRANSFORM ON A DFT TRACE USING MAGNITUDE AND PHASE DATA.       C
0249    C                                                                      C
0250    C                                                                      C
0251    C**********************************************************************C
0252    C
0253            SUBROUTINE IFOUR(F,FMAG,PHAS,T,Y)
0254    C
0255            DIMENSION   T(1024),Y(1024)
0256            DIMENSION   F(401),DFTRE(401),DFTIM(401),FMAG(401),PHAS(401)
0257            DIMENSION   FQ(20)
0258            COMPLEX     X(1024)
0259    C
0260    C..DEFINE DFT SETTINGS
0261    C
0262            NPTS - 1024
0263            NPOW - 10
0264            NFREQ - 401
0265            FSPAN - F(401) - F(1)
0266            PERIOD - FLOAT( (NFREQ-1) ) / FSPAN
0267            BW - F(2) - F(1)
0268            DELTA - PERIOD / FLOAT( (NPTS-1) )
0269            PRINT *, PERIOD
0270            PRINT *, BW
0271    C
0272    C INITIALIZE TIME, AND DFT ARRAYS
0273    C
0274            DO 100 I-1,NPTS
0275                T(I) - DELTA * FLOAT( I-1 )
```

77

```
0276              X(I) - ( 0.,0. )
0277    100       CONTINUE
0278  C
0279  C  CONVERTING PHASE AND MAGNITUDE TO REAL AND IMAGINARY FFT VALUES
0280  C
0281              PI - 3.1415927
0282              DO 300, I-1,NFREQ
0283              RAD - PHAS(I)*PI/180.
0284              DFTRE(I) - FMAG(I) * COS(RAD)
0285              DFTIM(I) - FMAG(I) * SIN(RAD)
0286    300       CONTINUE
0287  C
0288  C..PERFORM INVERSE DFT ON REAL PART
0289  C
0290              IFLAG - 1
0291              DO 2200 I-1,NFREQ
0292                  X(I) - CMPLX( DFTRE(I),0. )
0293    2200      CONTINUE
0294              CALL FFT( IFLAG,NPOW,X )
0295              DO 2300 I-1,NPTS
0296                  Y(I) - REAL( X(I) )
0297    2300      CONTINUE
0298  C
0299  C..PERFORM INVERSE DFT ON IMAGINARY PART
0300  C
0301              DO 2400 I-1,NFREQ
0302                  X(I) - CMPLX( DFTIM(I),0. )
0303    2400      CONTINUE
0304              DO 2500 I-NFREQ+1,NPTS
0305                  X(I) - ( 0.,0. )
0306    2500      CONTINUE
0307              CALL FFT( IFLAG,NPOW,X )
0308              DO 2600 I-1,NPTS
0309                  Y(I) - Y(I) - AIMAG( X(I) )
0310    2600      CONTINUE
0311  C
0312          RETURN
0313          END
0314  C
0315  C
0316  C****************************************************************C
0317  C                                                              C
0318  C    ROUTINE:  FFT                                             C
0319  C                                                              C
0320  C****************************************************************C
0321  C
0322          SUBROUTINE FFT( IFLAG,NPOW,X )
0323          DIMENSION  X(1),CS(2),MSK(13)
0324          COMPLEX    X,CXCS,HOLD,XA
0325          EQUIVALENCE (CXCS,CS)
0326  C
0327          PI - 3.141 592 7
0328          NMAX - 2**NPOW
0329          ZZ - 2. * PI * FLOAT(IFLAG) / FLOAT(NMAX)
0330          MSK(1) - NMAX / 2
```

78

```
0331            DO 15 I=2,NPOW
0332                MSK(I) - MSK(I-1) / 2
0333      15        CONTINUE
0334            NN - NMAX
0335            MM - 2
0336  C
0337  C..LOOP OVER NPOW LAYERS
0338  C
0339            DO 45 LAYER=1,NPOW
0340                NN - NN / 2
0341                NW - 0
0342                DO 40 I=1,MM,2
0343                    II - NN * I
0344  C
0345  C..CXCS - CEXP( 2*PI*NW*FLOAT(IFLAG)/FLOAT(NMAX) )
0346  C
0347                    W - FLOAT(NW) * ZZ
0348                    CS(1) - COS( W )
0349                    CS(2) - SIN( W )
0350  C
0351  C..COMPUTE ELEMENTS FOR BOTH HALVES OF EACH BLOCK
0352  C
0353                    DO 20 J=1,NN
0354                        II - II + 1
0355                        IJ - II - NN
0356                        XA - CXCS * X(II)
0357                        X(II) - X(IJ) - XA
0358                        X(IJ) - X(IJ) + XA
0359      20                CONTINUE
0360  C
0361  C..BUMP UP SERIES BY 2, COMPUTE REVERSE ADDRESS
0362  C
0363                    DO 25 LOC=2,NPOW
0364                        LL - NW - MSK(LOC)
0365                        IF( LL ) 30,35,25
0366      25                NW - LL
0367      30                NW - MSK(LOC) + NW
0368                        GOTO 40
0369      35                NW - MSK(LOC+1)
0370      40                CONTINUE
0371                MM - MM * 2
0372      45        CONTINUE
0373  C
0374  C..DO FINAL REARRANGEMENT, ALSO MULTIPLY BY DELTA.
0375  C
0376            NW - 0
0377            DO 80 I=1,NMAX
0378                NW1 - NW + 1
0379                HOLD - X(NW1)
0380                IF( NW1-I ) 60,55,50
0381      50        X(NW1) - X(I)
0382      55        X(I) - HOLD
0383  C
0384  C..BUMP UP SERIES BY 1, AND COMPUTE REVERSE ADDRESS.
0385  C
```

```
0386   60        DO 65 LOC=1,NPOW
0387                 LL = NW - MSK(LOC)
0388                 IF( LL )  70,75,65
0389   65            NW = LL
0390   70        NW = MSK(LOC) + NW
0391             GOTO 80
0392   75        NW = MSK(LOC+1)
0393   80        CONTINUE
0394         RETURN
0395         END
0396   C
0397   C
0398   C***********************************************************************C
0399   C                                                                      C
0400   C     ROUTINE: FILTER                                                  C
0401   C                                                                      C
0402   C     THIS SUBROUTINE USES FILTERS A, B, AND C DEFINED IN THE MAIN     C
0403   C     PROGRAM TO FILTER OUT ANY NON-GEAR-RELATED SIGNALS FROM THE      C
0404   C     ANALYSIS. (BEARING NOISE, SLAVE GEAR NOISE, Etc.)                C
0405   C                                                                      C
0406   C                                                                      C
0407   C***********************************************************************C
0408   C
0409         SUBROUTINE FILTER(FREQ,FMAG,FFMAG,AFS,AFE,BFS,BFE,CFS,CFE)
0410   C
0411         DIMENSION FREQ(401),FMAG(401),FFMAG(401)
0412   C
0413         DO 100, I=1,401
0414         FFMAG(I) = FMAG(I)
0415         IF((FREQ(I) .GE. AFS) .AND. (FREQ(I) .LE. AFE)) THEN
0416         FFMAG(I) = 0.0
0417         ENDIF
0418         IF((FREQ(I) .GE. BFS) .AND. (FREQ(I) .LE. BFE)) THEN
0419         FFMAG(I) = 0.0
0420         ENDIF
0421         IF((FREQ(I) .GE. CFS) .AND. (FREQ(I) .LE. CFE)) THEN
0422         FFMAG(I) = 0.0
0423         ENDIF
0424   100 CONTINUE
0425         RETURN
0426         END
0427   C
0428   C
0429   C***********************************************************************C
0430   C                                                                      C
0431   C     ROUTINE: FFM4                                                    C
0432   C                                                                      C
0433   C     THIS SUBROUTINE FILTERS OUT ALL AMPLITUDES EXCEPT: PRIMARY       C
0434   C     MESH FREQUENCY AND FIRST HARMONIC AND THEIR FIRST CORRESPONDING  C
0435   C     SIDEBANDS, AND PRIMARY SHAFT FREQ. (PER STEWART'S 1977 PAPER)    C
0436   C                                                                      C
0437   C                                                                      C
0438   C***********************************************************************C
0439   C
0440         SUBROUTINE FFM4(FREQ,FFMAG,PRIM,SPD,RMAG)
```

```
0441  C
0442          DIMENSION FREQ(401),FFMAG(401),RMAG(401)
0443  C
0444          HARM = PRIM * 2.
0445          LPRIM = PRIM - 1.5 * SPD
0446          HPRIM = PRIM + 1.5 * SPD
0447          LHARM = HARM - 1.5 * SPD
0448          HHARM = HARM + 1.5 * SPD
0449          LSHAFT = 0.5 * SPD
0450          HSHAFT = 1.5 * SPD
0451  C
0452          DO 100, I=1,401
0453          RMAG(I) = 0.0
0454          IF((FREQ(I) .GT. LPRIM) .AND. (FREQ(I) .LT. HPRIM)) THEN
0455          RMAG(I) = FFMAG(I)
0456          ENDIF
0457          IF((FREQ(I) .GT. LHARM) .AND. (FREQ(I) .LT. HHARM)) THEN
0458          RMAG(I) = FFMAG(I)
0459          ENDIF
0460          IF((FREQ(I) .GT. LSHAFT) .AND. (FREQ(I) .LT. HSHAFT)) THEN
0461          RMAG(I) = FFMAG(I)
0462          ENDIF
0463   100 CONTINUE
0464          RETURN
0465          END
0466  C
0467  C
0468  C************************************************************************C
0469  C                                                                      C
0470  C      ROUTINE: STDEV                                                   C
0471  C                                                                      C
0472  C      THIS SUBROUTINE COMPUTES THE STANDARD DEVIATION OF THE          C
0473  C      DIFFERENCE TIME SIGNAL (ORIGINAL - REGULAR COMPONENTS).         C
0474  C                                                                      C
0475  C                                                                      C
0476  C************************************************************************C
0477  C
0478          SUBROUTINE STDEV(DYO,N,DBAR,SD)
0479  C
0480          DIMENSION DYO(220)
0481          ASUM = 0.0
0482          DO 100, I=1,N
0483          ASUM = (DYO(I) - DBAR)**2. + ASUM
0484    100 CONTINUE
0485          SD = (ASUM/FLOAT(N))**.5
0486          RETURN
0487          END
0488  C
0489  C
0490  C************************************************************************C
0491  C                                                                      C
0492  C      ROUTINE: KURTOS                                                  C
0493  C                                                                      C
0494  C      THIS SUBROUTINE COMPUTES THE NORMALIZED KURTOSIS OF THE         C
0495  C      DIFFERENCE TIME SIGNAL (ORIGINAL - REULAR COMPONENTS)           C
```

```
0496  C                                                                                    C
0497  C                                                                                    C
0498  C******************************************************************C
0499  C
0500        SUBROUTINE KURTOS(DYO,N,DBAR,RKT)
0501  C
0502        DIMENSION DYO(220)
0503  C
0504        TSUM = 0.0
0505        DO 100, I=1,N
0506        TSUM = TSUM + (DYO(I) - DBAR)**4.
0507    100 CONTINUE
0508  C
0509        BSUM = 0.0
0510        DO 200, I=1,N
0511        BSUM = BSUM + (DYO(I) - DBAR)**2.
0512    200 CONTINUE
0513  C
0514        RKT = (FLOAT(N) * TSUM)/BSUM**2.
0515        RETURN
0516        END
```

```
0001    C**************************************************************C
0002    C                                                            C
0003    C                                                            C
0004    C       PROGRAM:  HILB.FOR              REVISION:       A     C
0005    C                                       REVISION DATE: 05-12-89   C
0006    C       PROGRAMMER: J.J. Zakrajsek      DATE CREATED: 05-03-89    C
0007    C                                                            C
0008    C       THIS PROGRAM USES THE HILBERT TRANSFORM THEORY TO CONVERT   C
0009    C       THE TIME SIGNAL TO A COMPLEX FUNCTION TO DEMODULATE THE     C
0010    C       SIDEBANDS FROM THE CARRIER FREQUENCY. THIS METHOD IS BASED  C
0011    C       ON THE 1986 PAPER BY P. D. McFADDEN, AND THE 1988 PAPER BY  C
0012    C       D. A. WALLACE AND M. K. DARLOW.                      C
0013    C                                                            C
0014    C       REV A: ADD VARIABLE RAMP FREQUENCY ANALYTIC PHASE VALUE    C
0015    C              CORRECTION FUNCTION.                          C
0016    C                                                            C
0017    C**************************************************************C
0018    C
0019          DIMENSION TIME(50),AMAGN(220),APHAS(220),PPHAS(220),CPHAS(220)
0020          DIMENSION FREQ(401),FMAGRMS(401),FMAG(401),PHAS(401),FFMAG(401)
0021          DIMENSION TO(1024),YACT(1024),YHIL(1024),POINT(60)
0022          CHARACTER*22 LIST1,LIST3,AMPLF,PHASEF
0023          CHARACTER*22 AAMPLF,APHASF
0024          COMPLEX X(1024)
0025    C
0026    C ENTER GENERAL PARAMETERS AND FILE NAMES
0027    C
0028          PRINT *, 'ENTER NUMBER OF DATA POINTS (INTEGER)'
0029          READ(*,*) K
0030          PRINT *, 'ENTER CARRIER FREQUENCY (PRIMARY OR FIRST HARMONIC)'
0031          READ(*,*) PRIM
0032          PRINT *, 'ENTER ROTATIONAL SPEED IN REV/SEC (Hz)'
0033          READ(*,*) SPD
0034          PRINT *, 'ENTER NUMBER OF TIME DATA POINTS PER CYCLE'
0035          PRINT *, '( INTEGER, 220 MAXIMUM )'
0036          READ (*,*) NCYC
0037    C
0038    C DEFINITION OF FREQUENCY BAND TO BE USED IN ANALYSIS
0039    C
0040          PRINT *, 'THIS ANALYSIS IS BASED ON A BAND OF FREQUENCY DATA'
0041          PRINT *, 'SURROUNDING THE MESH FREQUENCY CHOSEN ABOVE. THE '
0042          PRINT *, 'NUMBER OF SIDEBANDS ON EACH SIDE OF THE FREQUENCY'
0043          PRINT *, 'OF INTEREST ARE CHOSEN BY THE USER. DATA OUTSIDE THIS'
0044          PRINT *, 'BAND, ALONG WITH THE FREQUENCY CHOSEN ABOVE, ARE'
0045          PRINT *, 'FILTERED OUT OF THE ANALYSIS.'
0046          PRINT *, '        '
0047    C
0048          PRINT *, 'ENTER NUMBER OF SIDEBANDS TO BE PASSED BELOW'
0049          PRINT *, 'CHOSEN FREQUENCY ( REAL NUMBER XX.)'
0050          READ(*,*) FILTS
0051          PRINT *, 'ENTER NUMBER OF SIDEBANDS TO BE PASSED ABOVE'
0052          PRINT *, 'CHOSEN FREQUENCY (REAL NUMBER XX.)'
0053          READ(*,*) FILTE
0054    C
0055    C INPUT PRIMARY FILE NAMES FILES
```

83

```
0056  C
0057        PRINT *, 'ENTER  TXXLIST1.FIL  INPUT FILES FILENAME'
0058        READ(*,'(A22)') LIST1
0059        PRINT *, 'ENTER  TXXLIST3.FIL  OUTPUT FILES FILENAME'
0060        READ(*,'(A22)') LIST3
0061  C
0062  C OPEN PRIMARY FILES
0063  C
0064        OPEN(3,FILE=LIST1,IOSTAT=IOERR)
0065        IF(IOERR .GT. 0) GOTO 999
0066        OPEN(4,FILE=LIST3,IOSTAT=IOERR)
0067        IF(IOERR .GT. 0) GOTO 999
0068  C
0069  C STARTING POINT OF ANALYSIS LOOP FOR EACH DATA POINT
0070  C
0071        DO 111, J=1,K
0072        PRINT *, 'PROCESSING DATA POINT NO. :',J
0073        READ(3,300) AMPLF,PHASEF
0074    300 FORMAT(A22,A22)
0075        READ(4,400) AAMPLF,APHASF
0076    400 FORMAT(A22,A22)
0077  C
0078  C OPEN LOOP DEPENDANT FILES
0079  C
0080        OPEN(5,FILE=AMPLF,IOSTAT=IOERR)
0081        IF(IOERR .GT. 0) GOTO 999
0082        OPEN(6,FILE=PHASEF,IOSTAT=IOERR)
0083        IF(IOERR .GT. 0) GOTO 999
0084        OPEN(8,FILE=AAMPLF,IOSTAT=IOERR)
0085        IF(IOERR .GT. 0) GOTO 999
0086        OPEN(9,FILE=APHASF,IOSTAT=IOERR)
0087        IF(IOERR .GT. 0) GOTO 999
0088  C
0089  C READ IN PHASE AND FREQUENCY FILES
0090  C
0091        DO 222, I=1,401
0092        READ(5,500) FREQ(I),FMAGRMS(I)
0093    500 FORMAT(4X,F12.3,20X,F16.8)
0094        FMAG(I) = FMAGRMS(I) * (2.**.5)
0095        READ(6,600) PHAS(I)
0096    600 FORMAT(20X,F12.3)
0097    222 CONTINUE
0098  C
0099  C PERFORM BANDPASS FILTERING
0100  C
0101        CALL FILTER(FREQ,FMAG,FFMAG,FILTS,FILTE,PRIM,SPD)
0102  C
0103  C PERFORM IFFT ON FILTERED FREQUENCY COMPONENTS OF ACTUAL SIGNAL
0104  C
0105        IFL = 1
0106        CALL IFOUR(FREQ,FFMAG,PHAS,TO,YACT,IFL)
0107  C
0108  C OBTAIN HILBERT TRANSFORM OF ACTUAL SIGNAL
0109  C
0110  C PERFORM IFFT ON FREQUENCY COMPONENTS OF HILBERT TRANSFORM OF SIGNAL
```

```
0111   C
0112         IFL = 2
0113         CALL IFOUR(FREQ,FFMAG,PHAS,TO,YHIL,IFL)
0114   C
0115   C DETERMINATION OF ANALYTIC FUNCTION MAGNITUDE AND PHASE
0116   C
0117         PI = 3.1415927
0118         DO 444, I=1,NCYC
0119         AMAGN(I) = (YACT(I)**2. + YHIL(I)**2.)**(.5)
0120         APHAS(I) = (ATAN2(YHIL(I),YACT(I)))*(180./PI)
0121     444 CONTINUE
0122   C
0123   C CORRECT PHASE VALUES FOR NOMINAL GEAR MESH FREQUENCY
0124   C
0125   C ADD 180 DEGREES TO ALL PHASE VALUES
0126   C
0127         DO 210, I=1,NCYC
0128         PPHAS(I) = APHAS(I) + 180.
0129     210 CONTINUE
0130   C
0131   C DETERMINE FREQUENCY OF RAMP FUNCTION
0132   C
0133         NCT = 0
0134         LIM = NCYC - 1
0135         DO 211, I=1,LIM
0136         N = I + 1
0137         XCHK = PPHAS(I) - PPHAS(N)
0138         IF(XCHK .GT. 200.) THEN
0139         NCT = NCT + 1
0140         POINT(NCT) = (TO(I) + TO(N))/2.
0141         ENDIF
0142     211 CONTINUE
0143         SFREQ = FLOAT(NCT-1)/(POINT(NCT) - POINT(1))
0144         PRINT *, SFREQ
0145   C
0146   C DETERMINE INITIAL OFFSET OF RAMP FUNCTION
0147   C
0148         I = 0
0149     212 CONTINUE
0150         I = I + 1
0151         N = I + 1
0152         XCHK = PPHAS(I) - PPHAS(N)
0153         IF(XCHK .GT. 200.) GOTO 213
0154         GOTO 212
0155     213 PERIOD = 1.0/SFREQ
0156         OFFSET = PERIOD - (TO(I) + TO(N))/2.0
0157         PRINT *, OFFSET
0158   C
0159   C CORRECT PHASE ANGLE VARIATION FOR NOMINAL TOOTH MESH FREQUENCY
0160   C
0161         DO 214, I=1,NCYC
0162         IF(I .EQ. 1) THEN
0163         FC = 1.0
0164         ENDIF
0165         IF(I .EQ. 1) GOTO 379
```

```
0166          N = I - 1
0167          XCHK = PPHAS(N) - PPHAS(I)
0168          IF(XCHK .GT. 200.) THEN
0169          M = I - 1
0170    377   M = M + 1
0171          MN = M + 1
0172          CCHK = PPHAS(M) - PPHAS(MN)
0173          IF(CCHK .GT. 200.) GOTO 378
0174          GOTO 377
0175    378   LL = I - 1
0176          ULIM = (TO(MN) + TO(M))/2.0
0177          BLIM = (TO(I) + TO(LL))/2.0
0178   C      PRINT *, ULIM
0179   C      PRINT *, BLIM
0180          CFREQ = 1.0/(ULIM - BLIM)
0181          FC = CFREQ/SFREQ
0182          OFFSET = -1.0*BLIM
0183          ENDIF
0184    379   CONTINUE
0185          CPHAS(I) = PPHAS(I) - (360.)*SFREQ*FC*(TO(I) + OFFSET)
0186    214   CONTINUE
0187   C
0188   C WRITE RESULTS TO FILES
0189   C
0190          DO 777, I=1,NCYC
0191          WRITE(8,700) TO(I),AMAGN(I)
0192    700   FORMAT(F16.8,4X,F16.8)
0193    777   CONTINUE
0194   C
0195          DO 778, I=1,NCYC
0196          WRITE(9,700) TO(I),CPHAS(I)
0197    778   CONTINUE
0198   C
0199   C CLOSE LOOP DEPENDANT FILES
0200   C
0201          CLOSE(5,IOSTAT=IOERR)
0202          IF(IOERR .GT. 0) GOTO 999
0203          CLOSE(6,IOSTAT=IOERR)
0204          IF(IOERR .GT. 0) GOTO 999
0205          CLOSE(8,IOSTAT=IOERR)
0206          IF(IOERR .GT. 0) GOTO 999
0207          CLOSE(9,IOSTAT=IOERR)
0208          IF(IOERR .GT. 0) GOTO 999
0209   C
0210   C CLOSE LOOP, MOVE TO NEXT DATA POINT
0211   C
0212    111   CONTINUE
0213   C
0214   C
0215          PRINT *, 'VALUES STORED IN FILES ON DISK :A'
0216          STOP
0217    999   PRINT *, 'ERROR NO. ',IOERR
0218          END
0219   C
0220   C
```

```
0221  C END OF MAIN PROGRAM
0222  C
0223  C
0224  C*******************************************************************C
0225  C                                                                 C
0226  C      ROUTINE: IFOUR                                             C
0227  C                                                                 C
0228  C      THIS SUBROUTINE PERFORMS AN INVERSE DISCRETE FOURIER       C
0229  C      TRANSFORM ON A DFT TRACE USING MAGNITUDE AND PHASE DATA.    C
0230  C                                                                 C
0231  C                                                                 C
0232  C*******************************************************************C
0233  C
0234        SUBROUTINE IFOUR(F,FMAG,PHAS,T,Y,IFL)
0235  C
0236        DIMENSION  T(1024),Y(1024)
0237        DIMENSION  F(401),DFTRE(401),DFTIM(401),FMAG(401),PHAS(401)
0238        DIMENSION  FQ(20)
0239        COMPLEX    X(1024)
0240  C
0241  C..DEFINE DFT SETTINGS
0242  C
0243        NPTS = 1024
0244        NPOW = 10
0245        NFREQ = 401
0246        FSPAN = F(401) - F(1)
0247        PERIOD = FLOAT( (NFREQ-1) ) / FSPAN
0248        BW = F(2) - F(1)
0249        DELTA = PERIOD / FLOAT( (NPTS-1) )
0250        PRINT *, PERIOD
0251        PRINT *, BW
0252  C
0253  C INITIALIZE TIME, AND DFT ARRAYS
0254  C
0255        DO 100 I=1,NPTS
0256            T(I) = DELTA * FLOAT( I-1 )
0257            X(I) = ( 0.,0. )
0258  100     CONTINUE
0259  C
0260  C  CONVERTING PHASE AND MAGNITUDE TO REAL AND IMAGINARY FFT VALUES
0261  C
0262        PI = 3.1415927
0263  C
0264  C  ACTUAL SIGNAL ALGORYTHM (IFL = 1)
0265  C
0266        IF(IFL .EQ. 1) THEN
0267            DO 300, I=1,NFREQ
0268            RAD = PHAS(I)*PI/180.
0269            DFTRE(I) = FMAG(I) * COS(RAD)
0270            DFTIM(I) = FMAG(I) * SIN(RAD)
0271  300     CONTINUE
0272        ENDIF
0273  C
0274  C  HILBERT TRANSFORM ALGORYTHM (IFL = 2)
0275  C
```

87

```
0276          IF(IFL .EQ. 2) THEN
0277              DO 303, I=1,NFREQ
0278              RAD = PHAS(I)*PI/180.
0279              DFTRE(I) = FMAG(I)*SIN(RAD)
0280              DFTIM(I) = (-1.0)*FMAG(I)*COS(RAD)
0281      303     CONTINUE
0282          ENDIF
0283  C
0284  C..PERFORM INVERSE DFT ON REAL PART
0285  C
0286          IFLAG = 1
0287          DO 2200 I=1,NFREQ
0288              X(I) = CMPLX( DFTRE(I),0. )
0289     2200     CONTINUE
0290          CALL FFT( IFLAG,NPOW,X )
0291          DO 2300 I=1,NPTS
0292              Y(I) = REAL( X(I) )
0293     2300     CONTINUE
0294  C
0295  C..PERFORM INVERSE DFT ON IMAGINARY PART
0296  C
0297          DO 2400 I=1,NFREQ
0298              X(I) = CMPLX( DFTIM(I),0. )
0299     2400     CONTINUE
0300          DO 2500 I=NFREQ+1,NPTS
0301              X(I) = ( 0.,0. )
0302     2500     CONTINUE
0303          CALL FFT( IFLAG,NPOW,X )
0304          DO 2600 I=1,NPTS
0305              Y(I) = Y(I) - AIMAG( X(I) )
0306     2600     CONTINUE
0307  C
0308          RETURN
0309          END
0310  C
0311  C
0312  C****************************************************************C
0313  C                                                              C
0314  C     ROUTINE:  FFT                                            C
0315  C                                                              C
0316  C****************************************************************C
0317  C
0318          SUBROUTINE FFT( IFLAG,NPOW,X )
0319          DIMENSION  X(1),CS(2),MSK(13)
0320          COMPLEX    X,CXCS,HOLD,XA
0321          EQUIVALENCE (CXCS,CS)
0322  C
0323          PI = 3.141 592 7
0324          NMAX = 2**NPOW
0325          ZZ = 2. * PI  * FLOAT(IFLAG) / FLOAT(NMAX)
0326          MSK(1) = NMAX / 2
0327          DO 15 I=2,NPOW
0328              MSK(I) = MSK(I-1) / 2
0329      15     CONTINUE
0330          NN = NMAX
```

```
0331        MM - 2
0332 C
0333 C..LOOP OVER NPOW LAYERS
0334 C
0335        DO 45 LAYER=1,NPOW
0336            NN - NN / 2
0337            NW - 0
0338            DO 40 I=1,MM,2
0339                II - NN * I
0340 C
0341 C..CXCS - CEXP( 2*PI*NW*FLOAT(IFLAG)/FLOAT(NMAX) )
0342 C
0343                W - FLOAT(NW) * ZZ
0344                CS(1) - COS( W )
0345                CS(2) - SIN( W )
0346 C
0347 C..COMPUTE ELEMENTS FOR BOTH HALVES OF EACH BLOCK
0348 C
0349                DO 20 J=1,NN
0350                    II - II + 1
0351                    IJ - II - NN
0352                    XA - CXCS * X(II)
0353                    X(II) - X(IJ) - XA
0354                    X(IJ) - X(IJ) + XA
0355   20           CONTINUE
0356 C
0357 C..BUMP UP SERIES BY 2, COMPUTE REVERSE ADDRESS
0358 C
0359                DO 25 LOC=2,NPOW
0360                    LL - NW - MSK(LOC)
0361                    IF( LL )   30,35,25
0362   25               NW - LL
0363   30           NW - MSK(LOC) + NW
0364                GOTO 40
0365   35           NW - MSK(LOC+1)
0366   40           CONTINUE
0367            MM - MM * 2
0368   45       CONTINUE
0369 C
0370 C..DO FINAL REARRANGEMENT, ALSO MULTIPLY BY DELTA.
0371 C
0372        NW - 0
0373        DO 80 I=1,NMAX
0374            NW1 - NW + 1
0375            HOLD - X(NW1)
0376            IF( NW1-I )  60,55,50
0377   50       X(NW1) - X(I)
0378   55       X(I) - HOLD
0379 C
0380 C..BUMP UP SERIES BY 1, AND COMPUTE REVERSE ADDRESS.
0381 C
0382   60       DO 65 LOC=1,NPOW
0383                LL - NW - MSK(LOC)
0384                IF( LL )  70,75,65
0385   65           NW - LL
```

```
0386   70         NW - MSK(LOC) + NW
0387              GOTO 80
0388   75         NW - MSK(LOC+1)
0389   80         CONTINUE
0390          RETURN
0391          END
0392   C
0393   C
0394   C******************************************************************C
0395   C                                                                  C
0396   C      ROUTINE: FILTER                                             C
0397   C                                                                  C
0398   C      THIS SUBROUTINE FILTERS OUT ALL FREQUENCY COMPONENTS        C
0399   C      OUTSIDE THE FREQUENCY BAND CHOSEN IN THE MAIN PROGRAM.      C
0400   C      THE CARRIER FREQUENCY IS ALSO FILTERED OUT.                 C
0401   C                                                                  C
0402   C                                                                  C
0403   C******************************************************************C
0404   C
0405          SUBROUTINE FILTER(FREQ,FMAG,FFMAG,FS,FE,PRIM,SPD)
0406   C
0407          DIMENSION FREQ(401),FMAG(401),FFMAG(401)
0408   C
0409          SBL - PRIM - (FS + .5)*SPD
0410          PL - PRIM - (.5*SPD)
0411          PU - PRIM + (.5*SPD)
0412          SBU - PRIM + (FE + .5)*SPD
0413   C
0414          DO 100, I-1,401
0415          FFMAG(I) - 0.0
0416          IF((FREQ(I) .GE. SBL) .AND. (FREQ(I) .LE. PL)) THEN
0417          FFMAG(I) - FMAG(I)
0418          ENDIF
0419          IF((FREQ(I) .GE. PU) .AND. (FREQ(I) .LE. SBU)) THEN
0420          FFMAG(I) - FMAG(I)
0421          ENDIF
0422   100 CONTINUE
0423          RETURN
0424          END
```

90

```
0001   C**************************************************************C
0002   C                                                            C
0003   C                                                            C
0004   C     PROGRAM: PARAM.FOR     CREATED: 05-05-89   REVISED: XX-XX-XXXX C
0005   C                                                            C
0006   C     PROGRAMMER: J.J. ZAKRAJSEK                             C
0007   C                                                            C
0008   C     THIS PROGRAM COMPUTES SEVERAL FAULT DETECTION PARAMETERS C
0009   C     BASED ON THE A-B-C FILTERED SIGNAL CALCULATED IN THE PROGRAM C
0010   C     TFM4.FOR. THE BASIS OF THE PARAMETERS ARE SUMMARIZED BELOW. C
0011   C                                                            C
0012   C     CREST FACTOR (CF) - PEAK LEVEL / TOTAL RMS LEVEL       C
0013   C                                                            C
0014   C     SIDEBAND LEVEL FACTOR (SBLF) - FIRST ORDER SIDEBANDS (PRIMARY) C
0015   C                                          TOTAL RMS LEVEL   C
0016   C                                                            C
0017   C     WEAR ENERGY RATIO - RMS LEVEL OF NON-PERIODIC PART OF SIGNAL C
0018   C        (WER)            / RMS LEVEL OF PERIODIC PART OF SIGNAL  C
0019   C                                                            C
0020   C                                                            C
0021   C**************************************************************C
0022   C
0023         DIMENSION TIME(50),FSIG(220),RSIG(220),DSIG(220)
0024         DIMENSION FREQ(500), AMPL(500)
0025         CHARACTER*22 FMOF,PARAMF,LIST2,LIST1,AMPLF
0026         CHARACTER*18 FTIMEF,RTIMEF,DTIMEF
0027   C
0028   C ENTER INITIAL DATA AND FILE NAMES
0029   C
0030         PRINT *, 'ENTER NUMBER OF DATA POINTS'
0031         READ(*,*) K
0032         PRINT *, 'ENTER MESH FREQ (XXXX.)'
0033         READ(*,*) PRIM
0034         PRINT *, 'ENTER ROTATIONAL SPEED (REV/SEC)'
0035         READ(*,*) SPD
0036   C
0037         PRINT *, 'ENTER OUTPUT DATA FILE NAME (\TXXPARAM.DAT)'
0038         READ (*,'(A22)') PARAMF
0039         OPEN(7,FILE=PARAMF,IOSTAT=IOERR)
0040         IF (IOERR .GT. 0) GOTO 999
0041         PRINT *, 'ENTER FILE NAMES ARRAY FILE (\TXXLIST1.FIL)'
0042         READ(*,'(A22)') LIST1
0043         OPEN(6,FILE=LIST1,IOSTAT=IOERR)
0044         IF(IOERR .GT. 0) GOTO 999
0045         PRINT *, 'ENTER FILE NAMES ARRAY FILE (\TXXLIST2.FIL)'
0046         READ(*,'(A22)') LIST2
0047         OPEN(8,FILE=LIST2,IOSTAT=IOERR)
0048         IF(IOERR .GT. 0) GOTO 999
0049         PRINT *, 'ENTER PREVIOUS TFM0 FILE (\TXXFM0.DAT)'
0050         READ(*,'(A22)') FMOF
0051         OPEN(9,FILE=FMOF,IOSTAT=IOERR)
0052         IF(IOERR .GT. 0) GOTO 999
0053         PRINT *, 'ENTER NUMBER OF TIME DATA POINTS PER CYCLE (INTEGER)'
0054         READ(*,*) NCYC
0055   C
```

```
0056  C START TIME LOOPING, PROCESSING DATA AT EACH TIME INTERVAL
0057  C
0058        DO 300, J=1,K
0059        PRINT *, 'ACCESSING AND PROCESSING DATA FILE NO:',J
0060        READ(6,600) AMPLF
0061   600  FORMAT(A20)
0062        READ(8,800) FTIMEF,RTIMEF,DTIMEF
0063   800  FORMAT(A18,A18,A18)
0064        READ(9,900) TIME(J)
0065   900  FORMAT(F8.2)
0066        OPEN(4,FILE=FTIMEF,IOSTAT=IOERR)
0067        IF (IOERR .GT. 0) GOTO 999
0068        OPEN(3,FILE=RTIMEF,IOSTAT=IOERR)
0069        IF (IOERR .GT. 0) GOTO 999
0070        OPEN(2,FILE=DTIMEF,IOSTAT=IOERR)
0071        IF (IOERR .GT. 0) GOTO 999
0072        OPEN(5,FILE=AMPLF,IOSTAT=IOERR)
0073        IF (IOERR .GT. 0) GOTO 999
0074  C
0075  C READ IN AND FIND THE MAX VALUE OF THE FILTERED TIME RECORD
0076  C
0077        PKL = 0.0
0078        DO 100, I=1,NCYC
0079        READ(4,400) FSIG(I)
0080   400  FORMAT(20X,F16.8)
0081        AVALU = ABS(FSIG(I))
0082        IF( AVALU .GT. PKL ) THEN
0083        PKL = AVALU
0084        ENDIF
0085   100  CONTINUE
0086  C
0087  C FIND FIRST ORDER SIDEBANDS LEVEL
0088  C
0089        DO 301, I=1,401
0090        READ(5,500) FREQ(I),AMPL(I)
0091   500  FORMAT(4X,F12.3,20X,F16.8)
0092   301  CONTINUE
0093  C
0094        CALL FOSB(FREQ,AMPL,PRIM,SPD,SBL)
0095  C
0096  C FIND TOTAL RMS LEVEL OF SIGNAL
0097  C
0098        CALL STDEV(FSIG,NCYC,FSD)
0099  C
0100  C FIND RMS LEVEL OF PERIODIC COMPONENTS
0101  C
0102        DO 120, I=1,NCYC
0103        READ(3,400) RSIG(I)
0104   120  CONTINUE
0105  C
0106        CALL STDEV(RSIG,NCYC,RSD)
0107  C
0108  C FIND RMS LEVEL OF DIFFERENCE SIGNAL (SIGNAL - PERIODIC COMPONENTS)
0109  C
0110        DO 140, I=1,NCYC
```

```
0111          READ(2,400) DSIG(I)
0112      140 CONTINUE
0113   C
0114          CALL STDEV(DSIG,NCYC,DSD)
0115   C
0116   C COMPUTE CREST FACTOR
0117   C
0118          CF - PKL/FSD
0119   C
0120   C FIND SIDEBAND LEVEL FACTOR
0121   C
0122          SBLF - SBL/FSD
0123   C
0124   C FIND WEAR ENERGY RATIO
0125   C
0126          WER - DSD/RSD
0127   C
0128   C CLOSE LOOP DEPENDANT FILE, AND WRITE CALCULTED DATA TO FILE
0129   C
0130          CLOSE(4,IOSTAT-IOERR)
0131          IF (IOERR .GT. 0) GOTO 999
0132          CLOSE(2,IOSTAT-IOERR)
0133          IF (IOERR .GT. 0) GOTO 999
0134          CLOSE(3,IOSTAT-IOERR)
0135          IF (IOERR .GT. 0) GOTO 999
0136          CLOSE(5,IOSTAT-IOERR)
0137          IF (IOERR .GT. 0) GOTO 999
0138          WRITE (7,700) TIME(J),CF,SBLF,WER
0139      700 FORMAT(F8.2,F10.4,F10.4,F10.4)
0140      300 CONTINUE
0141   C
0142          PRINT *, 'PARAMETER VALUES STORED IN FILE:',PARAMF
0143          STOP
0144      999 PRINT *, 'ERROR NO.',IOERR
0145          END
0146   C
0147   C
0148   C ****** END OF MAIN PROGRAM ******
0149   C
0150   C
0151   C**********************************************************************C
0152   C                                                                    C
0153   C     ROUTINE: FOSB        (FIRST ORDER SIDEBANDS)                    C
0154   C                                                                    C
0155   C**********************************************************************C
0156   C
0157          SUBROUTINE FOSB(FREQ,AMPL,PRIM,SPD,SBL)
0158   C
0159          DIMENSION FREQ(500),AMPL(500)
0160          BSBS - PRIM - 1.5*SPD
0161          BSBE - PRIM - .5*SPD
0162          USBS - PRIM + .5*SPD
0163          USBE - PRIM + 1.5*SPD
0164          BSB - 0.0
0165          USB - 0.0
```

93

```
0166          DO 200, I=1,401
0167          IF((FREQ(I).GT.BSBS) .AND. (FREQ(I).LT.BSBE)) THEN
0168          IF(AMPL(I) .GT. BSB) BSB - AMPL(I)
0169          ENDIF
0170          IF((FREQ(I).GT.USBS) .AND. (FREQ(I).LT.USBE)) THEN
0171          IF(AMPL(I) .GT. USB) USB - AMPL(I)
0172          ENDIF
0173     200 CONTINUE
0174          SBL - (BSB + USB)/2.0
0175          RETURN
0176          END
0177   C
0178   C
0179   C*******************************************************************C
0180   C                                                                  C
0181   C     ROUTINE: STDEV      (STANDARD DEVIATION OF TIME SIGNAL)      C
0182   C                                                                  C
0183   C*******************************************************************C
0184   C
0185          SUBROUTINE STDEV(DYO,N,SD)
0186   C
0187          DIMENSION DYO(220)
0188          DSUM - 0.0
0189          DO 100, I-1,N
0190          DSUM - DSUM + DYO(I)
0191     100 CONTINUE
0192          DBAR - DSUM/FLOAT(N)
0193   C
0194          ASUM - 0.0
0195          DO 200, I-1,N
0196          ASUM - (DYO(I) - DBAR)**2. + ASUM
0197     200 CONTINUE
0198          SD - (ASUM/FLOAT(N))**.5
0199          RETURN
0200          END
```

A	amplitude at mesh frequency and harmonics
A(t)	original signal after time synchronous averaging
AN(f)	analytic signal
D(t)	difference signal
d	discrete value in the difference signal, D(t)
$\bar{d}$	mean value of the difference signal, D(t)
F(m)	discrete value in a frequency array
f(n)	discrete value in a time record
$\bar{F}(m)$	discrete frequency array (discrete fourier transform of a time record)
$\bar{f}(n)$	discrete time record
F(w)	frequency domain function (fourier transform of a time domain function)
f	frequency (cycles/second)
f(min)	minimum resolution frequency
FOSL	first order sidebands level
Gxy(f)	cross power spectrum
Gxy*(f)	complex conjugate of Gxy(f)
Gyx(f)	cross power spectrum
Gxx(f)	auto power spectrum of input
Gyy(f)	auto power spectrum of output
H(f)	frequency response function
$\bar{H}yx(f)$	estimate of frequency response function
h(t)	unit impulse response function
K	kurtosis, fourth moment of an array of values
N	number of data points in a discrete time record
NK	normalized kurtosis

NS	number of samples
Nt	number of time averages
PL	peak level of signal
PP	peak to peak level of signal average
R(t)	regular meshing components of signal average
RMS	standard deviation of signal average
RMSDS	standard deviation of difference signal, D(t)
RMSRC	standard deviation of regular meshing components of signal, R(t)
S/N	signal to noise ratio
T	length of time record (seconds)
t	time (seconds)
w	frequency (radians/second)
X(f)	fourier transform of input signal
X*(f)	complex conjugate of X(f)
Y(f)	fourier transform of output signal

REFERENCES

1. Stewart, R.M.: Some Useful Data Analysis Techniques for Gearbox Diagnostics. Machine Health Monitoring Group, Institute of Sound and Vibration Research, University of Southhampton, Report MHM/R/10/77, July 1977.

2. McFadden, P.D.: Detecting Fatigue Cracks in Gears by Amplitude and Phase Demodulation of the Meshing Vibration. J. Vibration, Acoustics, Stress and Reliability in Design, vol. 108, no. 2, April 1986, pp. 165-170.

3. Swansson, N.S.: Application of Vibration Signal Analysis Techniques to Signal Monitoring, Conference on Friction and Wear in Engineering 1980, Institution of Engineers, Australia, Barton, Australia, 1980, pp. 262-267.

4. Goold, I.: Chinook Report Criticizes Boeing and Authorities. Flight Int., vol. 135, no. 4161, April 22, 1989, pp. 8-9.

5. Faulty Part Temporarily Grounds Marine Corps CH-53E's. Helicopter News, vol. 14, no. 21, Oct. 21, 1988, p. 8.

6. Gonzalez, R.C.; and Wintz, Paul: Digital Image Processing. Addison-Wesley Publishing Co., Reading, MA, 1977.

7. Bendat, J.S.; and Piersol, A.G.: Engineering Applicationns of Correlation and Spectral Analysis. John Wiley and Sons, New York, 1980.

8. Favaloro, S.C.: A Preliminary Evaluation of Some Gear Diagnostics Using Vibration Analysis. ARL-AERO-RPOP-TM-427, Aeronautical Research Laboratories, Department of Defense, Melbourne, Australia, 1985, (Avail. NTIS, AD-A161939).

9. Gu, A.L.; and Badgley, R.H.: Prediction of Vibration Sidebands in Gear Meshes. ASME Paper 74-DET-95, Oct, 1974.

10. Wallace, D.A.; and Darlow, M.S.: Hilbert Transform Techniques for Measurement of Transient Gear Speeds. Mechanical Systems and Signal Processing, vol. 2, Apr. 1988, pp. 187-194.

11. Dynamic Signal Analyzer Applications: Effective Machinery Maintenance Using Vibration Analysis. Hewlett Packard Application Note 243-1, Hewlett Packard, 1983.

12. Cooley, J.W.; and Tukey, J.W.: An Algorithm for the Machine Calculation of Complex Fourier Series. Math. of Comput., vol. 19, 1965, pp. 297-301.

NASA

National Aeronautics and
Space Administration

Report Documentation Page

1. Report No. NASA TM-102340 AVSCOM TM 89-C-005	2. Government Accession No.	3. Recipient's Catalog No.

4. Title and Subtitle

An Investigation of Gear Mesh Failure Prediction Techniques

5. Report Date

October 1989

6. Performing Organization Code

7. Author(s)

James J. Zakrajsek

8. Performing Organization Report No.

E-5049

10. Work Unit No.

505-63-51

1L162209A47A

9. Performing Organization Name and Address

NASA Lewis Research Center
Cleveland, Ohio 44135-3191
and
Propulsion Directorate
U.S. Army Aviation Research and Technology Activity—AVSCOM
Cleveland, Ohio 44135-3127

11. Contract or Grant No.

13. Type of Report and Period Covered

Technical Memorandum

12. Sponsoring Agency Name and Address

National Aeronautics and Space Administration
Washington, D.C. 20546-0001
and
U.S. Army Aviation Systems Command
St. Louis, Mo. 63120-1798

14. Sponsoring Agency Code

16. Abstract

A study was performed in which several gear failure prediction methods were investigated and applied to experimental data from a gear fatigue test apparatus. The primary objective was to provide a baseline under-standing of the prediction methods and to evaluate their diagnostic capabilities. The methods investigated use the signal average in both the time and frequency domain to detect gear failure. Data from eleven gear fatigue tests were recorded at periodic time intervals as the gears were run from initiation to failure. Four major failure modes, consisting of heavy wear, tooth breakage, single pits, and distributed pitting were observed among the failed gears. Results show that the prediction methods were able to detect only those gear failures which involved heavy wear or distributed pitting. None of the methods could predict fatigue cracks, which resulted in tooth breakage, or single pits. It is suspected that the fatigue cracks were not detected because of limitations in data acquisition rather than in methodology. Additionally, the frequency response between the gear shaft and the transducer was found to significantly affect the vibration signal. The specific frequencies affected were filtered out of the signal average prior to application of the methods. Keywords: Computer Aided Diagnosis Rotary Wing Aircraft,

17. Key Words (Suggested by Author(s))	18. Distribution Statement
Gears Failure prediction Diagnostics	Unclassified—Unlimited Subject Category 37

19. Security Classif. (of this report)	20. Security Classif. (of this page)	21. No of pages	22. Price*
Unclassified	Unclassified	98	A05